Molecular and Cellular Mechanisms of Mycobacterial Glycolipid Recognition by Human T Cells

Charlotte A. James

A dissertation

submitted in partial fulfillment of the

requirements for the degree of

Doctor of Philosophy

University of Washington

2020

Reading Committee:

Chetan Seshadri, Chair

Marion Pepper

Thomas R. Hawn

Program Authorized to Offer Degree:

Pathology

University of Washington

Abstract

Molecular and Cellular Mechanisms of Mycobacterial Glycolipid Recognition by Human T Cells

Charlotte A. James

Chair of the Supervisory Committee:
Chetan Seshadri, MD. Associate Professor.
Department of Medicine, Division of Allergy and Infectious Diseases

Tuberculosis (TB) is of high global health importance and disproportionately affects individuals in resource-limited settings. A major challenge to reducing the global burden of this disease is the lack of effective vaccines and diagnostics. At present, the intricacies of the immune response to this disease are not understood well enough to rationally develop efficacious vaccines. Peptide-specific T cells have been implicated as a critical component of the immune response to TB. However, there are few studies that investigate the role of T cells that recognize non-peptide antigens in the immune response to TB. T cells can recognize lipid antigens presented by CD1 molecules, but how these antigens are recognized and the impact that antigen recognition has on lipid-specific T cell activation and functional differentiation is not understood. Here, we elucidate the molecular and cellular factors that affect lipid antigen recognition by human T cells, and what impact these factors have on T cell activation and function. This work focused on a family of mycobacterial lipids, diacylated sulfoglycolipids (Ac_2SGL), which are only expressed by virulent

strains of *Mycobacterium tuberculosis,* the causative agent of TB. The first aim of this work utilized synthetic Ac_2SGL analogs, a panel of T cell clones, and antigen presenting cells that express mutated CD1 molecules to probe the specificity with which these antigens are recognized by T cells to inform which molecular moieties are essential for Ac_2SGL recognition by T cells. The second aim investigated the impact of T cell receptor co-receptors on antigen recognition at the cellular level, as this influences the magnitude of activation and functional differentiation of T cells. We found that co-receptors augmented T cell affinity for Ac_2SGL and these molecules impact T cell function *in vitro* and *ex vivo*. Together, our data support an emerging model that related but chemically distinct antigens and T cell subpopulations should be studied independently to fully understand the T cell response to mycobacterial lipid antigens. As Ac_2SGL holds promise as a target for novel vaccination and diagnostic strategies for TB, these studies will inform the development of tools to address these two major needs.

ACKNOWLEDGEMENTS

This work would not have been possible without the support of some truly remarkable individuals.

I would first like to thank my PhD thesis advisor, Dr. Chetan Seshadri, whose untold levels experimental advice and thoughtful mentorship have shaped me into the scientist that I am today. I am grateful for the wisdom he has passed on to me, as well as his ability to creatively solve problems and approach all issues with an open mind. I will forever admire the carefulness with which he cultivated a supportive lab environment that enabled me to thrive during my time in graduate school. I would like to thank the members of my supervisory committee for their helpful and constructive advice throughout my time in graduate school. This work was greatly improved from your support and scientific guidance. This includes Professors Thomas Hawn, Marion Pepper, Martin Prlic, and Ian N. Crispe.

These studies would not have been possible without our many collaborators who lent protocols, experimental knowledge, and reagents. These include the laboratories of Drs. D. Branch Moody, Ildiko Van Rhijn, Daniel Pellici, Dale Godfrey, Martine Gilleron, Adriaan Minnaard, Edus H. Warren, Mark Davis, David Koelle and Martin Prlic. I would like to give a particular thank you to Drs. Lichen Jing and Yuexin Xu for their hands-on assistance in transferring methods to the Seshadri Lab. I would also like to thank our clinical collaborators, Cheryl Day, Thomas Scriba, and Stephen De Rosa for providing access to patient samples, and the patients themselves for volunteering for these studies. I would also like to thank the incredibly skilled members of the core facilities I used to generate the data in this dissertation. This includes the UW South Lake Union Cell Analysis Facility, the Fred Hutchinson Cancer Research Center Genomics Core, and the NIH Tetramer Core Facility.

I would like to thank all the members of the Seshadri Lab and the Center for Emerging and Re-emerging Infectious Diseases, past and present, for their technical and scientific support. I am especially grateful for Dr. Krystle Yu, whose guidance and support during my graduate work cannot be overstated. I would also like to thank Drs. Megan Zuck, Mark Fernandez, Soumik Barman, and Austin Haynes for their experimental advice, patient listening, and comic relief during the last four years. I would also like to acknowledge those who contributed to this work directly, Malisa Smith, Malisa Smith, Erik Layton, Paula Marsland, and Natalie Erjavec.

I would like to thank the members of the M3D PhD Program, for being my constant cheerleaders and fountains of wisdom. I would particularly like to thank Bill Mahoney, Daniel Promislow, Steve Berard, and Meghan Barker for their tireless efforts to ensure every member of our program is supported and cared for.

This work was supported by the National Institute of Allergy and Infectious Disease of the National Institutes of Health (R01 AI125189), the Doris Duke Charitable Foundation, the Institute of Translational Health Sciences (TL1 TR002318), and the Molecular Medicine Training Program (T32 GM095421).

Lastly, I would like to thank my extraordinary friends and family. Without their encouragement and levity I would not be where I am today. And lastly to John, for truly being the most kind, thoughtful, and supportive husband, and for always pretending to enjoy the things that I stress-bake, even when they are not very nice.

DEDICATION

To my Mum and Dad, Linda and Steve James.

For their unwavering support and unconditional love that enabled me to achieve anything I set my mind to.

TABLE OF CONTENTS

LIST OF FIGURES

LIST OF TABLES

Chapter 1. INTRODUCTION

Adapted from James C.A., Seshadri C. (2020). T Cell Responses to Mycobacterial Glycolipids: On the Spectrum of "Innateness". *Frontiers in Immunology.* 11, 170. doi: 10.3389/fimmu.2020.00170.

1.1 T CELL RESPONSES TO *MYCOBACTERIUM TUBERCULOSIS*

Tuberculosis (TB) is of high global health importance and disproportionately affects individuals in resource-limited settings. In 2018, an estimated 10 million individuals fell ill with TB and 1.5 million people succumbed to the infection (WHO Report, 2018). These statistics are further complicated by the estimated 1.8 billion individuals who are quiescently infected with *Mycobacterium tuberculosis* (M.tb), the causative agent of the disease (WHO Report, 2018). While individuals with dormant M.tb infection are not contagious, an estimated 5-10% of individuals with latent disease will go on to develop transmissible active disease (WHO Report, 2018). A major challenge to reducing the global burden of these diseases is the lack of effective diagnostics and vaccines.

The attenuated *Mycobacterium bovis* stain, Bacillus Calmette-Guérin (BCG), is the only licensed vaccine for TB. This vaccine provides protection against disseminated forms of the disease in children, but provides only partial and variable efficacy against pulmonary TB in adults (Fine, 1995; Mangtani et al., 2014; Trunz et al., 2006). As TB is spread through airborne droplets that are produced when an infected individual with active disease coughs, adults with pulmonary TB are thought to be the primary individuals who transmit this disease to others.

Further, the current standard for the diagnosis of TB infection is the IFN-γ release assay (Pai et al., 2014). This assay detects memory T cell responses to early secreted antigen 6 kilodaltons (ESAT-6) and culture filtrate protein-10 (CFP-10), two secreted proteins that are

specific to M.tb. While this test has improved specificity over the traditional tuberculin skin test (TST), neither test accurately predicts which patients will eventually develop active pulmonary disease.

Thus, effective vaccines and diagnostics that prevent or detect progression to active pulmonary TB in adults are necessary to limit the spread of this disease. To rationally design these tools, we must first obtain a clearer understanding of the immune response to this disease. Several studies in murine and non-human primate models implicate T cells as necessary to control M.tb (Lin et al., 2012; Mogues et al., 2001). Specifically, these studies led to a focus on T cells that recognize peptide antigens presented by major histocompatibility complex (MHC) molecules, in part because MHC class II (MHC-II) knockout mice infected with M.tb had a significantly shorter life-span than MHC-I knockout or wild-type mice (Mogues et al., 2001). These studies are underscored by the clinical observation that depleted $CD4^+$ T cell counts in individuals living with human immunodeficiency virus (HIV) infection is associated with increased risk of pulmonary and disseminated TB (Zumla et al, 2013). Consequently, the majority of new vaccine development efforts have been focused on eliciting robust $CD4^+$ T cell responses to mycobacterial protein antigens (Méndez-Samperio, 2018; Rowland and McShane, 2011). However, such vaccine strategies have exhibited mixed results in clinical trials (Tameris et al., 2013; Van Der Meeren et al., 2018).

Such results have led to the consideration of including non-peptide antigens in novel vaccine strategies for TB through whole cell mycobacterial vaccines that include a variety of antigenic types. However, there are relatively few studies that investigate the role of T cells that recognize non-peptide antigens in the immune response to TB. T cells can recognize lipids and microbial metabolites, presented by cluster of differentiation 1 (CD1) and MHC-related protein 1

(MR1), respectively (Beckman et al., 1994; Kjer-Nielsen et al., 2012). These CD1- and MR1-restricted T cells have been largely defined as "innate-like" T cells due to their unique biology. The two major populations of CD1- and MR1-restricted T cells are invariant natural killer T (iNKT) cells and mucosal associated invariant T (MAIT) cells, respectively (Figure 1A). Notably, iNKT and MAIT cells represent only a subset of T cells that recognize non-peptide antigens.

Lipids found in the mycobacterial cell wall, collectively termed mycolipids here, have been shown to bind CD1 molecules and activate human T cells (Beckman et al., 1994; Calabi et al., 1989; Martin et al., 1986) (Figure 1A, 1B). Long-chain mycolipids preferentially bind to CD1b due to its large binding pocket, while comparatively shorter lipids and lipopeptides are presented by CD1c and CD1a, respectively (Beckman et al., 1996; Moody et al., 2004; Rosat et al., 1999). Mycolic acid (MA) was the first mycobacterial lipid antigen shown to be recognized by T cells via the CD1b antigen presentation pathway (Beckman et al., 1994). Since then, glucose monomycolate (GMM) and glycerol monomycolate (GroMM) were discovered as glycated forms of mycolic acid that are also recognized as T cell antigens (Layre et al., 2009; Moody et al., 1997). In addition to the mycolates, lipoarabinomannan (LAM) and its constituent lipid phosphotidyl-*myo*-inositol mannoside (PIM) are abundant cell surface mycolipids recognized by human T cells (de la Salle et al., 2005; Sieling et al., 1995). Finally, diacylated sulfogylcolipids (Ac_2SGL), which are uniquely expressed in the cell wall of virulent strains of M.tb, are also T cell antigens (Gilleron et al., 2004). Thus, six structurally defined mycolipids are presented by CD1b to human T cells (Figure 1B). In addition, mannosyl-β-1-phosphoketide (MPM) antigen presentation is restricted by CD1c (Moody et al., 2000) and didehydroxymycobactin (DDM) is a lipopeptide antigen presented by CD1a (Moody et al., 2004).

T cell responses to many of these antigens have been detected among individuals infected with M.tb. GMM- and SGL-specific T cells have been detected at a higher frequency in individuals infected with M.tb than healthy individuals (Gilleron et al., 2004; Layton et al., 2018). Mycolipid-specific T cells have also been studied directly from the peripheral blood of individuals with active TB (Ulrichs et al., 2003).

iNKT cells and MAIT cells may contribute to protection from M.tb based on data derived from *in vitro* and *in vivo* models of TB. Patients with active TB have reduced levels of iNKT and MAIT cells in peripheral blood or bronchoalveolar lavage samples when compared to healthy donors and individuals with latent TB, suggesting that these cells home to the lung to mediate a protective immune response (Gold et al., 2010; Kee et al., 2012; Malka-Ruimy et al., 2019; Paquin-Proulx et al., 2018). In a murine model, pulmonary mycobacterial infection leads to recruitment of MAIT cells in the lung, and this was associated with reduced bacterial burden during infection (Sakala et al., 2015). While MAIT cells from this study exhibited diverse functional profiles, no particular functional profile was associated with reduction in disease burden (Sakala et al., 2015). iNKT cells can recognize infected macrophages and kill intracellular mycobacteria in a granulocyte-macrophage colony-stimulating factor (GM-CSF) dependent manner (Rothchild et al., 2014; Sada-Ovalle et al., 2008).

The role of mycolipid-specific T cells in mediating protection has been evaluated in two animal models. Guinea pigs immunized with purified or synthetic mycobacterial lipids showed reduced lung pathology upon subsequent challenge with M.tb (Dascher et al., 2003; Larrouy-Maumus et al., 2017). In a humanized CD1 transgenic mouse model, MA-specific T cells that were adoptively transferred trafficked to the lung during M.tb challenge and led to decreased bacterial burden in a CD1-dependent manner (Zhao et al., 2015). Interestingly, MA-specific T

cells were activated earlier in the course of M.tb infection than MHC class II-restricted T cells that recognized antigen 85B (Ag85B) (Zhao et al., 2015). MA-specific T cells isolated from the lung secreted TNF, IFN-γ, IL-2, and expressed CD107a, a surrogate marker of cytotoxic activity (Zhao et al., 2015). Taken together, these data suggest that mycolipid-specific T cells can provide protection from mycobacterial infection, given they efficiently traffic to the lung during the early stages of infection.

Here, we summarize the existing data that pertains to recognition of mycolipid antigens, including the factors that affect T cell activation, memory phenotype acquisition, and functional profiles. In addition, we highlight the research priorities and knowledge gaps addressed by studies discussed in this dissertation. We also provide context for the existing data with respect to a large body of literature examining T cells with adaptive or innate-like phenotypes. Our analysis suggests that mycolipid-specific T cells lie somewhere in the middle of this spectrum, which will influence how we leverage their unique biology to improve vaccines and diagnostics for TB.

1.2 Antigen Recognition by Mycolipid-specific T Cells

T cells recognize their cognate antigens through a heterodimeric surface protein known as a T cell receptor (TCR) (Murphy, 2017). To recognize the diverse suite of antigens presented to T cells, TCR diversity is generated as a result of genetic recombination of variable (V), diversity (D), and joining (J) gene segments, through a process known as VDJ recombination (Murphy, 2017). At the intersection of these gene segments, known as the complementarity determining region 3 (CDR3), nucleotides are stochastically added or subtracted to further enhance the diversity of TCRs (Murphy, 2017). TCRs recognize their cognate antigen through a highly specific

interaction between the TCR and the antigen-loaded antigen presenting molecule complex (Murphy, 2017). As a result of MHC polymorphism, MHC-restricted T cells exhibit diverse TCRs that are unlikely to be shared across individuals, even for a specific peptide antigen.

By contrast, the CD1 and MR1 antigen presentation systems are highly conserved across human populations (Han et al., 1999; Parra-Cuadrado et al., 2000). Thus, one defining feature of iNKT and MAIT cells is the expression of a semi-invariant TCR that is shared across genetically unrelated individuals. The canonical TCR that is expressed by iNKT cells includes an invariant TCR α chain that is comprised of a TRAV10/TRAJ18 gene rearrangement (Dellabona et al., 1994; Porcelli et al., 1993). The canonical TCR expressed by MAIT cells expresses a TCR α chain comprised of a TRAV1-2/TRAJ33,12,22 gene rearrangements (Gold et al., 2014; Lepore et al., 2014; Porcelli et al., 1993). While MHC-restricted T cells are typically activated by a single peptide antigen, iNKT and MAIT cells that express the canonical invariant TCR α chain have the ability to recognize multiple ligands. iNKT cells are defined by their recognition of α-galactosylceramide (α-GalCer), which is a potent and high affinity antigen (Kitamura et al., 1997; Sidobre et al., 2002). However, iNKT cells can also recognize a variety of other antigens presented by CD1d, such as lyso-phospholipids, glycosphingolipids, and sulfatides (Fox et al., 2009; Jahng et al., 2004; Kinjo et al., 2005; Zhou et al., 2004). The canonical ligand for MAIT cells is 5-(2-oxopropylideneamino)-6-D-ribitylaminouracil (5-OP-RU) presented by MR1, which is recognized with high affinity (Corbett et al., 2014; Kjer-Nielsen et al., 2012). MAIT cells can also recognize chemically diverse small molecules such as drugs, drug metabolites, and drug-like molecules (Keller et al., 2017).

The development of CD1b tetramers for GMM, SGLs, and MA have enabled the isolation of mycolipid-specific T cells to study the TCR repertoire and functional diversity directly *ex vivo*

(DeWitt et al., 2018; James et al., 2018; Kasmar et al., 2011; Van Rhijn et al., 2013, 2014, 2017). TCR diversity among T cells specific for mycolipids has been best studied using GMM as the model antigen. Like iNKT and MAIT cells, a subset of GMM-specific T cells present in genetically unrelated donors expresses a semi-invariant TCR. This TCR is termed the germline-encoded mycolyl-reactive (GEM) TCR and includes a conserved TCR α chain that consists of a TRAV1-2/TRAJ9 gene rearrangement (Van Rhijn et al., 2013). However, recent data suggest that GMM-specific T cells expressing this conserved TCR may actually constitute the minority of GMM-specific T cells, which have been shown to express a more diverse TCR repertoire (DeWitt et al., 2018; Van Rhijn et al., 2014). GMM-specific TCRs have also been shown to display varying levels of affinity and specificity for GMM. A GMM-specific T cell clone with a TCR that uses TRAV1-2 has a higher affinity for GMM-CD1b tetramer and expresses a similar but distinct cytokine profile than a T cell clone that does not use TRAV1-2 (Van Rhijn et al., 2014). Further, the GMM-specific T cell clone LDN5 displays such fine specificity that alterations to the sugar head group or lipid tail moieties distal to the head group can abrogate antigenicity (Moody et al., 1997). A different GMM-specific T cell clone expressing the semi-invariant TCR α chain was shown to recognize both GMM and MA, which lacks a sugar head group (Gras et al., 2016; Van Rhijn et al., 2013). The mechanism for this promiscuity is not fully understood but may relate to modulation of the CD1b surface by the embedded lipid tails (Chancellor et al., 2017). Future studies comparing TCR sequences may reveal whether a molecular or structural pattern is responsible for the TCR being permissive to multiple mycolate ligands.

Of note, NKT cells can also express diverse TCRs and are collectively referred to as Type II iNKT cells (Arrenberg et al., 2010; Dhodapkar and Kumar, 2017). Similarly, T cells that are restricted by MR1 can also express TCRs that do not contain the TRAV1-2 gene segment

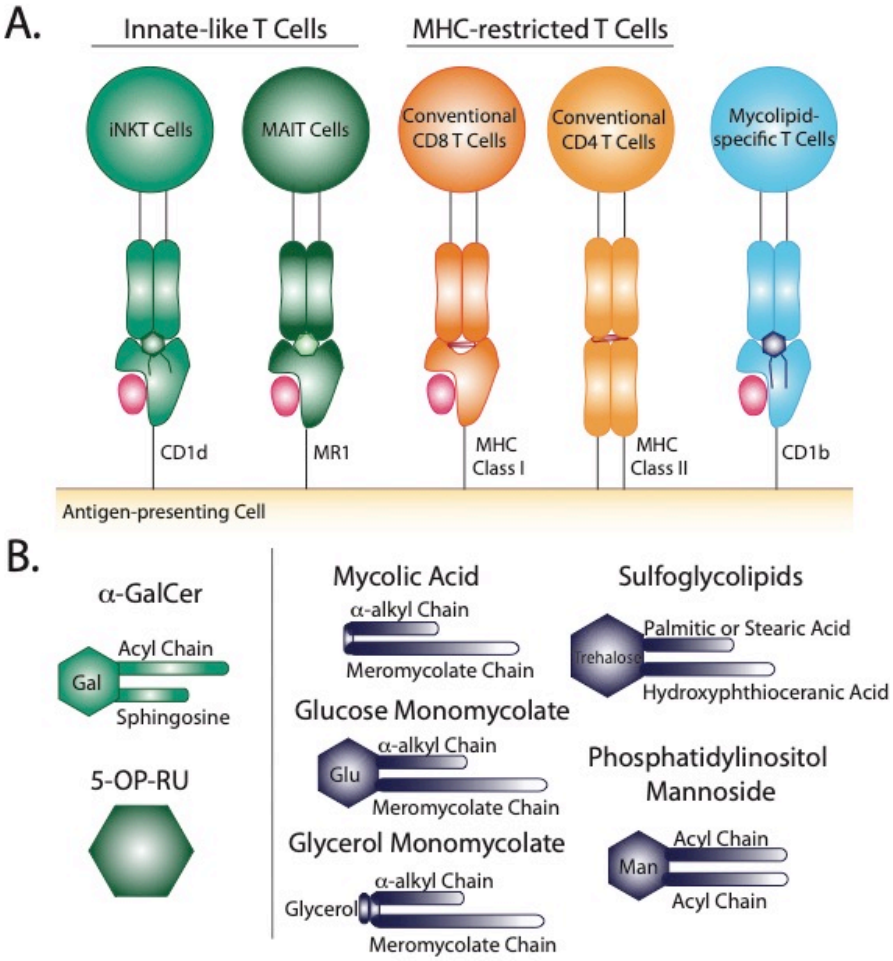

Figure 1.1. **T cell subsets that respond to M.tb infection and depiction of non-classical T cell antigens.**

(A). Graphical depiction of innate-like (green), MHC-restricted (orange), and mycolipid-specific T cells (blue). (B). Graphical depictions of canonical innate-like antigens or mycolipid antigens presented by CD1b. α-galactosyl ceramide (α-GalCer) is recognized by iNKT cells when presented by CD1d and is comprised of a galactose head group and a sphingosine and acyl chain. 5-(2-oxopropylideneamino)-6-D-ribitylaminouracil (5-OP-RU) is recognized by MAIT cells when presented by MR1. Mycolic acid is comprised of an α-alkyl and meromycolate chain. Glucose monomycolate and glycerol monomycolate are comprised of a mycolic acid base with a glucose and glycerol head group, respectively. Sulfoglycolipids are comprised of a sulfated trehalose headgroup and an hydroxyphthioceranic acid and palmitic acid or stearic acid chains. Phosphatidyl-*myo*-inositol mannoside is comprised of two acyl chains and two or more mannose residues as a headgroup.

(Lepore et al., 2017; Meermeier et al., 2016). This is similar to the pattern of GMM-specific TCR diversity that has been described above as some GMM-specific T cells express a semi-invariant TCR, but others exhibit diverse TCRs.

Thus, GMM-specific TCRs exhibit properties of both innate and adaptive T cells. On the one hand, they are characterized by diverse TCRs with varying affinity, but there is also a dominant and conserved semi-invariant TCR that is shared across individuals. While several mycolipid-restricted TCRs have been identified, we provide a further analysis of large numbers of T cells specific to Ac_2SGL to determine if common TCR genes or motifs are shared between T cells from unrelated donors. This is accomplished using targeted TCR sequencing of mycolipid-specific T cells. Further, antigenic determinants that affect antigen recognition by Ac_2SGL-specific T cells are investigated to further understand TCR promiscuity and specificity in this system.

1.3 Mycolipid-specific T cell Activation and Memory Phenotype

Naive MHC-restricted T cells are present at low frequency and require TCR ligation by their cognate antigen as well as additional stimulation by professional antigen presenting cells to become activated (Gonzalo et al., 2001; London et al., 2000; Schlienger et al., 2000). These T cells will then undergo a rapid expansion, up to 25-fold in 72 hours, and differentiate into effector T cells (Gudmundsdottir et al., 1999). Upon clearance of antigen, the effector T cell population will then contract and form long-lived memory T cells that have enhanced proliferative potential and more rapid activation and cytokine production upon subsequent encounter with antigen (Rogers et al., 2000).

By contrast, iNKT and MAIT cells do not necessarily require cognate recognition of antigen to be activated in the periphery, and they acquire their effector memory phenotype during

development, as described above. For example, bacterial infection and toll-like receptor (TLR) agonists can induce interferon (IFN-)γ production in MAIT cells, through an IL-12- and IL-18-dependent mechanism (Ussher et al., 2014). It was also shown that MAIT cells derived from human peripheral blood produce IFN-γ and tumor necrosis factor (TNF) when stimulated with IL-12, IL-15, and IL-18 (Slichter et al., 2016). Further, TCR signaling is not sufficient for MAIT cell activation in the absence of these inflammatory signals (Slichter et al., 2016). iNKT cells express high levels of IL-12 receptor, and IFN-γ production during *in vitro* stimulation is dependent on IL-12 signaling (Brigl et al., 2011). In the absence of activation, iNKT and MAIT cells are present at high frequency, comprising up to 1% and 10% of circulating T cells, respectively (Gherardin et al., 2018; Lee et al., 2002b; Montoya et al., 2007). However, they have an impaired proliferative potential compared to MHC-restricted T cells after stimulation (Gutierrez-Arcelus et al., 2019).

It is unknown what factors are required for activation of naive mycolipid-specific T cells. Mycolipid-specific T cells are found at a higher frequency in individuals with documented exposure to mycobacteria, suggesting prior antigen exposure drives activation and proliferation (Gilleron et al., 2004; Layton et al., 2018). There is evidence that immunization of cattle with GMM produces GMM-specific T cells with enhanced proliferative potential, also suggesting that exposure to antigen can lead to activation and enhanced recall responses (Nguyen et al., 2009). In addition, a study of *ex vivo* GMM-specific T cells showed that over 80% of this population expresses CD45RO, further suggesting that they are antigen experienced (Kasprowicz et al., 2016).

The proportion of different memory subsets found in antigen-experienced individuals is currently unknown, and whether antigen experience is required for memory phenotype acquisition also remains to be determined (Table 1.1). This could be comprehensively examined by looking at the memory phenotype of mycolipid-specific T cells using CD1 tetramers cohort studies. Other

metrics of T cell memory should also be investigated, such as clonal expansion, using *ex vivo* TCR profiling in antigen-exposed individuals. Finally, it is unknown whether mycolipid-specific T cells can be activated in a cytokine-driven and TCR-independent manner (Table 1.1). This could be investigated using *in vitro* activation studies such as IFN-γ secretion or activation marker upregulation (e.g., CD69) as assessed by flow cytometry.

1.4 MYCOLIPID-SPECIFIC T CELL FUNCTION

The phenotypes of MHC-restricted T cells are broadly dictated by the inflammatory environment, TCR co-receptor expression, and TCR affinity (Zhu et al., 2010). Largely, these functional categories are pro-inflammatory (Th1, Th2, and Th17), cytotoxic, or regulatory (Treg). The pro-inflammatory subsets are regulated by the transcription factors T-bet, GATA3, and ROR-γt, respectively (Ivanov et al., 2006; Szabo et al., 2000; Zhen and Flavell, 1997). Regulatory T cells are regulated by the transcription factor FOXP3 (Fontenot et al., 2003; Hori et al., 2003). However, there is evidence that MHC-restricted T cells exhibit functional plasticity and can alter their functional program over the course of the T cell's life-span (Sallusto et al., 2018).

iNKT cells are largely characterized by constitutive IFN-γ expression and IL-4 production, a phenotype not commonly exhibited by MHC-restricted T cells (Coquet et al., 2008; Gumperz et al., 2002). MAIT cells are capable of secreting a variety of cytokines, such as IL-17, IFN-γ, IL-2 and TNF (Gherardin et al., 2018). The functional subsets of iNKT and MAIT cells are largely defined by the magnitude of PLZF expression and the expression of the master transcription factors that define MHC-restricted T cell functional subsets (Coquet et al., 2008; Lee et al., 2013; Rahimpour et al., 2015). However, no Th2 equivalent has been identified for MAIT cells (Garner et al., 2018; Rahimpour et al., 2015).

Most of the data regarding mycolipid-specific T cells have been obtained through studies of *in vitro*-derived T cell clones, which have been shown to express IFN-γ, TNF, and IL-17, as well as lyse M.tb-infected cells and control M.tb replication *in vitro* (Busch et al., 2016; Gilleron et al., 2004; Moody et al., 1997; Sieling et al., 2000; Van Rhijn et al., 2013; Zhao et al., 2015). T cells with different affinities for GMM-loaded CD1b tetramers have been shown to have different functional capabilities. The high affinity GMM-specific T cells expressed high levels of Th1 cytokines, whereas the lower affinity T cells expressed Th1 cytokines along with IL-17 (Van Rhijn et al., 2014). The most comprehensive study performed on cells stimulated directly *ex vivo* showed that $CD4^+$ mycolipid-specific T cells secrete IFN-γ, TNF, IL-2, and IL-17 in polyfunctional combinations (Seshadri et al., 2015). Notably, different lipid antigens yielded unique functional profiles with GMM-specific T cells being the most polyfunctional, while GroMM-specific T cells largely expressed IL-2 alone (Seshadri et al., 2015).

The factors that dictate mycolipid-specific T cell function are not understood. Here, we investigate the role of various factors that affect peptide-specific T cell affinity on mycolipid-specific T cell function. In addition, whether mycolipid-specific T cells can be categorized into traditional T-helper lineages based on expression of canonical transcription factors is currently unknown. These questions can be investigated in human cohorts using tetramers to isolate antigen-specific T cells from peripheral blood mononuclear cells (PBMC) and profiling transcription factor and cytokine expression through targeted gene expression analysis.

In summary, several factors suggest that mycolipid-specific T cells may be more like MHC-restricted T cells than iNKT or MAIT cells in their functional qualities (Figure 1.2). These include a low precursor frequency, increased frequency in mycobacteria-infected individuals, lack of PLZF expression, and the preliminary evidence of antigen-dependent activation, proliferation,

Table 1.1. Summary of properties exhibited by innate-like, MHC-restricted, and mycolipid-specific T cells.

Topic	Innate-like T Cells	MHC-restricted T Cells	Mycolipid-specific T Cells
TCR Diversity	Semi-Invariant	Highly Diverse	Semi-Invariant Highly Diverse
TCR Promiscuity	Yes	No	Yes
Activation Requirements	TCR dependent and independent	TCR dependent	TCR dependent?
Memory Phenotype	Acquired during development	Acquired after development	Unknown
Functional Profiles	Th1, Th17	CD4 (Th1, Th2, Th17) CD8 (CTL)	Th1 and CTL, some Th17

Table 1.1. Summary of properties exhibited by innate-like, MHC-restricted, and mycolipid-specific T cells. This table compares the major aspects of T cell biology between innate-like T cells, MHC-restricted T cells, and mycolipid-specific T cells. TCR diversity is evaluated by conservation of TCR sequences across genetically unrelated donors. TCR promiscuity is defined as the ability of the same TCR to recognize several chemically unrelated ligands. The activation requirements for T cell subsets are described as the reliance on TCR ligation for T cell activation. As all three T cell subsets have been shown to exhibit T cell memory in some capacity, we summarized the differences between memory phenotype as acquisition during or after T cell development. Lastly, the functional profiles for these subsets are summarized as the major functional profiles that have been described for T cells in each subset. These are summarized using the designations for the T-helper subsets or cytotoxic T lymphocytes (CTL).

and memory phenotype acquisition. However, some studies have shown that a subset of mycolipid-specific T cells exhibit innate-like qualities as well, such as expression of a semi-invariant TCR and promiscuous ligand recognition. On the whole, mycolipid-specific T cells have qualities of both innate-like and MHC-restricted T cells and exist on a spectrum of "innateness" (Figure 1.2).

1.5 Central Question

Thus, the central question this work aims to further the literature summarized above by elucidating the molecular and cellular mechanisms that affect lipid antigens are recognized by T cells, and what impact these factors have on T cell activation and function. This work is focused on the mycobacterial lipid antigen Ac_2SGL, using our understanding of peptide-specific, innate-like, and GMM-specific T cell biology to contextualize our findings. As Ac_2SGL holds promise as a target for novel vaccination and diagnostic strategies for M.tb due to the hypothetical lack of sensitization to this antigen by BCG-vaccinated individuals, these studies will inform the development of tools to address these two major needs.

The first aim of this work utilizes novel synthetic Ac_2SGL analogs to probe the specificity with which this antigen is recognized by T cells and to inform which molecular moieties are essential for recognition by Ac_2SGL-specific T cells. This work also validates a Ac_2SGL-loaded CD1b tetramer that can now be used in large-scale clinical studies to further elucidate the role(s) this T cell population may exhibit during M.tb infection. The second aim is to understand the factors that can affect antigen affinity at the cellular level, as this measure influences the magnitude of activation and functional differentiation of T cell responses during infection and vaccination. In this work, we highlight the role of TCR co-receptors in augmenting T cell affinity for Ac_2SGL

and the subsequent impact on T cell function in *in vitro* and *ex vivo* studies. Together, these studies inform how Ac_2SGL-specific T cells can be leveraged in novel diagnostic and vaccination strategies for TB.

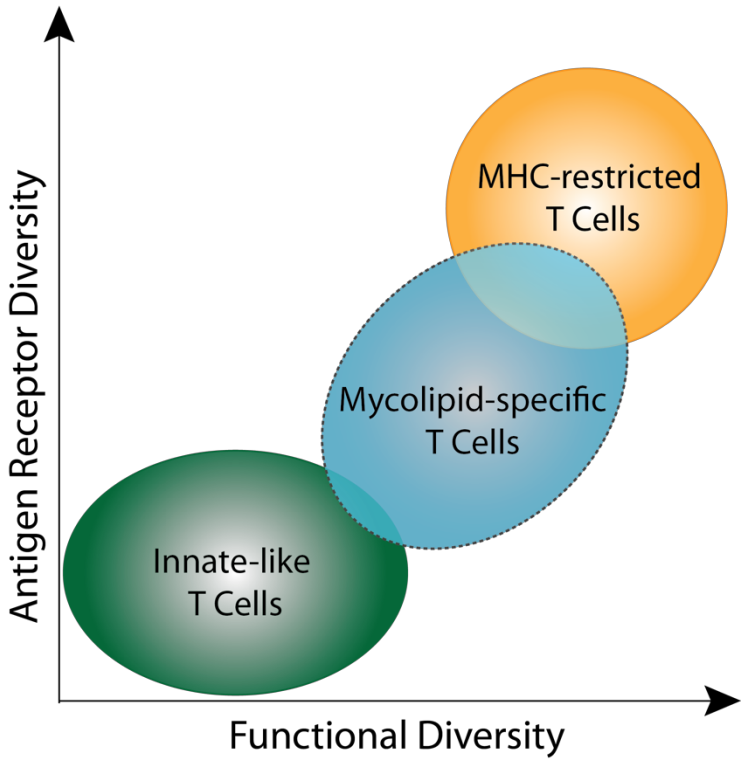

Figure 1.2. **Comparison of innate-like, MHC-restricted, and mycolipid-specific T cells.**
Summary of the key determinants of T cell "innateness." Innate-like T cells (green) have low antigen receptor diversity and fewer functional subsets. Peptide-specific T cells (orange) exhibit high antigen receptor diversity and higher functional diversity and plasticity. Mycolipid-specific T cells (blue) have qualities that overlap with both innate-like and MHC-restricted T cells, but are functionally more similar to MHC-restricted T cells.

Chapter 2. MOLECULAR FACTORS THAT AFFECT MYCOBACTERIAL GLYCOLIPID RECOGNITION BY HUMAN T CELLS

Adapted from: James CA*, Yu KKQ*, et al. (2018). CD1b Tetramers Identify T Cells that Recognize Natural and Synthetic Diacylated Sulfoglycolipids from *Mycobacterium tuberculosis*. *Cell Chemical Biology*. 25(4):392–402.e14. doi:10.1016/j.chembiol.2018.01.006
*These authors contributed equally to this work.

Methods section adapted from: Yu KKQ, Wilburn DB, Hackney JA, Darrah PA, Foulds KE, James CA, et al. (2019). Conservation of molecular and cellular phenotypes of invariant NKT cells between humans and non-human primates. *Immunogenetics*. 71:465–478. doi:/10.1007/s00251-019-01118-9

2.1 INTRODUCTION

Sulfoglycolipids (SGLs) are a family of cell wall lipids found only in M.tb that consist of a sulfotrehalose core with up to four acyl chains that differ in length and composition (Goren, 1970). Among the acylations there is typically a phthioceranic or hydroxyphthioceranic acid with multiple methyl groups (Goren et al., 1971; Layre et al., 2011a). SGLs were first described in virulent M.tb, and SGL synthesis is regulated by PhoP, a transcription factor expressed by M.tb that has a well-established role as a virulence factor (Chesne-Seck et al., 2008; Goren, 1970; Lee et al., 2008). One possible mechanism for the role that SGL plays as a virulence factor is that guinea pigs that are infected with an M.tb strain that is unable to synthesize sulfolipid-1 (SL-1) do not exhibit cough reflexes while infected, and SL-1 directly interacts with nociceptive neurons, such as the ones that innervate the lung and initiate coughs (Ruhl et al., 2020).

Additional studies allowed identification and characterization of a family of SGLs (acylated trehalose 2'-sulphate) that were detectable only in M.tb and SGL levels correlated with

the relative virulence in guinea pigs (Goren et al., 1974). Presence of SGL in virulent bacteria, but not in environmental strains or vaccine strains, is also supported by lipidomic profiling of the cell wall of M.tb and the *M. bovis* BCG vaccine strain (Layre et al., 2011b). The preferential expression of SGLs by pathogenic M.tb strains suggests that SGL-specific T cells could be harnessed to develop novel lipid-based strategies for specifically diagnosing or treating tuberculosis.

Diacylated SGL (Ac_2SGL) is one of only eight cell wall lipids from M.tb that have been identified as CD1-presented antigens for human T cells (Beckman et al., 1994; Gilleron et al., 2004; Layre et al., 2009; Moody, 1997; Sieling et al., 1995). Proof-of-principle that Ac_2SGL is presented by CD1b to T cells was obtained using two *in vitro* derived T cell clones named Z4B27 and Z4A26 derived from a healthy donor with latent M.tb infection (Gilleron et al., 2004). In addition, recall responses to Ac_2SGL by primary lymphocytes isolated from patients depends on prior exposure to M.tb but is not affected by a history of vaccination with BCG (Gilleron et al., 2004). This is in contrast to the tuberculin skin test (TST), which is commonly used to diagnose M.tb infection in humans but is limited by false positive responses in BCG-vaccinated populations (Farhat et al., 2006). Further translational work on Ac_2SGL-specific T cells has been hampered for two main reasons. First, Ac_2SGLs exist at low abundance in the M.tb cell wall, so purifying a sufficient quantity to perform a large-scale clinical study is economically and logistically prohibitive. Characteristic markers for SGL-specific T cells other than an antigen-specific T cell receptor (TCR) are not known, so there are no tools to facilitate their identification in *ex vivo* blood or tissue samples.

Synthetic analogs of Ac_2SGL have been reported previously, and their biological potency compared to the natural compounds has been assessed using Z4B27 and Z4A26 T cell clones (Gau et al., 2013; Guiard et al., 2008, 2009). These data have revealed that the presence of a hydroxyl

group, the number of C-methyl substituents on the acyl chains, the configuration of the chiral centers, and the respective localization of the two different acyl chains on the sugar moiety govern TCR recognition and T cell activation (Guiard et al., 2009). Comparing C16, C24, and C32 long chain tri-methylated fatty acids revealed increased stimulatory capacity of analogs with the longer alkyl chain lengths (Gau et al., 2013). These findings were supported by a crystal structure which showed that part of the Ac_2SGL lipid tail is exposed to the solvent above the binding plane, explaining why the methyl groups on the tail of the lipid are important for antigenicity (Garcia-Alles et al., 2011).

Here, we utilized a novel analog of a naturally occurring Ac_2SGL that can be generated in large quantities. This analog contains hydroxyphthioceranic acid, which is a key antigenic determinant of Ac_2SGL. We used this analog to generate a fluorescent probe, called a tetramer, to study antigen-specific T cells. CD1b-Ac_2SGL tetramers are multimers of CD1 proteins that are fluorescently labeled and loaded with Ac_2SGL that bind polyclonal T cells even when present in low numbers of total blood cells. This powerful technique can be used to detect antigen specific T cells in patients, isolate T cell clones of interest, or investigate T cell fine specificity for structurally related antigens. We used CD1b tetramers loaded with natural and synthetic versions of Ac_2SGL antigens and used these reagents to study human Ac_2SGL-specific T cells. Our data reveal the fine specificity of human T cells for Ac_2SGL for fully saturated antigens, and highlight the antigenic importance of hydroxyphthioceranic acid. In the four T cell clones analyzed here, our data show an important lack of cross-reactivity between structurally related antigens.

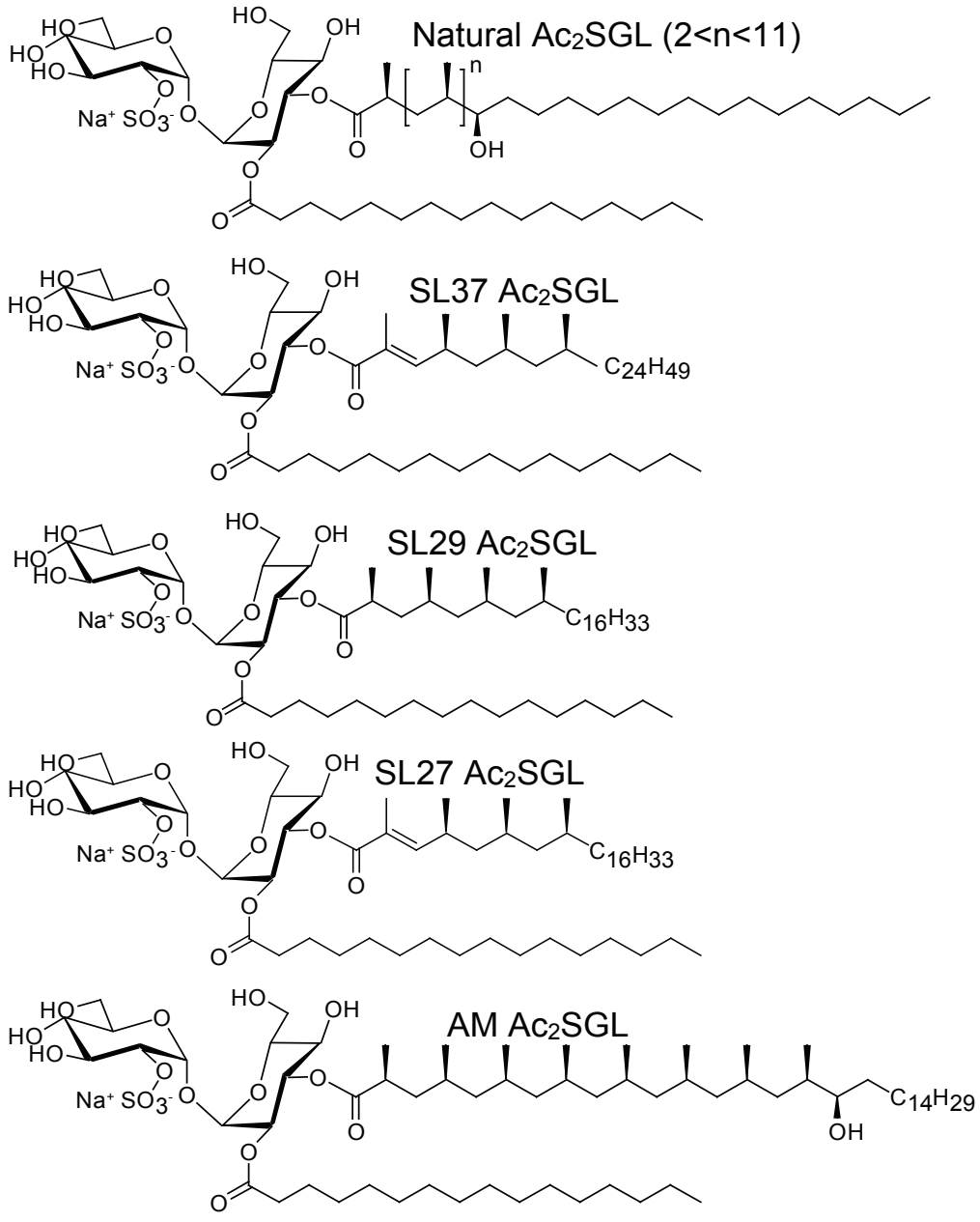

Figure 2.1. Structure of diacylated sulfoglycolipids and their analogs.

Structures of natural Ac_2SGL purified from M.tb and four synthetic forms that have been previously described: SL37 Ac_2SGL, SL27 Ac_2SGL, SL29 Ac_2SGL, AM Ac_2SGL.

2.2 STRUCTURES OF SULFOGLYCOLIPID ANALOGS

Ac_2SGL purified from M.tb (referred to as natural Ac_2SGL) is a family of molecules containing a sulfotrehalose core, which is diacylated with a phthioceranoyl or a hydroxyphthioceranoyl group at the 3 position and a palmitoyl or stearoyl group at the 2 position (Goren et al., 1971; Layre, Paepe, et al., 2011). The hydroxyphthioceranoyl group varies in alkyl chain length (C22-C42) and in the number of methyl groups, ranging from 2 to 11 (Layre, Paepe, et al., 2011). The combined effect of positional, chain length, and methylation variants leads to thousands of known molecular SGL variants cataloged in the MycoMass database and other sources (Layre, Sweet, et al., 2011; Sartain et al., 2011). Four different analogs differing only in the structure of the alkyl chain in position 3 of the sulfotrehalose core were used in this study (Figure 2.1).

The first molecule has a sulfotrehalose core with a palmitoyl and a tetramethylated unsaturated fatty acid (compound 21c of reference (Gau et al., 2013)), which we will refer to as SL37 Ac_2SGL (Fig. 2.1). Two additional compounds, SL27 (SGL12 of reference (Guiard et al., 2009)) and SL29 Ac_2SGL (SGL8 of reference (Guiard et al., 2009)), have the same sulfotrehalose core with a palmitic acid linked as in SL37 Ac_2SGL, but the tetramethylated fatty acid is eight carbons shorter. SL27 Ac_2SGL is further distinguished from SL29 due to the unsaturation on the first methyl group in the chain (Fig 2.1). The fourth molecule, called AM Ac_2SGL exactly mimics the structure of one of the compounds in the natural Ac_2SGL mixture.

2.3 Derivation of Sulfoglycolipid-specific T Cell Lines

We next used natural and synthetic Ac_2SGL preparations to generate CD1b-Ac_2SGL tetramers that enabled us to sort and expand T cells specific for these lipid antigens. Based on a long term goal of detecting SGL-specific T cells in large cohorts of tuberculosis patients, we first generated CD1b tetramers loaded with natural Ac_2SGL by adapting our recently published method for generating human CD1b tetramers (Kasmar et al., 2011).

Subsequently, peripheral blood mononuclear cells (PBMC) from a subject with latent tuberculosis were stained with the tetramer along with markers to label T cells and cell viability (Figure 2.2.A, left). Even though we did not yet confirm that the tetramers were sufficiently loaded, we detected a rare population (0.008%) of T cells that stained with CD1b-natural Ac_2SGL tetramer. These T cells were sorted and expanded *in vitro*. We named the resulting T cell line A01 and noted that 64% of A01 T cells stained with CD1b-natural Ac_2SGL tetramer (Figure 2.2.A, center). These results suggest stable loading of CD1b with natural Ac_2SGL. We used an antibody against the CD4 co-receptor to discover that the majority of Ac_2SGL-specific T cells within the A01 T cell line did not express CD4 (Figure 2.2.A, right). These results are in contrast to mycobacterial glucose monomycolate (GMM)-specific T cells, which commonly express CD4 (Kasmar et al., 2011; Van Rhijn et al., 2013). We generated another T cell line (A05) specific for natural Ac_2SGL by first stimulating PBMC with the antigen in the presence of monocyte-derived dendritic cells and subsequently sorted using CD1b-natural Ac_2SGL tetramer (Figure 2.2.B, left).

We noted that 92% of A05 T cells stained with CD1b-natural Ac_2SGL tetramer (Figure 2.2.B, center) and predominantly express the CD4 co-receptor (Figure 2B, right). Further, we generated SL37 Ac_2SGL-loaded CD1b tetramers and isolated SL37 Ac_2SGL-specific T cells from two additional subjects with latent tuberculosis to create two additional T cell lines, named 56SL37

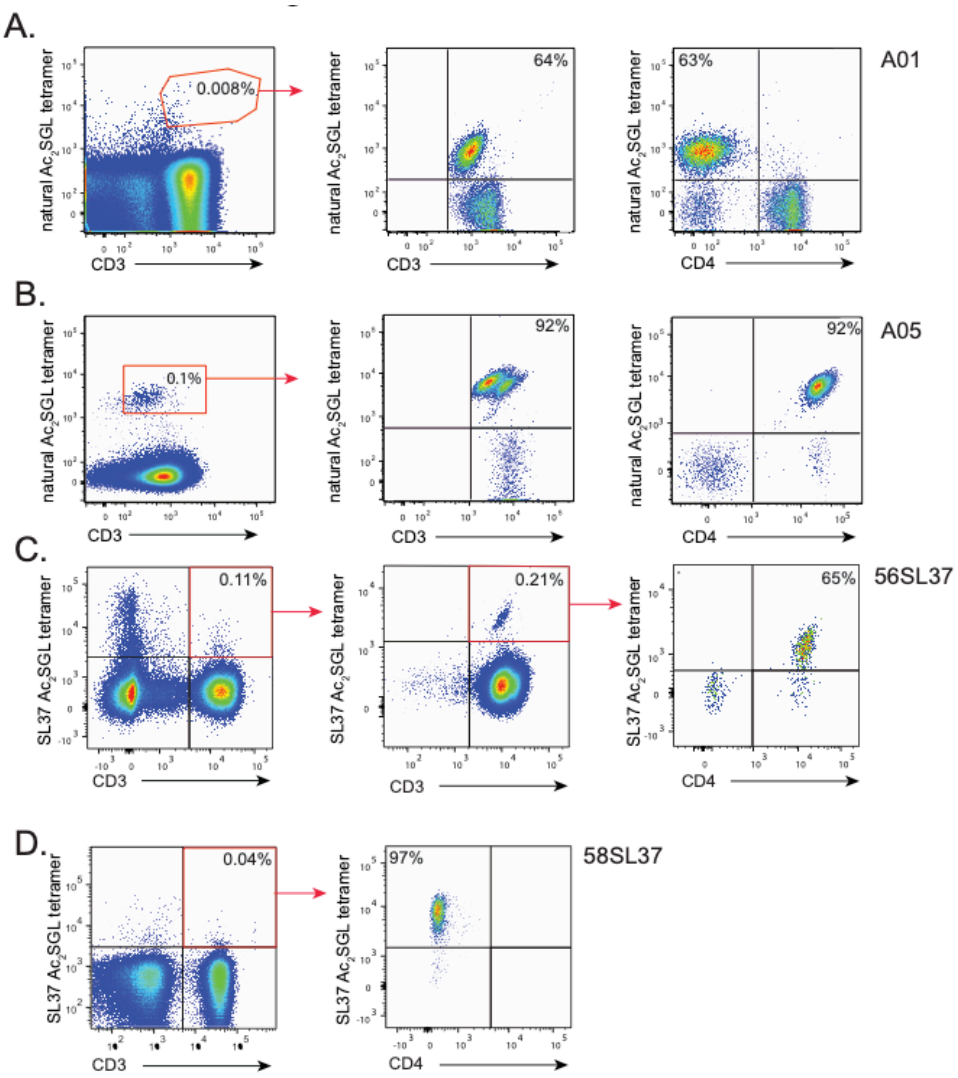

Figure 2.2. Generation of Ac_2SGL-specific T cell clones.
T cell lines were generated from peripheral blood mononuclear cells (PBMC) by sorting rare T cells that bound to Ac_2SGL-loaded tetramers followed by *in vitro* expansion. Specificity of the resulting T cell lines was confirmed by staining with the same tetramer used in the sort and reveal greater than 100-fold enrichment of antigen-specific T cells. CD4 co-receptor expression was also examined using a specific antibody. (A) A01 T cell line lacks CD4 expression and was created after two rounds of *in vitro* expansion after sorting with natural Ac_2SGL-loaded tetramers (red polygon). (B) A05 T cell line expresses CD4 and was generated by first stimulating PBMC with natural Ac_2SGL in the presence of monocyte-derived dendritic cells and sorting with natural Ac_2SGL tetramer following *in vitro* expansion (red box) (C) 56SL37 T cell line expresses CD4 and was created after multiple round of *in vitro* expansion and re-sorting using SL37 Ac_2SGL-loaded tetramers (red box). (D) 58SL37 T cell line generated in a manner similar to 56SL37 but lacks CD4 expression. Sorting data are representative of a single experiment, but tetramer staining of T cell lines was confirmed in two or more experiments.

and 58SL37, one from each subject. We noted that these two T cell lines differed with respect to the expression of the CD4 co-receptor (Figures 2.2.C and 2.2.D). These results validate CD1b tetramers loaded with natural Ac_2SGL or SL37 Ac_2SGL and describe four new SGL-specific T cell lines.

2.4 Activation of Ac_2SGL-specific T cell Lines by Sulfoglycolipid Analogs

We then explored the reactivity of the newly derived T cell lines to natural and synthetic SGLs. We noted that natural Ac_2SGL and AM Ac_2SGL stimulated A01 with half-maximal effective concentration (EC_{50}) of 0.04 μg/ml and 0.006 μg/ml respectively in an IFN-γ ELISPOT assay (Figure 2.3.A). Similarly, AM Ac_2SGL is a potent antigen for A05, with an estimated EC_{50} value of 0.0006 μg/ml (Figure 2.3.A). However, SL37 Ac_2SGL was a much less potent antigen for both A01 and A05, with an average EC_{50} of 0.11 μg/ml. In addition, SL27 Ac_2SGL, which has a shorter methylated carbon chain than SL37 Ac_2SGL, had an average EC_{50} of 0.01 μg/ml, while SL29 Ac_2SGL, which lacks the unsaturation in methylated carbon chain, has an EC_{50} of 0.009 μg/ml, similar to that of AM Ac_2SGL (Figure 2.3.B). Collectively, the low EC_{50} estimates using AM Ac_2SGL and SL29 Ac_2SGL to activate both the A01 and A05 T cell lines demonstrate the importance of using fully saturated analogs similar to that present in natural Ac_2SGL to induce strong activation of the T cells. Further, these data suggest that the extra methylations and hydroxyl group present in AM Ac_2SGL and lacking in SL29 Ac_2SGL are not required to reproduce the activity of the native mixture (Figure 2.1.A).

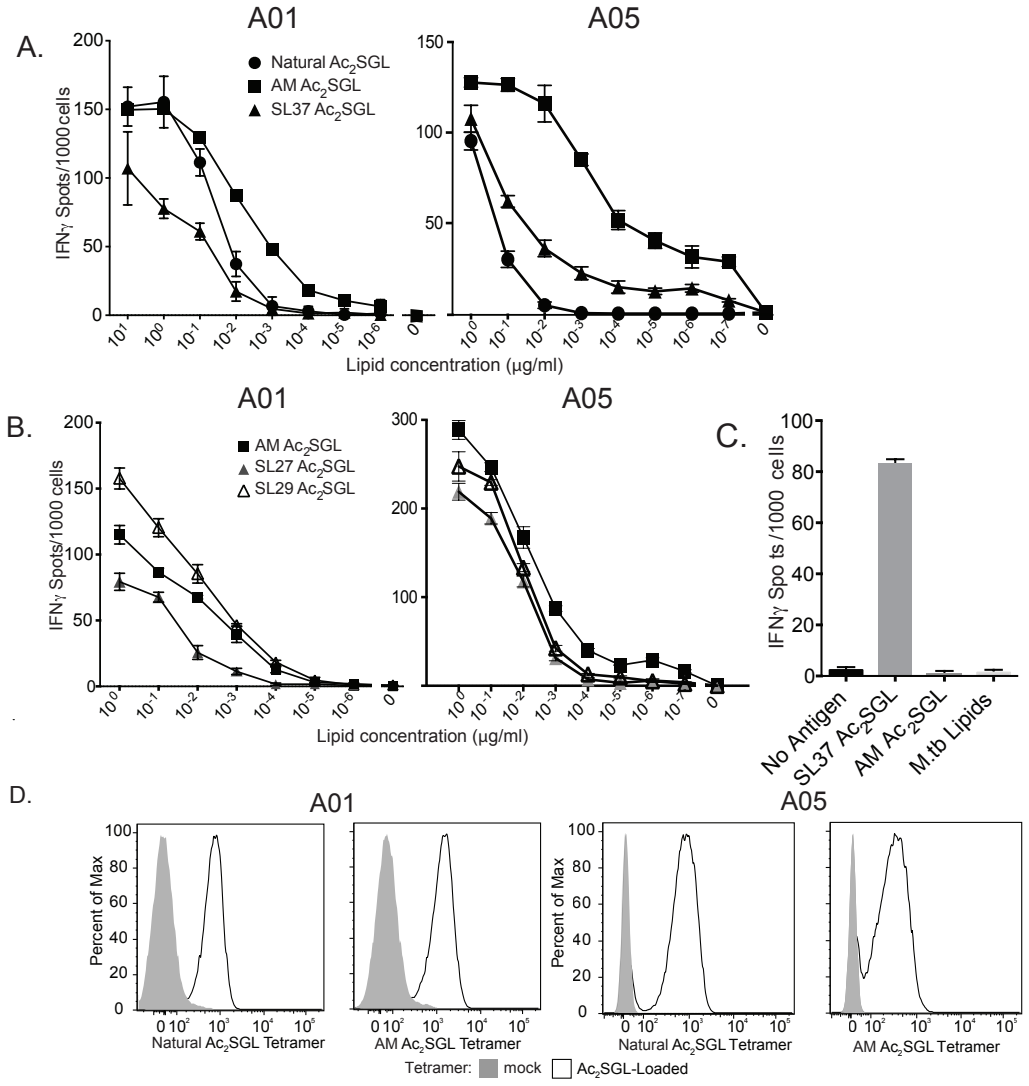

Figure 2.3. **Fine specificity of Ac_2SGL-specific T cell clones.**

(A) IFN-γ production by A01 and A05 in response to titrating amounts of natural Ac_2SGL, AM Ac_2SGL, and SL37 Ac_2SGL as measured by an IFN-γ ELISPOT. (B) IFN-γ production by A01 and A05 in response to titrating amounts of AM Ac_2SGL, SL29 Ac_2SGL, and SL27 Ac_2SGL as measured by an IFN-γ ELISPOT. (C) IFN-γ production by C56SL37 in response to 5 μg/ml SL37 Ac_2SGL, AM Ac_2SGL, or whole mycobacterial lipid extract. T cell clone activation was blocked using the anti-CD1b antibody BCD1b.3 (10 μg/ml). (D) A01(left) and A05 (right) was stained with mock loaded CD1b tetramer (shaded histogram) or CD1b loaded with either natural or AM Ac_2SGL (open histograms). Data are representative of two or three independent experiments. Error bars represent standard deviation of triplicate wells in an ELISPOT assay.

The T cell lines C56SL37 and C58SL37, which were derived using SL37 Ac_2SGL-loaded tetramers, were activated by SL37 Ac_2SGL as expected, and this was blocked by anti-CD1b (Figure 3C and data not shown). However, neither AM Ac_2SGL nor M.tb lipid extract containing natural Ac_2SGL were stimulatory for C56SL37 and C58SL37. Because the three Ac_2SGL variants tested here share an identical sulfated trehalose head group and 2-palmitoylation, the data confirm that T cells display specificity for the acylation at the 3 position of the Ac_2SGL synthetic analogs (Gau et al., 2013; Guiard et al., 2009). Finally, we stained A01 using CD1b tetramers treated with natural Ac_2SGL or AM Ac_2SGL to validate its ability to recognize each lipid variant. Tetramers treated with natural Ac_2SGL or the synthetic analog AM Ac_2SGL stained equivalently sized populations of the A01 and A05 T cell lines (Figure 2.3.D). Together, these data suggest that AM Ac_2SGL and SL29 Ac_2SGL are bio-equivalent to natural Ac_2SGL (Figure 2.1).

2.5 Effect of CD1b Point Mutations on Ac_2SGL Antigen Recognition

Next, we asked whether mutations in the CD1b binding surface would influence recognition of Ac_2SGLs. We generated a library of mutations in the $\alpha1$ and $\alpha2$ domains of CD1b to selectively modify the surface available for contacting the TCR (Figure 2.4.A). The mutations are not predicted to change the antigen-binding cleft. C1R cells were transduced with the mutant CD1b constructs and used as antigen presenting cells for T cells. Importantly, all of these transfectants expressed similar levels of CD1b at the cell surface (Figure 2.4.B). We examined the effect of each of these mutations on activation of A01 and A05 T cell lines in response to AM Ac_2SGL. Amino acid D83 markedly reduced activation of both A01 and A05 T cell lines (Figure

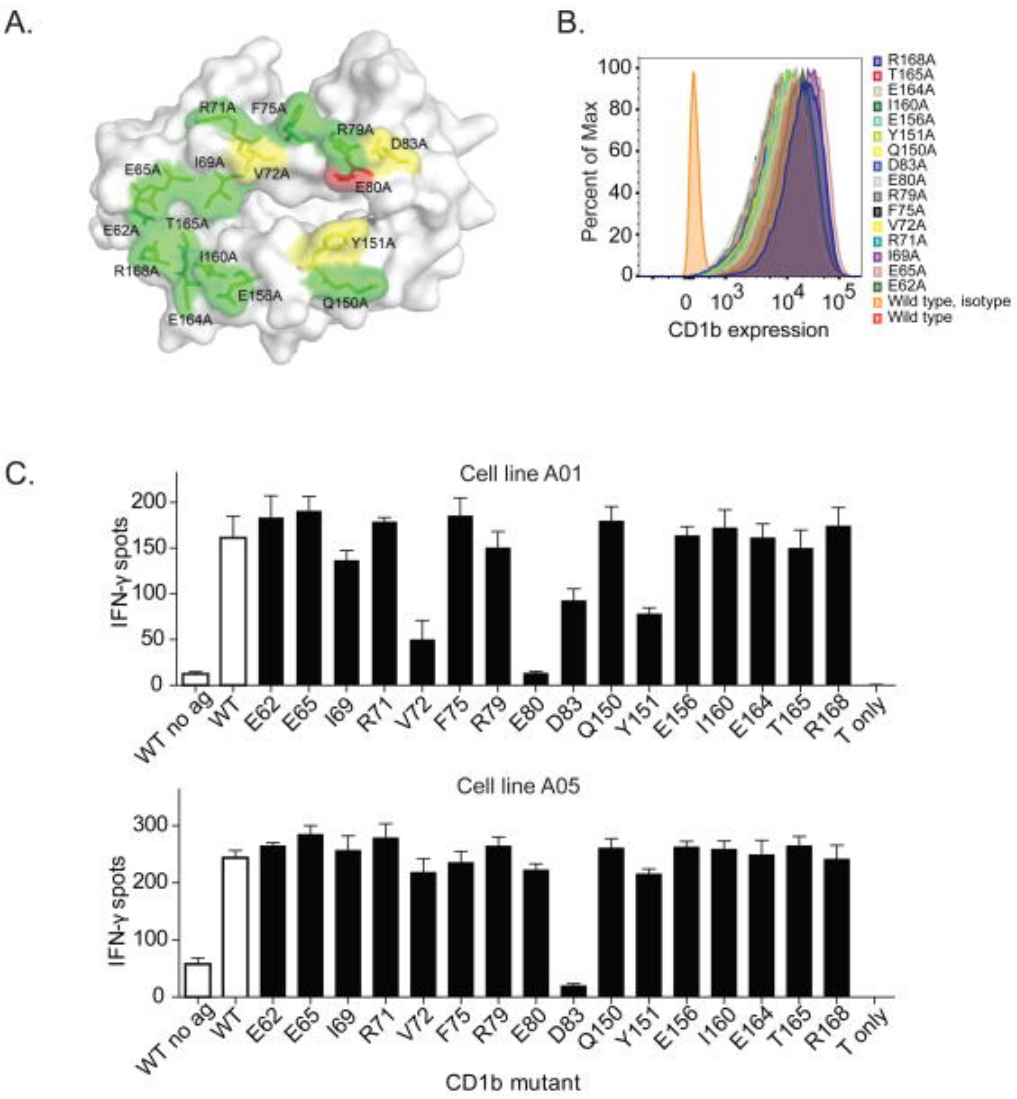

Figure 2.4. **Effect of CD1b point mutations on Ac_2SGL antigen recognition.**

(A) Location of CD1b point mutations in stably transfected C1R cells. The figure is based on PDB entry 1GZP (Gadola et al., 2002). Substitutions at residues colored green did not show an effect on A01 T cell activation, while residues colored yellow showed moderate inhibition, and residues colored red showed complete inhibition (B) Expression of CD1b by each of the transfected C1R cells. Isotype indicates staining with an isotype control antibody. (C) IFN-γ production by A05 and A01 T cell clones in the presence of AM Ac_2SGL and transfected C1R cells. WT = wild type. Controls are shown as white bars and CD1b mutants are shown as black bars. Data are representative of three independent experiments with triplicate wells. Error bars represent SEM of triplicate wells. Work was completed in collaboration with Michael NT Souter, Dale I Godfrey, and Daniel G. Pellici (Department of Microbiology and Immunology, University of Melbourne, Melbourne, Australia).

2.4.C). Additionally, we noted that amino acids Y151, E80, and V72, which are located near the center of the CD1b platform near the site of the expected SGL headgroup protrusion, significantly abrogated T cell activation of the A01 but had more modest effects on A05 (Figure 2.4.C). These data emphasize the critical nature of centrally located residues in both the α1 and α2 domains of CD1b on T cell recognition of SGLs (Garcia-Alles et al., 2011).

2.6 Synthetic Ac_2SGL Analogs are Recognized by Diverse T Cell Receptors

Finally, we used commercial immunosequencing or single-cell multiplex PCR to obtain the sequences for the TCR α and β chain of A01, A05, C56SL37, and C58SL37. We further confirmed the TCR sequence by staining all four lines with the predicted anti-TCR Vβ antibody (data not shown). We found no overlap in dominant TCR sequences among the four lines (Table 2.1). Unlike recent results with mycobacterial GMM-reactive clones, this survey of four Ac_2SGL-specific TCRs failed to demonstrate conservation of TCRs that bind antigens with identical head groups but differ in the composition of only one of two lipid tails.

To test whether the TCR alone is sufficient to convey antigen specificity, we transduced Jurkat 76 cells that lack CD4 and CD8 co-receptor molecules with the dominant C58SL37, A01, and A05 TCR α and β chain, and isolated clones using limiting dilution. We tested TCR-transduced C58SL37 clones that stained with SL37 Ac_2SGL-loaded tetramers, but not with mock loaded tetramers (Figure 2.5.A). These data confirm the identity of the dominant clone within the C58SLS37 T cell line. We then tested one A01 and A05 clone that stained with AM Ac_2SGL-loaded tetramer, but not with mock loaded tetramer (Figure 2.5.C). Stimulation with CD1b-transfected, but not CD1a-transfected antigen presenting cells, activated TCR-transduced cells in

the presence but not in the absence of SL37 Ac_2SGL (Figure 2.5.B). Further, the A01 and A05 clones produced IFN-γ when stimulated with K562 cells transfected with CD1b and AM Ac_2SGL, but produced no IFN-γ in the absence of antigen (Figure 2.5.D). Together, these data reveal that TCR interaction with CD1b and SGL antigen is sufficient to mediate T cell activation, and that diverse T cell receptors are capable of recognizing Ac_2SGLs.

Table 2.2. TCRs expressed by Ac_2SGL-specific T Cell Lines

T cell receptor gene usage, CDR3 region amino acid sequence, of Ac_2SGL and SL37 specific T cell clones. Variable and joining gene segment names were assigned using the International ImMunoGeneTics (IMGT) Database.

Clone	TCR	Variable	CDR3	Joining
A01	α	TRAV8-6	CAVKAGYSSASKIIF	TRAJ3
	β	TRBV12-4	CASKGKQGPEQFF	TRBJ2-1
A05	α	TRAV13-2	CAEVLGGTSYGKLTF	TRAJ52
	β	TRBV20-1	CSASGRRGYGYTF	TRBJ1-2
56SL37	α	TRAV14	CAMRRGFQKLVF	TRAJ8
	β	TRBV4-1	CASSQALLTGSYEQYF	TRBJ2-7
58SL37	α	TRAV17	CATPNTGGFKTIF	TRAJ9
	β	TRBV6-2	CASSSPFRRASVGELFF	TRBJ2-2

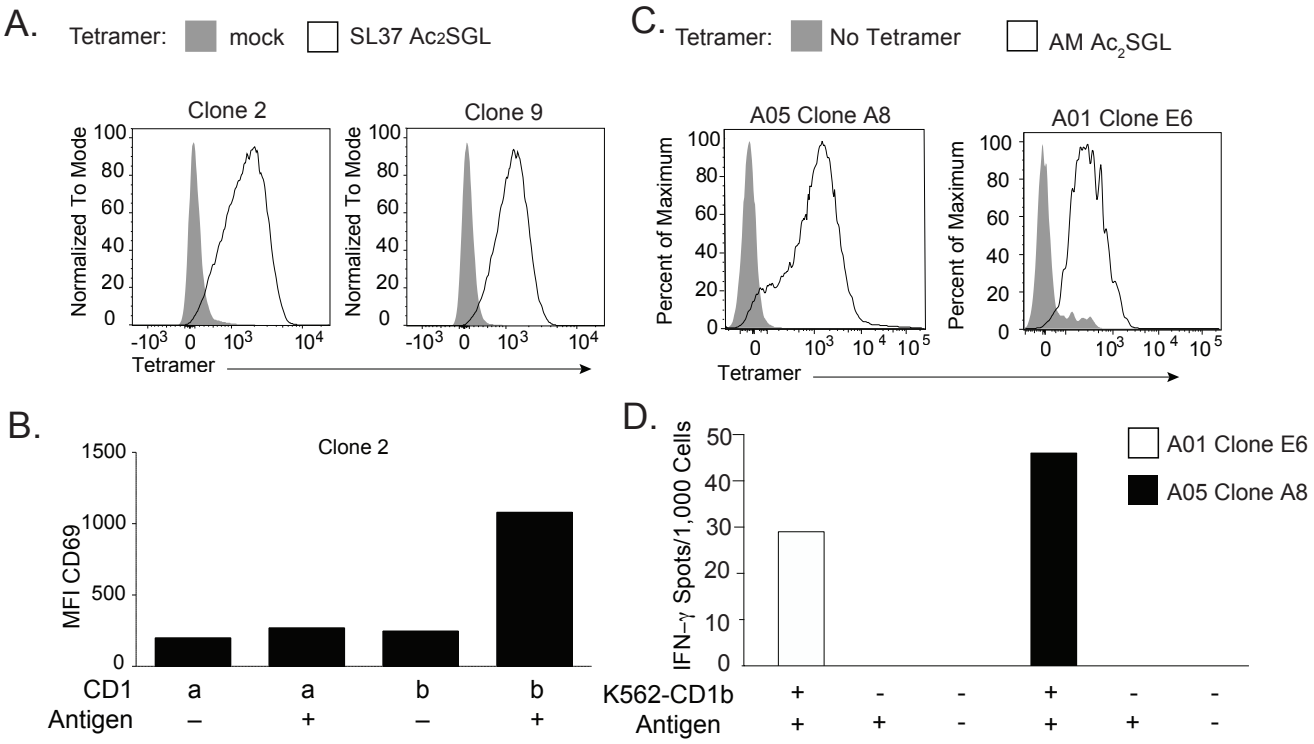

Figure 2.5. **Ac_2SGL-specific TCR transduction confers antigen specificity.**

(A) Jurkat cells were transduced with the dominant TCR α and TCR β of C58SL37 and clones were isolated by limiting dilution. Two independent clones, clone 2 and clone 9, were stained with SL37 Ac_2SGL-loaded tetramers (white) or mock loaded (grey) tetramers. (B) C1R cells (20,000) transfected with CD1a or CD1b were loaded with SL37 Ac_2SGL, mixed with clone 2 cells (100,000) and incubated overnight before staining with an antibody against CD69 as a marker of T cell activation. MFI = mean fluorescence intensity. Data are representative of four independent experiments. (C) Jurkat cells were transduced with the dominant TCR α and TCR β of A01 and A05 and clones were isolated by limiting dilution cloning. One clone was selected and stained with AM Ac_2SGL-loaded tetramers (white) and compared to a no tetramer (grey) control sample. (D) K562 cells transfected with CD1b were loaded with AM Ac2SGL and co-incubated with 1,000 A05 clone A8 or A01 clone E6 and incubated overnight. T cell activation was measured using IFN-γ ELISPOT.

2.7 SUMMARY

The discovery that human T cells recognize bacterial lipid antigens bound to CD1 proteins opened new areas of investigation with potential applications in pathogen-specific immunity (Beckman et al., 1994; Porcelli et al., 1992). However, key reagents and tools to conduct studies in human populations have been lacking. Here, we describe two main results that will advance translational studies of CD1-restricted T cells in TB patients. First, we report the generation and validation of Ac_2SGL-loaded CD1b tetramers, a new tool that will allow us to probe the phenotypes and functions of Ac_2SGL-specific T cells *ex vivo*. Second, we provide insights in cross-reactivity patterns among human Ac_2SGL-specific T cell lines that will guide choices concerning the development of synthetic Ac_2SGL analogs into vaccine components. Because SGLs are normally produced in many hundreds of forms, but will be developed as vaccines and recall reagents using chemically simplified versions, understanding whether multiple forms are bio-equivalent is essential. Our data show that synthetic analogs of SGLs are not equivalent, and understanding the specific chemical basis of divergence is important. Previous studies have demonstrated that phthioceranic acid and hydroxyphthioceranic acid are key antigenic determinants of Ac_2SGL, but synthesis of these complex lipids required multiple steps and were typically not of sufficient yield to enable large scale clinical studies (Geerdink et al., 2013; Geerdink and Minnaard, 2014; Gilleron et al., 2004; Guiard et al., 2009; Rasappan and Aggarwal, 2014). The A01 and A05 T cell lines that we isolated based on recognition of natural Ac_2SGL cross-react strongly with AM Ac_2SGL, a synthetic molecule that is a component of the natural Ac_2SGL mixture that includes eight methylated carbons on the hydroxyphthioceranic acid and corresponds to the major acyl form at *m/z* 1249.9. It also cross-reacts strongly with SL29 Ac_2SGL, which has a fully saturated tetramethylated phthioceranic acid. By contrast, A01 reacts weakly

with SL37 Ac_2SGL, a molecule that is not identical to any form of naturally occurring Ac_2SGL. Further, we show that T cell lines from two different blood donors that were isolated based on recognition of SL37 Ac_2SGL are unable to recognize natural Ac_2SGL. Thus, even though the Z4B27 T cell clone originally reported to recognize natural Ac_2SGL was broadly cross reactive and recognized nature-identical and modified versions of Ac_2SGL, this is not a general rule and has implications for the use of synthetic Ac_2SGL in future designs of vaccines against TB (Gilleron et al., 2004).

Our findings have immediate relevance for the development of novel whole cell and subunit vaccines for tuberculosis. MTBVAC is an attenuated strain of M.tb that recently completed Phase I clinical trials and has entered efficacy testing (Spertini et al., 2015). MTBVAC contains inactivating mutations in fadD26 and phoP, thus it would not be expected to express SGLs and induce Ac_2SGL-specific T cell responses (Arbues et al., 2013). Induction and expansion of SGL-specific T cells could be measured using tetramers and used as a surrogate marker of infection with M.tb in efficacy studies of MTBVAC. Another approach would be to consider vaccinating with lipid antigens themselves. CD1-restricted T cells have anti-bacterial effector functions and lyse M.tb-infected target cells *in vitro* (Rosat et al., 1999; Stenger et al., 1997). Humanized mouse models have shown that these cells can provide protection against M.tb challenge *in vivo* (Zhao et al., 2015). In a recently published guinea pig vaccination model, natural and SL37 Ac_2SGL containing liposomes conferred modest protection to M.tb challenge (Larrouy-Maumus et al. 2017). These results may reflect suboptimal cross-reactivity with SGL antigens present in M.tb and could be improved if T cells were primed using a different synthetic analog, such as AM or SL29 Ac_2SGL. Our data show that there is a human T cell repertoire for natural and synthetic forms of Ac_2SGL, so it might be possible to use synthetic analogs other than SL37 to prime T cells

by immunization. The immunogenicity of these vaccines in humans can then be evaluated using the SGL-loaded CD1b tetramers.

Furthermore, these results are consistent with data from two recent studies. First, a study of mycolated recognition by GMM-specific T cell receptors by Chancellor et al., demonstrated that changes to the lipid tails are "communicated" to the surface of CD1b through subtle changes to the binding surface that then affect antigen recognition (Chancellor et al., 2017). Next, a study by Van Rhijn et al., demonstrated that moieties within the meromycolate chain of mycolic acid are key antigenic determinants for T cells (Van Rhijn et al., 2017). Thus, one proposed model is that individual lipids within a group of structurally related antigens may elicit diverse responses by distinct TCRs. Further, careful selection of particular antigens from within a group of related antigens may be a strategy to fine-tune T cells responses to lipid antigens in future vaccine strategies. This work is highlighted by the functional differences in cytokine release and cytotoxicity that GMM-specific T cells exhibit when activated by various structurally related antigens (Chancellor et al., 2017). Elucidating the ability of glycolipid-specific T cells to discriminate between lipid tail structures in *in vivo* studies remains a key area of investigation.

The newly developed Ac_2SGL-loaded CD1b tetramers will be useful in probing the functions of Ac_2SGL-specific T cells because it is generally not known which functional classes exist among lipid-specific T cells *in vivo.* Tetramer staining can be used in combination with staining for markers of T cell function, including cytokine production, or to isolate single Ac_2SGL-specific T cells for RNA sequencing. Further, the TCR repertoire of Ac_2SGL-specific T cells can now be studied using tetramers. We describe four newly discovered TCRs here with different patterns of reactivity against natural and synthetic SGLs. High throughput sequencing of T cells that bind to tetramers loaded with natural or AM Ac_2SGL could potentially lead to the

identification of a highly relevant new population of invariant T cells. It is worth noting that one of our T cell clones contained a TRAV17 to TRAJ9 rearrangement. Though the CDR3 regions are markedly different, we have previously reported TRAV17 to TRAJ9 rearrangements among a group of CD1b and glucose monomycolate-specific T cells that are called "LDN5-like T cells" (Van Rhijn et al., 2014). Thus, TRAV17 and TRAJ9 may be part of a general molecular pattern that is associated with CD1b recognition.

We used CD1b point mutants to study the influence of specific residues located at the CD1b surface on T cell activation and found that mutation of V72, E80, D83, or Y151 reduces T cell activation. This reduction could be caused by diminished direct interaction between these residues and the TCR. An alternative possibility is that these residues are required to "lock" the SGL antigen in the CD1b binding groove, so that lack of T cell activation reflects a lack of antigen. Supporting the latter model is the published crystal structure of CD1b bound to SL27 Ac_2SGL, which reveals a dramatic conformational change and decreased groove volume compared to unloaded soluble CD1b in which E80 and Y151 are responsible for occluding the F' entrance of the CD1b binding pocket (Garcia-Alles et al., 2011). The authors also show that replacement of E80 and Y151 with alanine completely abrogated the activation of T cell clone Z4B27 to both natural Ac_2SGL as well as SL27 Ac_2SGL. Further, in a published ternary crystal structure of the semi-invariant germline-encoded mycolyl-reactive (GEM) TCR in complex with glucose monomycolate (GMM)-loaded CD1b, the authors highlight that alanine substitution of E80 abrogates GMM-loaded CD1b tetramer staining of GEM cells, and that this residue forms a salt bridge with R109 in the CDR2 loop of the TCR β chain (Gras et al., 2016). The E80 residue also contacts R110 within the CDR2 loop of a TCR that recognizes phosphatidylglycerol (PG90) (Shahine et al., 2019). However, the salt bridge is not conserved between all auto-reactive TCRs (Shahine et al., 2019). These published

data are consistent with our results and suggest shared molecular mechanisms underlie recognition of CD1b-presented SGL antigens from natural and synthetic sources, and CD1b antigens generally.

Our findings may also have implications for the improved diagnosis of M.tb infection in humans. We recently published that T cell responses to mycobacterial proteins and lipids are poorly correlated in a South African cohort, revealing the complementary nature of immunity to these two classes of antigens (Seshadri et al., 2015). The data presented suggest measuring SGL-specific T cell responses using tetramers could improve existing diagnostic algorithms by providing complementary information. Unlike MHC tetramers, SGL-CD1b tetramers can be applied independently of genetic background because CD1 genes are structurally non-polymorphic (Han et al., 1999). SGL-loaded CD1b tetramers could also be used to detect SGL-specific T cell responses in the blood or lungs of patients with suspected active tuberculosis disease. Recent data have revealed that T cells specific for ESAT-6 and CFP-10 that expressed an activated phenotype was able to distinguish latent infection from active disease (Adekambi et al., 2015). SGL-CD1b tetramers could similarly be incorporated into multi-parameter flow cytometry assays designed to measure the activation status of lipid-specific T cells.

2.8 Materials and Methods

2.8.1 *Human Studies*

A01 and A05 T cell lines were derived from South African adults with latent tuberculosis infection. The individuals were enrolled in studies with IDs DN060-11 and DN070, respectively. The cell lines C58SL37 and C56SL37 were derived from PBMC obtained from a U.S. latent

tuberculosis patient and a random donor from the Massachusetts General Hospital blood bank, respectively. Informed consent was obtained from all subjects.

2.8.2 *Approving Bodies*

Blood was donated with informed consent by asymptomatic tuberculin positive subjects with no clinical or radiographic evidence of active tuberculosis, as approved by the institutional review boards of the Lemuel Shattuck Hospital and Partners Healthcare. The study was also approved by the IRB of the University of Washington and University of Cape Town.

2.8.3 *Isolation and Synthesis of Sulfoglycolipids*

Natural Ac_2SGL was purified from M.tb as previously described (Gilleron et al., 2004). Chemical synthesis of SL37 Ac_2SGL has also been described previously (Gau et al., 2013; Larrouy-Maumus et al., 2017). Chemical synthesis of AM Ac_2SGL consisted of a separate synthesis of hydroxyphthioceranic acid and a subsequent assembly of AM Ac_2SGL (James et al., 2018).

2.8.4 *Generation of SGL-loaded CD1b Tetramers*

Soluble biotinylated CD1b monomers were provided by the National Institutes of Health Tetramer Core Facility (Emory University, Atlanta, GA). The loading protocol for CD1b monomers was based on previously published glucose monomycolate loading protocols (Kasmar et al. 2011). Natural Ac_2SGL was dried down in a glass tube in a stream of nitrogen and sonicated into a 50 mM sodium citrate buffer at pH 4, containing 0.25% with 3-[(3-cholamidopropyl)dimethylammonio] -1-propanesulfonate (CHAPS) (Sigma, St. Louis, MO) for two minutes at 37°C. The sonicate was transferred to a microfuge tube, and 20 μg of CD1b

monomer was added and incubated in a 37°C water bath for 2 hours with vortexing every 30 minutes. At the end of the incubation, the solution was neutralized to pH 7.4 with 6 µl of 1M Tris pH 9. For SL37 Ac_2SGL and AM Ac_2SGL, the sonication was performed in 50 mM sodium citrate buffer at pH 7.4, containing 10 mM taurocholate (Sigma, St. Louis, MO) for 30 minutes at 37°C. After addition of CD1b, the mixture was incubated in a 37°C water bath for 2 hours. Finally, 10 µl of Streptavidin conjugated to allophycocyanin or phycoerythrin (Life Technologies, Carlsbad, CA) was added in ten aliquots of 1 µl every 10 minutes. The final product was filtered through a SpinX column (Sigma, St. Louis, MO) to remove aggregates and stored at 4°C until use.

2.8.5 *T cell Lines and Assays*

The cell line A01 was isolated from cryopreserved, CD14-depleted peripheral blood mononuclear cells (PBMC) from a South African adult with latent tuberculosis infection as defined by a positive QuantiFERON-TB Gold blood test. PBMC were thawed and washed in warm RPMI 1640 (Gibco, Waltham, MA) supplemented with 10% fetal bovine serum (Hyclone, Logan, UT) and 10 ml/ml Benzonase (Millipore, Billerica, MA) and enumerated using Trypan blue exclusion. T cell media consists of RPMI 1640 (Gibco, Waltham, MA) supplemented with 10% fetal bovine serum (Hyclone, Logan, UT), 100 U/ml Penicillin and 100 mg/ml Streptomycin (Gibco, Waltham, MA), 55 mM 2-mercaptoethanol (Gibco, Waltham, MA), 0.3X Essential Amino Acids (Gibco, Waltham, MA), 60mM Non-essential Amino Acids (Gibco, Waltham, MA), 11mM HEPES (Gibco, Waltham, MA), and 800mM L-Glutamine (Gibco, Waltham, MA). PBMC were then plated in a 24-well plate at a density of three million cells per well in T cell media and allowed to rest overnight at 37°C in humidified incubators supplemented with 5% CO2. The following day, PBMC were washed and blocked with 50% human serum (Valley Biomedical, Winchester, VA)

in PBS supplemented with 0.2% BSA (Sigma, St. Louis, MO) (FACS buffer) for 10 minutes at 4°C. The samples were washed twice with PBS and stained with Aqua Live/Dead stain (Life Technologies, Carlsbad, CA) according to the manufacturer's instructions. Following two additional PBS washes, cells were resuspended in 50 μL FACS buffer and 1 μL of either mock loaded CD1b tetramer or Ac_2SGL-loaded CD1b tetramer and incubated at room temperature for 40 minutes in the dark. Finally, cells were stained with anti-CD3-electron coupled dye (ECD) (Beckman Coulter, Brea, CA), washed twice in T cell media and filtered through a cell strainer tube (Falcon, Tewksbury, MA) prior to sorting. Tetramer-positive T cells were sorted using a FACS Aria II (BD, San Jose, CA) cell sorter equipped with 407nm, 488nm, and 641nm lasers.

Sorted T cells were washed and resuspended in T cell media supplemented with 10% human serum and divided among eight wells of a 96-well plate to create a T cell line. Irradiated PBMC (150,000 cells per well) were added as feeder cells along with phytohaemagglutinin (Remel, San Diego, CA) at a final concentration of 1.6 mg/ml. After two days in culture at 37˚C, 5% CO_2, 10 μl natural IL-2 (Hemagen, Columbia, MD) was added to each well. Half the media was replaced every two days with T cell media supplemented with 10% human serum and natural IL-2. When the cell clusters were large and round (approximately after eight days of growth), they were pooled into a 24-well plate. After 10 days in culture, the cell line was screened by tetramer staining or functional response to Ac_2SGL. We then further expanded the T cell line using a modified version of a previously published rapid expansion protocol (Riddell et al. 1992). Briefly, 200,000 T cells were mixed with 5 million irradiated EBV-transformed B cells and 25 million irradiated PBMC as feeder cells in 25 ml T cell media. Anti-CD3 (clone OKT3) was added a final concentration of 30 ng/ml, and the mixture was incubated overnight at 37˚C, 5% CO2. The following day, recombinant IL-2 (rIL-2) (UWMC Clinical Pharmacy) was added to a final

concentration of 50 U/ml. On day 4, the cells were washed twice in T cell media to remove OKT3, and fresh media supplemented with rIL-2 at 50 U/ml was added. Half the media was replaced every three days or split into new T25 tissue culture flasks (Costar, St. Louis, MO) as determined by cell confluency. After 13 days in culture, the line was screened by tetramer staining and then cryopreserved on day 14.

The cell lines C58SL37 and C56SL37 were derived from PBMC from a latent tuberculosis patient and a random blood bank donor, respectively. Cells were resuspended in 50 µl FACS buffer and 1 µL of either mock loaded CD1b tetramer or Ac_2SGL-loaded CD1b tetramer and incubated at room temperature for 20 minutes in the dark. Finally, cells were stained with anti-CD3-FITC (clone SK7, BD, San Jose, CA), washed twice in T cell media and filtered through a cell strainer tube (Falcon, Tewksbury, MA) prior to sorting. Tetramer-positive T cells were sorted using a FACS Aria II (BD, San Jose, CA) cell sorter equipped with 407nm, 488nm, and 641nm lasers. Sorted cells were expanded with the anti-CD3-based rapid expansion method seeding 1,000 T cells with 40,000 irradiated EBV-transformed B cells and 200,000 irradiated PBMC per well of a round bottom 96-well plate.

2.8.6 *IFN-γ ELISPOT*

We used an IFN-γ ELISPOT to determine the antigen specificity of our T cell lines. EMD Multiscreen-IP filter plates (Millipore, Billerica, MA) were coated with 1D1K antibody (Mabtech, Sweden) diluted 1:400 in PBS and incubated overnight at 4˚C. The following day, one thousand T cells were plated 1:50 with K562 cells stably transfected with CD1b or with a mock vector. Lipids antigens were stored in 2:1 chloroform:methanol and appropriate amount was dried using gaseous nitrogen. The lipids were sonicated into media to obtain a 4 µg/ml suspension and plated with the cells at a final concentration of 1 µg/ml. These cultures were incubated at 37˚C for approximately

16 hours. The following day, the cells were washed twice with sterile water to lyse the cells, and the plates were incubated with the detection antibody 7-B6-1-biotin (Mabtech, Sweden) diluted 1:1000 in PBS + 0.5% FCS and incubated for two hours at room temperature. The cells were then washed five times with PBS and incubated in ExtrAvidin-Alkaline Phosphatase (Sigma, St. Louis, MO) diluted 1:1000 in PBS and incubated for one hour at room temperature. The wells were then washed five times and incubated with BCIP/NBT substrate (Sigma, St. Louis, MO) for five minutes to develop the membrane. The wells and IFN-γ spots were counted using an ImmunoSpot S6 Core Analyzer (Cellular Technology Limited, Cleveland, OH).

2.8.7 *T cell Receptor Sequencing*

The TCRs of the A01 and A05 line were obtained using 5'-Rapid Amplification of cDNA Ends (5'-RACE). RNA was extracted from the T cell lines using a RNeasy Mini Kit (Qiagen, Hilden, Germany). cDNA was generated from 1 μg RNA using the SMARTer RACE 5′/3′ Kit (Clontech Laboratories, Inc., Mountain View, CA) and the manufacturer's protocol for preparing 5′-RACE-Ready cDNA. To determine the sequence of the T cell receptor (TCR)-β chain, 5′-RACE was performed according to the manufacturer's protocol using the following gene-specific primers for the human TCR β and TCR α chain constant region:

5′-GATTACGCCAAGCTTCCCATTCACCCACCAGCTCAGCTCCACG-3',

5'-GATTACGCCAAGCTTGTTGCTCCAGGCCACAGCACTGTTGCTC-3',

respectively. The RACE products were resolved through a 1% agarose (Thermo Fisher Scientific, Waltham, MA) gel supplemented with 1× SYBR Safe (Life Technologies, Carlsbad, CA) for 1 hour at 120 V, and the band located at ~ 700 bp was excised. The NucleoSpin Gel and PCR Clean-up kit (Macherey-Nagel, Duren, Germany) was used to extract DNA, and then In-Fusion Cloning of RACE Products was performed according to the 5′-RACE protocol according to manufacturer's

instructions. Plasmid DNA was extracted using the Plasmid Mini Kit (Qiagen, Hilden, Germany) and was submitted for sequencing (Genewiz, South Plainfield, NJ). The sequencing results for both TCR α and TCR β were cleaned using Sequencher software (Version 5.2.4) and analyzed using the IMGT/V-QUEST program version 3.4.7. Sequences were aligned using Serial Cloner version 2.6. The TCR sequences were confirmed using a single cell approach (Method detailed in Chapter 4).

The TCRs of C56SL37 and C58SL37 were sequenced by a single cell approach (Wang et al., 2012).

2.8.8 *T cell Receptor Cassette Construction*

Codon-optimized A01 and A05 T cell TCR sequences were assembled into a TCR cassette (Linnemann et al. 2013). In this construct, the TCR α and TCR β chain constant regions are replaced with modified murine TCR constant regions to facilitate measurement of TCR expression and to encourage pairing between exogenous TCR chains. The TCR cassettes were synthesized through Thermo Fisher GeneArt Synthesis service and were then cloned into pRRL.PPT.MP.GFPpre (Jing et al. 2016; Zhou et al. 2012) using BamHI and SalI restriction enzymes (New England BioLabs, Ipswich, MA). All plasmids were purified using Maxi Prep kits (Qiagen, Hilden, Germany).

2.8.9 *Generation of Lentivirus*

Lenti-X HEK293T cells (Clontech, Mountain View, CA) were seeded at 2 million cells per 100 mm tissue culture dish and incubated for 48 hours at 37˚C/5% CO2 in DMEM (Gibco, Waltham, MA) or until cells reached 75% confluency. The medium was replaced 4 hours before transfection. Cells were transfected with 10 μg pRRL-TCR plasmid, 5 μg pCI-VSVG envelope

plasmid, and 5 μg of a psPAX2 packaging vector (gifted from Dr. Stanley Riddell at Fred Hutchinson Cancer Research Center). Plasmids were mixed with Fugene 6 transfection reagent (Promega, Madison, WI) at a dilution of 1:12 in a total volume of 600 μl. Transfection mixture was added dropwise into the cell culture and incubated overnight in the conditions described above. The medium was then replaced and incubated for an additional 48 h. After this time, 20 μl of supernatant was titered using Lenti-X GoStix (Clontech, Mountain View, CA) per the manufacturer. Supernatant was then harvested every 12 hours for a total of three collections. At each collection, cell debris was removed by centrifugation at 1500 rpm for 5 minutes, and cleaned supernatant was reserved in a 50-ml conical and kept at 4˚C until three collections had been acquired. Supernatant was then incubated overnight with Lenti-X concentrator (Clontech, Mountain View, CA) at a ratio of 1:3. The following day, the supernatant was centrifuged at 1500×g for 45 minutes at 4˚C. Supernatant was then discarded, and the pelleted virions were resuspended in 300 μL R10 media and stored at -80˚C until use.

2.8.10 *Transduction of Jurkat Cells*

CD8-expressing Jurkat cells were seeded at 1 million cells per well in a 48-well plate in enhanced RPMI. The same day, the Jurkat cells were transduced with TCR lentivirus at an estimated multiplicity of infection (MOI) of 5 with 1 μL of polybrene at a final concentration of 4 μg/ml (Sigma, St. Louis, MO). Cells and virus were incubated for 4 hours at 37 °C/5% CO2 and washed with PBS (Gibco, Waltham, MA) to remove excess virus. Jurkat cells were maintained in culture for 1 week using enhanced RPMI and screened for TCR expression (Jing et al. 2016) using an anti-mouse TCR β chain APC antibody (BD Biosciences, San Jose, CA) and tetramer staining as described above. TCR constructs containing TCR α and TCR β separated by a p2A linker were synthesized (ThermoFisher, Waltham, MA) and inserted into pRRL vectors as previously

described (Holst et al. 2006). For the SL37-specific TCRs, TCR constructs containing TCR α and TCR β separated by a 2A linker were synthesized (Biocat, Germany) and inserted into pMIG2 vectors as previously described (Holst et al. 2006). Human embryonic kidney (293T) cells were transfected with TCR expression vector, pMIG expression vector containing CD3δγεζ sequence, packaging vectors pEQ-Pam3(-E) and pVSV-G using FuGENE 6 transfection reagent (Promega) (Szymczak et al. 2004). Retrovirus containing supernatant was collected twice daily and used to transduce the TCR-deficient T cell line Jurkat 76 in the presence of Polybrene (Sigma-Aldrich, St. Louis, MO) for a total of 4 days.

2.8.11 *Production of Wild-type and Mutant CD1b-expressing C1R cells*

Gene segments encoding full-length wild-type CD1b or single-site mutant CD1b (E62A, E65A, I69A, R71A, V72A, F75A, R79A, E80A, D83A, Q150A, Y151A, E156A, I160A, E164A, T165A and R168A) were purchased from Thermo Fisher Scientific, cloned into the pMIG retroviral vector and transfected into HEK293T cells to produce CD1b containing retrovirus. C1R cells were transduced with retroviral supernatants as previously described (Birkinshaw et al., 2015). Each of the CD1b transduced cell lines were stained with an anti-CD1b monoclonal antibody (SN13; Biolegend) and sorted by flow cytometry with a FACSAria III Cell Sorter (BD Biosciences) to ensure each line expressed similar levels of CD1b. These reagents were developed by Michael NT Souter, Dale I Godfrey, and Daniel G. Pellici (Department of Microbiology and Immunology, University of Melbourne, Melbourne, Australia).

2.8.12 *Quantification and Statistical Analyses*

GraphPad Prism (v.6.0) was used for all statistical analyses. Statistical details can be found in the figure legend. Estimated EC_{50} values were calculated based on a nonlinear

regression model of the means of triplicate wells.

Chapter 3. T CELL RECEPTOR CO-RECEPTORS ENHANCE GLYCOLIPID-SPECIFIC T CELL FUNCTIONAL AVIDITY

3.1 INTRODUCTION

Understanding the factors that influence T cell functional differentiation following antigen stimulation is central to leveraging T cells through vaccination. The inflammatory environment is the primary factor that influences T cell fate determination and effector function (Zhu et al., 2010). In addition, it has been well established that antigen avidity also has downstream effects on the level of proliferation, memory phenotype acquisition, and functional differentiation (Kersh et al., 1998; Viganò et al., 2012; Zehn et al., 2009)

There are four major factors that affect T cell avidity for antigens. These are the TCR affinity for the antigen presenting molecule, TCR affinity for the antigen-loaded antigen presenting molecule, the level of TCR expression, and the expression of TCR co-receptors on the cell surface (Stone et al., 2009). The aggregate impact that these factors have on the binding strength of the TCR for the antigen-loaded antigen presenting molecule is known as functional avidity, due to the multivalent and multifaceted nature of this interaction in live cells (Stone et al., 2009). These factors have largely been explored for peptide-specific and innate-like T cells, but not for T cells that recognize mycobacterial glycolipid antigens.

TCR affinity for antigen-loaded antigen presenting molecules has been explored in peptide-specific and innate-like T cells. Peptide-specific CD4 and CD8 T cells can exhibit a range of TCR affinities, from 1-150 μM and 10-200μM, respectively (Stone and Kranz, 2013). By contrast, the semi-invariant TCRs of iNKT cells have demonstrated a relatively uniform high affinity for α-GalCer-loaded CD1d, at approximately 2 μM (Patel et al., 2011). This high affinity interaction is

shared by the semi-invariant TCR of MAIT cells, which is also on the order of 2 μM (Eckle et al., 2014). A population of T cells specific for the mycobacterial glycolipid GMM expresses a semi-invariant TCR known as the germline-encoded mycolyl-reactive (GEM) TCR. These TCRs exhibit a range of affinities from 0.06 to 1.5 μM (Gras et al., 2016; Van Rhijn et al., 2014). In addition, another population of GMM-specific T cells known as LDN5-like T cells express a lower affinity TCR, which has an affinity of 39 μM (Van Rhijn et al., 2014). These two populations have been described as two "compartments" of GMM-specific T cells that are defined by TCR bias and affinity, but whether two "compartments" exist for other mycobacterial glycolipid-specific T cells is unknown.

Further, TCR co-receptor expression patterns have been extensively studied in peptide-specific and innate-like T cells. In human PBMC, approximately two-thirds of T cells express the CD4 co-receptor, and the remaining one-third express the CD8 co-receptor. Double negative (DN) and double positive (DP) T cells are rare in peripheral blood. Among invariant natural killer T (iNKT) cells, on average 15% of iNKT cells express CD4, 49% are double negative (DN), and roughly 34% express the CD8αα homodimer (O'Reilly et al., 2011). Among mucosal-associated invariant T (MAIT) cells, 35% express CD8αα and 44.7% express CD8αβ, making approximately 78% of MAIT cells $CD8^+$ T cells (Gherardin et al., 2018). However, some evidence suggests that CD8αβ MAIT cells also express CD8αα homodimers on the cell surface (Gherardin et al., 2018). Approximately 14% of MAIT cells are DN (Gherardin et al., 2018). CD4 and double positive (DP) MAIT cells are rare (Gherardin et al., 2018). GEM T cells exclusively express the CD4 co-receptor (Van Rhijn et al., 2013). But, LDN5-like T cells lack CD4 and CD8 co-receptor expression (Van Rhijn et al., 2014). This suggests that there is heterogeneity among the co-receptor expression and functional avidities that GMM-specific T

cells can exhibit. However, whether this phenomenon is generalizable to T cells that recognize other mycobacterial glycolipids, and whether TCR co-receptors are directly involved in mediating functional avidity of mycobacterial glycolipid-specific T cells is unknown.

Sensitivity to antigen-dependent activation is further enhanced when CD4 and CD8 proteins are simultaneously engaged (Janeway, 1992). In some instances, the presence of the CD4 co-receptor on the T cell surface can augment T cell activation up to 100-fold (Janeway, 1992). In addition, previous studies have described that CD4 potentiates iNKT cell activation leading to sustained TCR signaling and potentiation of effector responses (Thedrez et al., 2007). However, these factors have largely not been investigated for T cells that recognize mycobacterial lipid antigens.

Here, we study co-receptor expression on T cells specific to Ac_2SGL, and investigate the impact of co-receptor expression on T cell functional avidity. We examine co-receptor expression on Ac_2SGL-specific T cells in *ex vivo* studies, and the differences in AMSGL-CD1b tetramer binding in *ex vivo* T cells, *in vitro*-derived T cell lines, and manipulated transduced T cells. We found that *ex vivo* Ac_2SGL-specific T cells identified by tetramer show a bias toward CD4 co-receptor expression, and that CD4 T cells bind AMSGL-CD1b tetramer with a higher intensity than T cells that express the CD8 co-receptor or are DN.

3.2 CO-RECEPTOR EXPRESSION BY *EX VIVO* SULFOGLYCOLIPID-SPECIFIC T CELLS

To determine the co-receptor expression by Ac_2SGL-specific T cells, we used direct *ex vivo* tetramer staining using CD1b tetramers loaded with a synthetic analog of Ac_2SGL, AMSGL (James et al., 2018). We utilized a diverse sample of peripheral blood mononuclear cells (PBMC) from 5 US healthy donors, 5 South African adolescents with negative tuberculin skin tests (TST)

and negative IFN-γ release assay (IGRA), and 5 South African adolescents with positive TST and IGRA (demographic information summarized in Appendix A) (Mahomed et al., 2011). To ensure robust identification of these cells, we used AMSGL-CD1b tetramer labeled with two distinct fluorochromes (electron coupled dye (ECD) and allophycocyanin (APC)) and defined AMSGL-specific T cells as staining with both tetramers, while being unlabeled by a mock-loaded CD1b tetramer (Figure 3.1A). Gates defining AMSGL-CD1b tetramer-positive cells were set based on samples not stained with one of the tetramers, labeled ECD fluorescence minus one (FMO) and APC FMO (Figure 3.1A, left, middle). We also added an Ac_2SGL-specific T cell line at approximately 8% of total T cells to ensure that both tetramers were staining the appropriate T cell population (Figure 3.1A, right). Representative tetramer staining plots from one individual, including relevant gates are shown (Figure 3.1B). The full staining panel and gating strategy are described in the appendix (Appendix A).

After gating on putative Ac_2SGL-specific T cells, we examined CD4 and CD8 expression using CD4 and CD8β antibodies, and compared the percentage within each group to tetramer-negative T cells. Ac_2SGL-specific T cells exhibit a 18-fold enrichment of CD4 and CD8 double-positive (DP) and a 1.5-fold enrichment of CD4 T cells above $CD3^+$ T cells ($p < 0.0001$) (Figure 3.1C). This is accompanied by a 5.6-fold reduction of CD8 and a 2.8-fold reduction of CD4 and CD8 double negative (DN) T cells when compared to $CD3^+$ T cells ($p < 0.0001$). Further, DP, CD4, and CD8 AMSGL-specific T cells exhibit a modest, yet consistent, increase in AMSGL-CD1b APC tetramer MFI when compared to DN Ac_2SGL-specific T cells, 8%, 6%, and 2% respectively ($p < 0.0001$) (Figure 3.1D). These data reveal a hierarchy, where CD4 Ac_2SGL-specific T cells exist at a higher frequency and bind AMSGL-CD1b tetramer with a higher intensity, followed by CD8 and DN Ac2SGL-specific T cells, respectively.

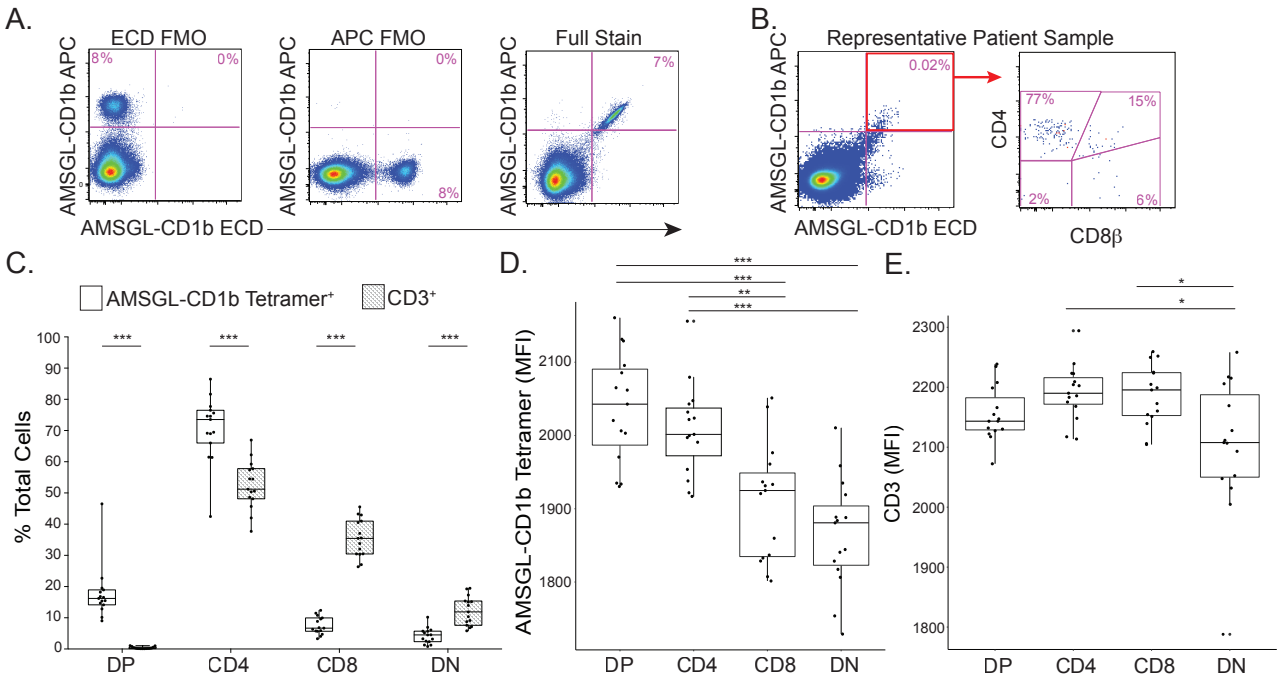

Figure 3.1. **Co-receptor expression by *ex vivo* Ac_2SGL-specific T cells**

AMSGL-CD1b tetramers were incorporated into a multi-parameter flow cytometry assay to measure co-receptor expression by Ac_2SGL-specific T cells. (A) The tetramer positive gate was defined by a 'Fluorescence Minus One' (FMO) negative control (left and center) and a positive control using Ac_2SGL-specific T cell lines diluted in donor PBMC (right). (B) Representative staining from a South African adolescent blood donor. The co-receptor expression of Ac_2SGL-CD1b tetramer positive T cells in the blood was quantified using cryopreserved PBMC obtained from three groups of healthy subjects: U.S. controls at low risk for M.tb exposure (n=5), South African adolescents with latent tuberculosis (IGRA-positive, n=5), and South African adolescents without latent tuberculosis (IGRA-negative, n=5). (C) Boxplots depict the median and interquartile range of tetramer-positive events (white) within each co-receptor group (double positive (DP), CD4, CD8, and double negative (DN), expressed as a percent of total tetramer-positive events. These were compared to the percent of cells in each group in total $CD3^+$ T cells (grey). (Mann-Whitney with Bonferroni Correction , *** = $p < 0.0001$, n = 15) Each dot represents the mean percent of one sample. (D) Boxplots depict the median and interquartile range of mean fluorescence intensity (MFI) of AMSGL-CD1b tetramer-positive events in each co-receptor group. Each dot represents the MFI of one sample. MFI was compared between groups (Kruskal-Wallis with post-hoc Dunn test, *** = $p < 0.0001$, ** = $0.0001 < p < 0.001$, n = 15). (E) Boxplots depict the median and interquartile range of mean fluorescence intensity (MFI) of CD3 among tetramer-positive events in each co-receptor group. Each dot represents the MFI of one sample. MFI was compared between groups (Kruskal-Wallis with post-hoc Dunn test, * = $0.001 < p < 0.05$, n = 15).

We considered the possibility that the difference in tetramer MFI between DP, CD4, CD8, and DN Ac_2SGL-specific T cells could be explained by differences in TCR expression. We compared the mean TCR expression of Ac_2SGL-specific T cells, as measured by CD3 MFI, and found no difference in CD3 expression between DP, CD4, and CD8 T cells (Figure 3.1E). However, we did detect a 4% lower CD3 MFI in DN T cells when compared to the other groups ($p = 0.02$) (Figure 3.1E). This data suggests that while there are slight differences in TCR expression between groups, CD4 Ac_2SGL-specific T cells may have a higher functional avidity than CD8 and DN Ac_2SGL-specific T cells. Additionally, the expression of the CD8 co-receptor may also confer a modest increase in functional avidity above DN T cells. However, these data are affected by the inherent limitations of direct *ex vivo* tetramer staining, including lack of external validation of antigen specificity.

3.3 Co-receptor Expression by *in vitro* Derived Sulfoglycolipid-specific T cell Lines

To address these limitations, we evaluated affinity differences between *in vitro*-derived SGL-specific T cell lines that have been previously described, named A01 and A05 (James et al., 2018). In brief, these T cell lines were isolated from South African adults with latent TB using Ac_2SGL-loaded CD1b tetramers, expanded *in vitro*, and screened for antigen specificity using tetramer staining and functional reactivity, as measured by interferon (IFN-)γ production following antigen stimulation (James et al., 2018).

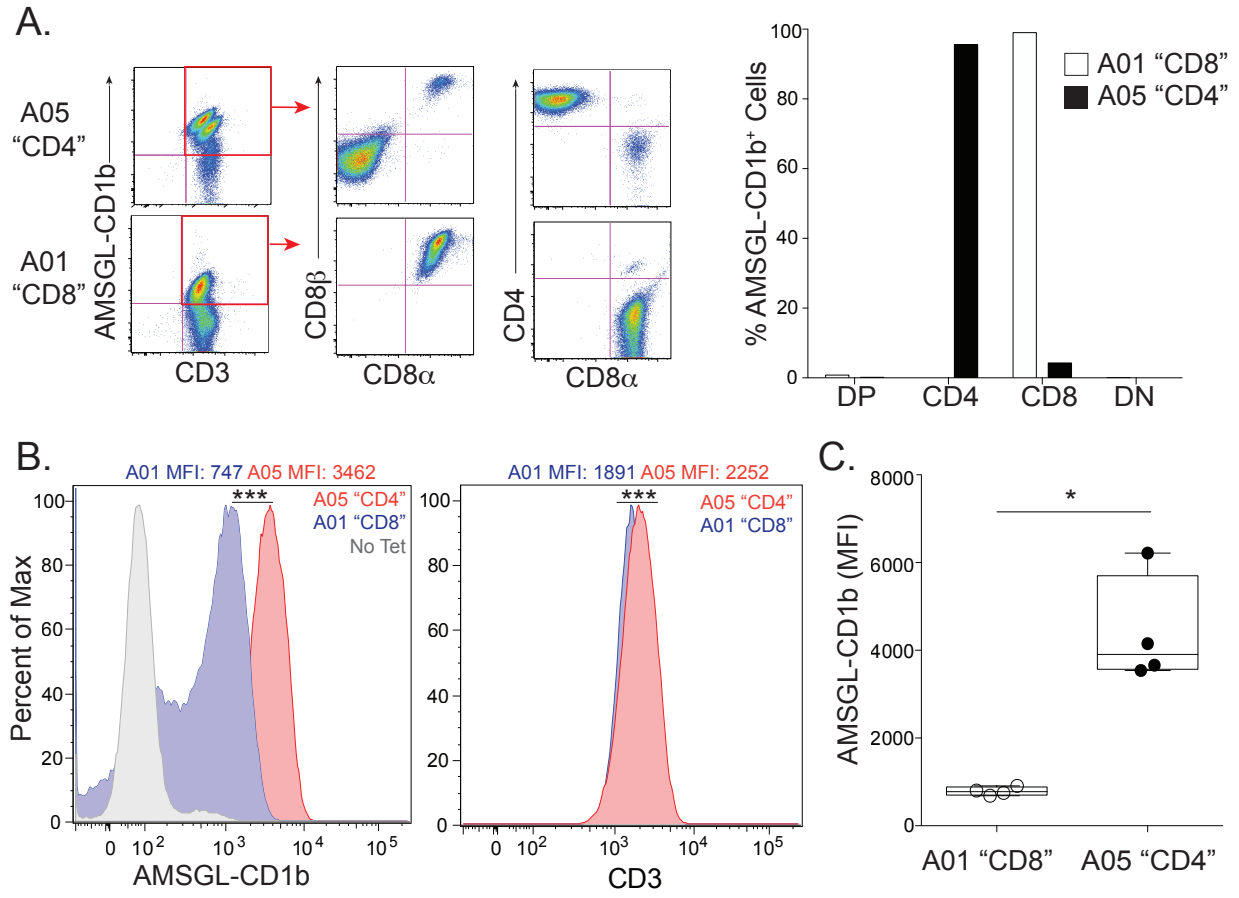

Figure 3.2. Co-receptor expression and functional avidity of *in vitro*-derived Ac_2SGL-specific T cell lines.

Previously described T cell lines were used for this study (James et al., 2018). CD4 and CD8 co-receptor expression was examined using a specific antibody. AMSGL-CD1b tetramer and CD3 MFI were also compared. (A) Tetramer-positive cells within the A05 T cell line expresses CD4, and lacks CD8α and CD8β expression (left, top). Tetramer-positive cells within the A01 T cell line expresses CD8α and CD8β, but lack CD4 expression (left, bottom). The percentage of each of the T cell lines in each co-receptor group is quantified in this bar plot (right). (B) A01 T cell line AMSGL-CD1b tetramer MFI (blue) is compared to A05 T cell line tetramer MFI (red). A no tetramer control is also represented (grey) (left). (Student's t-test, $p < 0.0001$, $n = 137{,}788$). CD3 MFI of both A01 (blue) and A05 (red) T cell lines is also compared. (Student's t-test, $p < 0.0001$, $n = 137{,}788$). (C) Boxplots depict the median and interquartile range of the AMSGL-CD1b MFI of A01 (white) and A05 (black) is compared from four independent experiments. (Mann-Whitney, $p = 0.028$, $n = 4$).

First, we evaluated the co-receptor expression by these T cell lines. The Ac_2SGL-specific T cell lines were stained with AMSGL-CD1b tetramer and CD4, CD8α, and CD8β antibodies. 99% of the cells that stain with AMSGL-CD1b tetramer within the A01 line express a heterodimeric CD8αβ co-receptor, while 96% of the cells that stain with AMSGL-CD1b tetramer in the A05 line expresses the CD4 co-receptor (Figure 3.2A). Further, the A05 T cell line exhibits an AMSGL-CD1b tetramer MFI of 3462, while the A01 T cell line MFI is 747 ($p < 0.0001$) (Figure 3.2B, left). The CD4 T cell line has a 1.2-fold higher CD3 MFI, suggesting that TCR expression may also be impacting the differences AMSGL-CD1b tetramer MFI ($p < 0.0001$) (Figure 3.2B, middle). Upon repeated testing, the difference in AMSGL-CD1b tetramer MFI between A01 and A05 is approximately 5.5-fold ($p = 0.028$) (Figure 3.2C). However, these data are limited by the differences in TCR sequences expressed by both the T cell lines, as the TCR sequence is likely to contribute to T cell functional avidity as well as the co-receptor (Table 2.1).

3.4 CD4 T CELLS TRANSDUCED WITH AN AC_2SGL-SPECIFIC TCR EXHIBIT A HIGHER FUNCTIONAL AVIDITY THAN CD8 PRIMARY T CELLS

To address this limitation, we generated an SGL-specific TCR cassette isolated from the CD4 T cell line and delivered the gene cassette using a lentiviral vector into polyclonal T cells (Figure 2.5C). This cassette contains a modified murine TCR α and TCR β constant region (mTCRBC) that contains an additional cysteine residue. This modification encourages binding with the other exogenous TCR chain and allows for determination of exogenous TCR expression by flow cytometry. Of note, we attempted a similar set of experiments with the low-affinity TCR from the CD8 T cell line, but exceptionally high levels of TCR expression are required for tetramer

binding, prohibiting TCR reconstitution in primary T cells (data not shown). Thus, these experiments focus exclusively on the TCR from the CD4 T cell line.

To determine differences in functional avidity between CD4, CD8, and DN T cells, we transduced the exogenous TCRs into primary $CD3^+$ T cells isolated from a blood bank donor. Among primary T cells that are not transduced with the exogenous TCR, 0% stain with AMSGL-CD1b tetramers or a mTCRBC antibody (Figure 3.3A). When transduced with the TCR, 88% of the cells stain with the both AMSGL-CD1b tetramer and the mTCRBC antibody, the cells stain with the both AMSGL-CD1b tetramer and the mTCRBC antibody, demonstrating that expression of this T cell receptor is necessary and sufficient for antigen-specific tetramer staining in primary T cells (Figure 3.3A).

The polyclonal transduced cells were then stained with AMSGL-CD1b tetramer, and the tetramer MFI of CD4, CD8, and DN T cell transductants were compared. The CD4 T cells transduced with an Ac_2SGL-specific TCR had an MFI of 1148, while the CD8 T cells had an MFI of 984 and DN T cells had an MFI of 921 ($p < 0.0001$) (Figure 3.3B). This suggests that Ac_2SGL-specific TCR transduction into CD4 T cells confers a higher functional avidity for AMSGL-loaded CD1b tetramer than when this same TCR is transduced into CD8 or DN T cells. However, the CD4, CD8, and DN transductant had a mTCRBC MFI of 2098, 1882, and 1774 respectively, suggesting that these populations also exhibit differences in the level of exogenous TCR expression post-transduction ($p < 0.0001$) (Figure 3.3B).

Next, the CD4 and CD8 T cell transductants were sorted to exclude non-transduced T cells and transduced T cells were subjected to limiting dilution cloning. We analyzed eight CD4 expressing clones and eight CD8 expressing clones. The CD4 T cell transduction clones had an MFI of 209, while the CD8 T cell transductant clones had an MFI of 125 ($p = 0.019$) (Figure 3.3C).

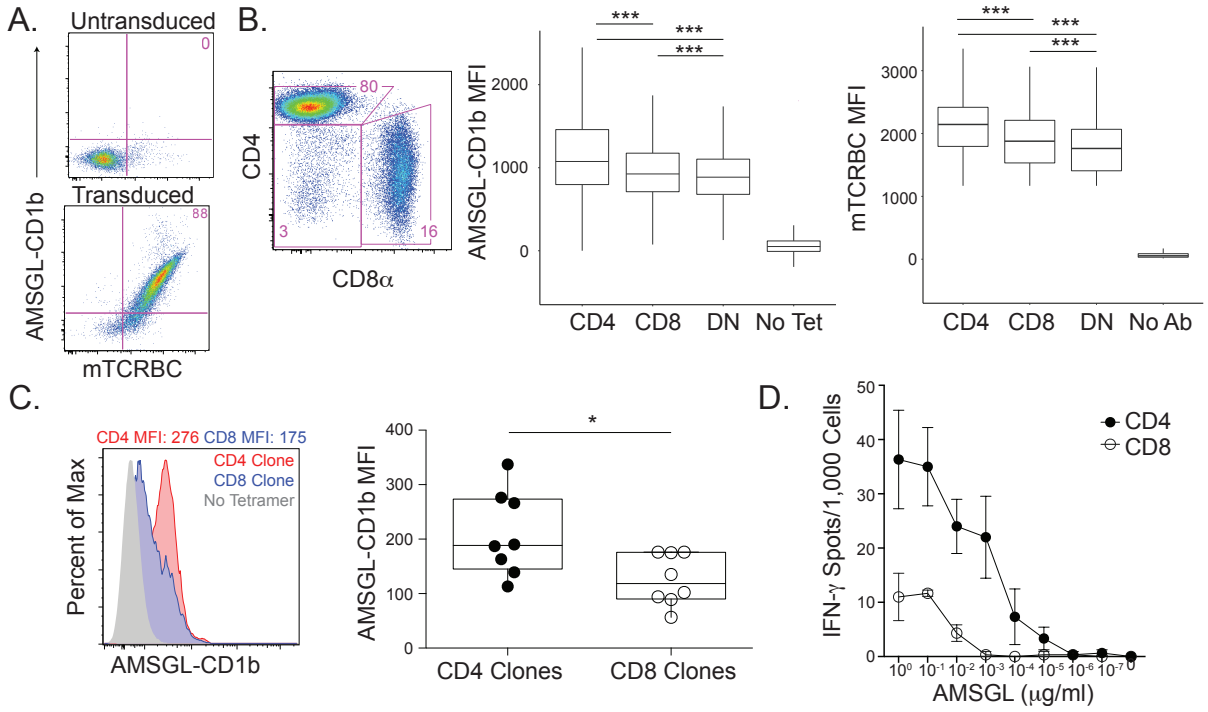

Figure 3.3. **Functional avidity of CD4, CD8, and DN primary T cells transduced with an Ac_2SGL-specific TCR.**

Primary T cells were transduced with the TCR from the A05 T cell line using a lentiviral vector. (A) Untransduced primary T cells do not stain with AMSGL-CD1b tetramer or a murine T cell receptor β chain constant region (mTCRBC) specific antibody (top). After transduction with the TCR, the cells stain with both the AMSGL-CD1b tetramer and mTCRBC antibody. (B) Flow plot depicts the percent of transduced T cells that are CD4, CD8, or DN. Boxplot depicts the median and interquartile range of the AMSGL-CD1b MFI of each CD4, CD8, and DN T cell that was transduced with the A05 TCR was compared (Two-way ANOVA, *** = $p < 0.0001$, n = 86,520). Boxplot depicts the median and interquartile range of the mTCRBC MFI of each CD4, CD8, and DN T cell that was transduced with the A05 TCR was compared (Two-way ANOVA, *** = $p < 0.0001$, n = 86,520). (C) CD4 and CD8 single cell clones were then generated from the primary T cell transductants. A representative CD4 (red) and CD8 (blue) T cell clone stained with AMSGL-CD1b tetramer is compared (left). A no tetramer control is also represented (grey) (left). Boxplots depict the median and interquartile range of AMSGL-CD1b MFI of CD4 (black) and CD8 (white) clones (Mann Whitney, $p = 0.019$, n = 16). (D) Antigen-specific activation of CD4 (black) and CD8 (white) T cell clones was measured using IFN-γ ELISPOT. Error bars represent standard deviation of triplicate wells. AMSGL was serially diluted log-fold from 1 μg/ml to 10^{-7} μg/ml.

While lower than the MFIs observed previously, these clones stain with AMSGL-CD1b tetramer above a no tetramer control, with an MFI of 35 (Figure 3.3.C). Despite attempts to generate a panel of clones with equivalent levels of exogenous TCR expression, the CD4 T cell clones had a mTCRBC MFI of 3637, while the CD8 clones had an MFI of 2923 ($p = 0.005$) (data not shown). This is consistent with our finding among bulk transduced cells and may suggest that CD4 T cells may intrinsically express higher levels of the exogenous TCR, particularly after *in vitro* culture, or possess intrinsic differences in their ability to be transduced with lentiviral vectors.

Finally, we assessed the impact of these observed differences in tetramer staining intensity on T cell activation between CD4 and CD8 T cells transduced with the A01 TCR by measuring IFN-γ production after antigen stimulation using IFN-γ ELISPOT. 1,000 tetramer-positive CD4 or CD8 T cells were co-incubated with K562 antigen presenting cells stably transfected with CD1b (K562-CD1b) and titrating concentrations of AMSGL. The CD4 T cell clone produced 36.3 IFN-γ spots per 1,000 cells at a lipid concentration of 1μg/ml, and displayed a half-maximal effective concentration (EC_{50}) of 0.0006 μg/ml (Figure 3.3D). However, the CD8 T cell clone produced 11 IFN-γ spots at a lipid concentration of 1μg/ml, and displayed an EC_{50} of 0.015 μg/ml (Figure 3.3D). These data show that transduced CD4 T cells are more sensitive to TCR-dependent antigen stimulation than transduced CD8 T cells, despite expressing the same T cell receptor.

We demonstrate here that transduced primary CD4 T cells bind AMSGL-CD1b tetramer with a higher MFI than CD8 and DN T cells, and are more sensitive to stimulation, even at low antigen concentrations. Further, our data suggest that transduced primary CD8 T cells bind AMSGL-CD1b tetramer with a higher intensity than DN T cells. These data show that TCR co-receptors are associated with higher tetramer MFI, but our data are limited by the inherent biological differences between CD4, CD8, and DN primary T cells.

3.5 CD8 JURKAT CELLS TRANSDUCED WITH AN AC_2SGL-SPECIFIC TCR EXHIBIT A HIGHER FUNCTIONAL AVIDITY THAN DN JURKAT CELLS

Thus, in these studies we demonstrate that the CD8 co-receptor expression is sufficient to confer increased tetramer binding in Jurkat cells transduced with the TCR from the A05 T cell line. We obtained a DN Jurkat cell line, and a Jurkat line that is derived from the DN line, but has been transduced to express CD8α homodimers. As these two lines are derived from the same parent Jurkat line, there should be no biological differences between these two lines, with the exception of CD8 expression.

First, to demonstrate that the A05 TCR is sufficient to confer AMSGL-CD1b tetramer binding in Jurkat cells, we transduced the CD8 Jurkat T cell line with the TCR of the A05 "CD4" T cell line. 0% of untransduced Jurkat cells bind both AMSGL-CD1b tetramer and a mTCRBC antibody (Figure 3.4A). After transduction with the A05 TCR, 77% of the Jurkat cells bind both AMSGL-CD1b tetramer and mTCRBC antibody, (Figure 3.4A). Thus, the A05 TCR is necessary and sufficient to confer antigen-specific tetramer staining in Jurkat cells.

Next, we transduced the DN and CD8 Jurkat cells with the A05 TCR and compared their ability to bind AMSGL-CD1b tetramer, as measured by MFI. Of note, the Jurkat cells that express CD8α display a gradient of expression, and the DN Jurkat cells exhibit low levels of CD4 co-receptor expression, (Figure 3.4.B, left). Thus, for this experiment we included only true CD8 and DN cells from the CD8 and DN line, respectively (Figure 3.4B, left). After staining both of the Jurkat T cell lines AMSGL-CD1b tetramer, the MFI of the CD8 line was 23043, while the MFI of the DN line was 13459, suggesting that the CD8 Jurkat line binds AMSGL-CD1b tetramer with a higher functional avidity ($p < 0.0001$) (Figure 3.4B, right). However, when we compared the

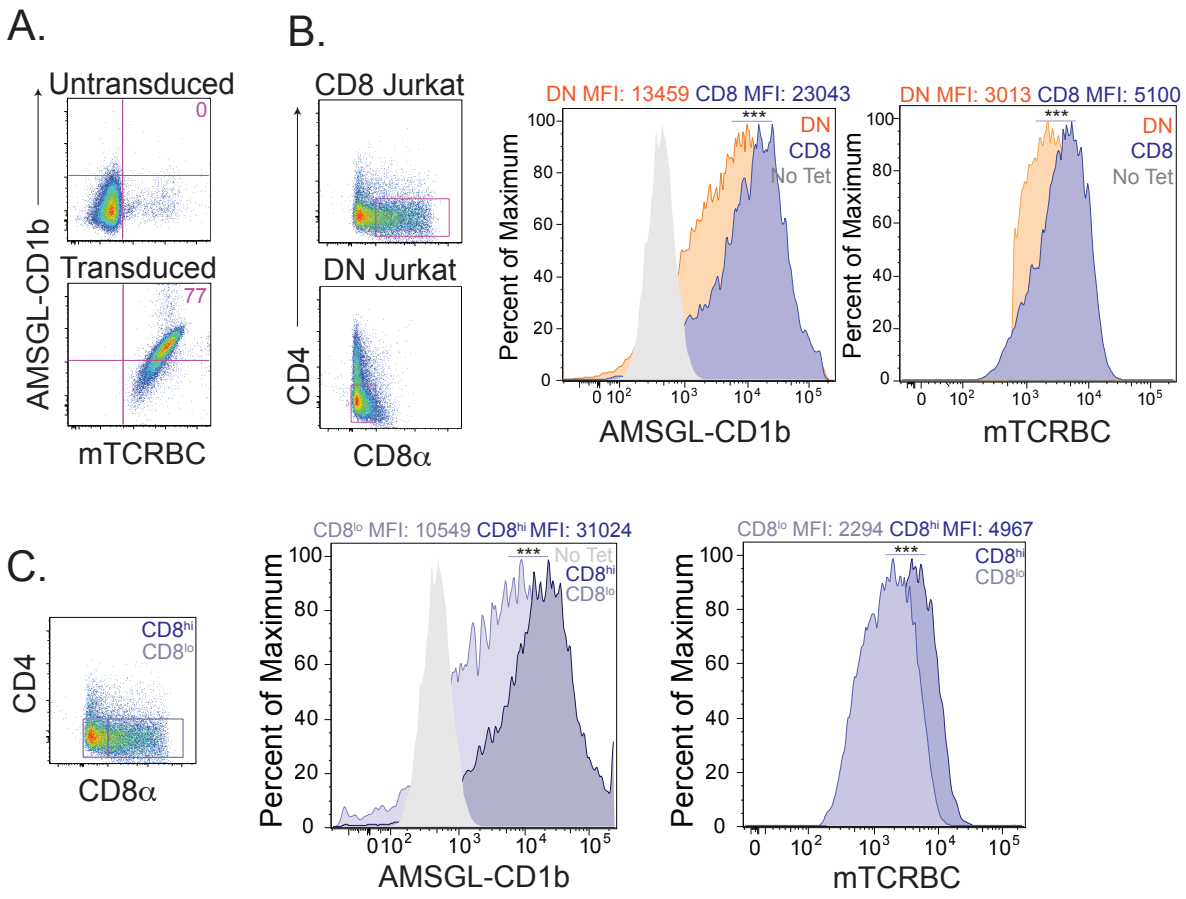

Figure 3.4. Functional avidity of CD8 and DN Jurkat T cells transduced with an Ac_2SGL-specific TCR.

DN and CD8 Jurkat cell lines were transduced with the TCR from the A05 T cell line. (A) Untransduced CD8 Jurkat cells do not stain with AMSGL-CD1b tetramer or a murine T cell receptor β chain constant region (mTCRBC) specific antibody (top). After transduction with the TCR, the cells stain with both the AMSGL-CD1b tetramer and mTCRBC antibody. (B) CD8 and DN Jurkat cells express a gradient of TCR co-receptor expression. For these studies, gates enclose true "CD8" (left, top) and "DN" (left, bottom) cells that express only CD8 or no co-receptors, respectively. The distributions of AMSGL-CD1b MFI of the DN (orange) and CD8 (blue) Jurkat cells were then compared (middle) (Student's t-test, $p < 0.0001$, $n = 29{,}195$). A no tetramer control is also represented (grey) (right). The distributions of mTCRBC MFI of the DN (orange) and CD8 (blue) Jurkat cells were also compared (right) (Student's t-test, $p < 0.0001$, $n = 29{,}195$). (C) The distributions of AMSGL-CD1b MFI of $CD8^{hi}$ (dark blue) (CD8α MFI of 10^3 to 10^5) and $CD8^{lo}$ (light blue) (CD8α MFI of 0 to 10^3) Jurkat cells were then compared (right) (Student's t-test, $p < 0.0001$, $n = 20{,}260$). A no tetramer control is also represented (grey) (right). The distributions of mTCRBC MFI of $CD8^{hi}$ (dark blue) and $CD8^{lo}$ (light blue) Jurkat cells were then compared (right) (Student's t-test, $p < 0.0001$, $n = 20{,}260$).

mTCRBC expression by both these lines, we found that the MFI of the CD8 line was 5100, while the MFI of the DN line was 3013, showing that the CD8 line expresses the exogenous TCR at a higher level, potentially contributing to the differences in functional avidity we observed ($p < 0.0001$) (Figure 3.4B). In fact, one explanation for the differences we observe in TCR expression between the CD4, CD8, and DN lines is that the expression of a TCR co-receptor on the surface stabilizes or otherwise increases the TCR expression on the surface of the cell to increase functional avidity.

To investigate this further, we compared AMSGL-CD1b MFI of the CD8α Jurkat cell line, and stratified Jurkats that expressed high ($CD8^{hi}$) and low levels ($CD8^{lo}$) of CD8α (Figure 3.4C, left). The $CD8^{hi}$ transductants had an MFI of 31024 and the MFI of the $CD8^{lo}$ Jurkat cells was MFI of 10549 ($p < 0.0001$) (Figure 3.4C, right). When we compared the level of mTCRBC expression, we found that the $CD8^{hi}$ transductants had an MFI of 4967 and the MFI of the $CD8^{lo}$ Jurkat cells was MFI of 2294 ($p < 0.0001$) (Figure 3.4C), consistent with our hypothesis that TCR co-receptor expression enhances TCR expression, which in turn may lead to the increase in functional avidity we describe here.

3.6 SUMMARY

In summary, we have shown that Ac_2SGL-specific T cells analyzed directly ex vivo exhibit a bias toward CD4 expression, and that CD4 Ac_2SGL-specific T cells have a higher functional avidity than CD8 Ac2SGL-specific T cells. Our data show that *ex vivo, in vitro*-derived, and transduced Ac_2SGL-specific T cells exhibit a consistent hierarchy in which CD4 T cells bind AMSGL-CD1b tetramer with a higher MFI, followed by CD8 T cells, and DN T cells. Further,

our data show that the surface expression of a TCR co-receptor is associated with increased levels of TCR expression, suggesting a potential mechanism for the increase in functional tetramer avidity we have observed.

However, several other potential mechanisms could be at play and these mechanisms are not mutually exclusive. First, as with peptide-specific T cells, the TCR co-receptors may physically bind to CD1b and augment TCR affinity for lipid-loaded CD1b (Janeway, 1992). However, due to the structural differences between MHC-II and CD1 molecules, putative binding sites for this interaction are unknown and should be the subject of future genetic and biophysical analyses. Further, it has been reported among peptide-specific T cells that the primary function of TCR co-receptors is to assist in recruitment of intracellular signaling molecules, and their role in stabilizing TCR-pMHC interactions contributes negligibly to T cell activation (Artyomov et al., 2010). In fact, T cells expressing mutant CD8 molecules that lack the ability to bind to MHC-I show similar activation levels to T cells expressing wild type CD8 (Hutchinson et al., 2003). As such, TCR co-receptors may not need to physically bind to CD1b for CD4 and CD8 to function as canonical TCR co-receptors.

Second, it has been shown in peptide-specific T cells expressing CD4 that precise spatial control of the immunologic synapse in part determines response to stimuli (Roh et al., 2015). One suggested mechanism for this is that the level of cholesterol in lipid rafts controls clustering of surface proteins at this site, which would affect T cell functional avidity and tetramer MFI (Schieffer et al., 2014). Studies have shown that CD4 and CD8 T cell lipid rafts are structured differently and do not reorganize the same way during TCR engagement, suggesting an alternate mechanism to the phenotypes we have observed here (Kabouridis, 2006). These additional

potential mechanisms should be the basis for future studies that investigate how TCR co-receptors affect glycolipid recognition by T cells.

Despite which factors influence these differences in functional avidity between CD4, CD8, and DN T cells, this phenomenon has significant implications for antigen recognition *in vivo*. Work from Chapter 2 and other studies has highlighted that subtle differences within the lipid tail can influence antigen affinity significantly (Chancellor et al., 2017, Van Rhijn et al., 2017). This work is furthered by the functional differences in cytokine release and cytotoxicity that GMM-specific T cells exhibit when activated by various chemically related but distinct antigens (Chancellor et al., 2017). Thus, an emerging model for glycolipid antigen recognition by human T cells is that the extent of activation and subsequent T cell function is directly related to antigen affinity. However, this model is obscured by the various factors that affect glycolipid-specific T cell affinity, which we currently model using antigen structure and T cell receptor sequence. As we now begin to understand that each chemically distinct antigen ought to be studied independently and that antigens can be recognized with high or low affinity depending on the T cell population, we propose that CD4, CD8, and DN glycolipid-specific T cells be treated as unique populations when studying glycolipid-specific T cell responses to M.tb infection or novel vaccine strategies.

Another significant implication of this study is that as CD4 mycobacterial glycolipid-specific T cells bind CD1b tetramers with higher functional avidity, human clinical studies using CD1b tetramers should be interpreted with caution. CD4 T cells may be more readily identified by tetramer staining due to their higher MFI and greater separation from the tetramer-negative population. In fact, the frequency of CD8 and DN mycobacterial glycolipid-specific T cells may be higher than reported due to this bias (Layton et al., 2018; Lopez et al., 2020). Complementary

methods for mycobacterial glycolipid-specific T cell identification should be considered to validate *ex vivo* findings, such as activation-based identification or higher valency molecular probes.

Future work should focus on two major areas. First, the impact that these differences in tetramer binding ability have on T cell activation and proliferation should be investigated in *in vitro* studies. Further, the effect of antigen exposure on CD4, CD8, and DN T cell frequency and memory phenotype *in vivo* should be robustly studied in human cohorts pre- and post-antigen exposure and in controlled animal studies. As our data demonstrate that most Ac_2SGL-specific T cells express CD4, one hypothesis that our data raises is that CD4 T cells may exist at a higher frequency because they expand more readily during antigen exposure due to their higher functional avidity. However, this could also be an artifact of the thymic selection process as CD4 T cells may have a higher affinity for CD1b during selection and may undergo positive selection more readily than CD8 CD1b-restricted T cells. These questions can be studied using a humanized transgenic murine model that has previously been used to examine thymic selection of a mycolic acid-specific T cell line that expressed neither CD4 or CD8 (Felio et al., 2009; Zhao et al., 2015)

In conclusion, we report that CD4 and CD8 TCR co-receptors increase mycobacterial-glycolipid-specific TCR binding strength to glycolipid-loaded CD1b tetramers. We have provided insights from *ex vivo* and *in vitro* studies that CD4 T cells exhibit higher functional avidity for Ac_2SGL-loaded CD1b, and that these differences may translate to differences in T cell activation and cytokine release.

3.7 MATERIALS AND METHODS

3.7.1 *Ethics Statement*

The study protocols were approved by the IRBs of the University of Washington, the Fred Hutchinson Cancer Research Center, or the University of Cape Town. Written informed consent was obtained from all adult participants as well as from the parents and/or legal guardians of the adolescents who participated. In addition, written informed assent was obtained from the adolescents.

3.7.2 *Clinical Cohorts*

For *ex vivo* analysis of Ac_2SGL-CD1b tetramer positive cells, we studied two cohorts of healthy subjects. First, U.S. healthy controls were recruited and enrolled at the Seattle HIV Vaccine Trials Unit as part of a cohort of healthy adults used to provide blood samples for developing and testing new assays. PBMC collected by leukapheresis from 20 HIV-seronegative individuals with a known Co-receptor response to CMV were used here. Second, we studied a subset of 6363 South African adolescents that were enrolled into a study that aimed to determine the incidence and prevalence of tuberculosis infection and disease (Mahomed et al., 2011). 12- to 18-year-old adolescents were enrolled at eleven high schools in the Worcester region of the Western Cape of South Africa. Subjects were screened for the presence of latent tuberculosis by a tuberculin skin test and IFN-γ release assay (IGRA) QuantiFERON-TB GOLD In-Tube (QFTG) (Cellestis Inc.) at study entry. PBMC were isolated from freshly collected heparinized blood via density centrifugation and cryopreserved. For this work, a sample of 10 M.tb-infected (QFTG+) and 8 M.tb-uninfected (QFTG-) adolescents were selected based on availability of PBMC.

3.7.3 *Culture Media*

Media (R10) for washing peripheral blood mononuclear cells (PBMC) consisted of RPMI 1640 (Gibco, Waltham, MA) supplemented with 10% fetal calf serum (Hyclone, Logan, UT). Our base T cell media (TCM) consisted of RPMI 1640 supplemented with 10% fetal calf serum, 100 U/ml Penicillin, 100 mg/ml Streptomycin, 55 mM 2-mercaptoethanol, 0.3X Essential Amino Acids, 60 mM Non-essential Amino Acids, 11 mM HEPES, and 800 mM L-Glutamine (Gibco, Waltham, MA) sterile-filtered. Our TCM containing human serum (TCM/HS) consisted of 10% human serum (derived from healthy donors), 100 U/ml Penicillin, 100 mg/ml Streptomycin, and 400 mM L-Glutamine (Gibco, Waltham, MA).

3.7.4 *Generation of SGL-loaded CD1 Tetramers*

Soluble biotinylated CD1b monomers were provided by the National Institutes of Health Tetramer Core Facility (Emory University, Atlanta, GA). The loading protocol for CD1b monomers was based on previously published glucose monomycolate loading protocols (Kasmar et al. 2011). AMSGL was dried down in a glass tube in a stream of nitrogen and sonicated into a 50 mM sodium citrate buffer at pH 4, containing 0.25% with 3-[(3-cholamidopropyl)dimethylammonio] -1-propanesulfonate (CHAPS) (Sigma, St. Louis, MO) for two minutes at 37°C. The sonicate was transferred to a microfuge tube, and 20 μg of CD1b monomer was added and incubated in a 37°C water bath for 2 hours with vortexing every 30 minutes. At the end of the incubation, the solution was neutralized to pH 7.4 with 6 μl of 1M Tris pH 9. After addition of CD1b, the mixture was incubated in a 37°C water bath for 2 hours. Finally, 10 μl of Streptavidin conjugated to ECD or APC (Life Technologies, Carlsbad, CA) was added in

ten aliquots of 1 µl every 10 minutes. The final product was filtered through a SpinX column (Sigma, St. Louis, MO) to remove aggregates and stored at 4°C until use.

3.7.5 *Tetramer Staining*

For *ex vivo* analysis of Ac_2SGL-CD1b tetramer positive cells, PBMC were thawed in warm thaw media (R10 with 2 µl/ml Benzonase (Millipore, Billerica, MA) sterile-filtered) and centrifuged at 1500 rpm for 5 minutes. The supernatant was decanted, and the cells were resuspended in R10 and counted by Trypan Blue (Millipore, Billerica, MA) exclusion. The cells were centrifuged at 1500 rpm for 5 minutes and plated at a density of 1 million cells per well in a 96-well U-bottom plate. A portion of the PBMC were resuspended in R10 at a density of 2 million cells per ml in 50 ml conicals with the caps lightly in place and rested overnight at 37°C in humidified incubators supplemented with 5% CO_2. The PBMC in the 96-well plate were washed with FACS buffer (1x phosphate-buffered saline (PBS) (Gibco, Waltham, MA) supplemented with 0.2% bovine serum albumin (BSA) (Sigma, St. Louis, MO) and centrifuged at 1800 rpm for 3 minutes. Next, the cells were washed twice with PBS and stained with Aqua Live/Dead stain (Life Technologies, Carlsbad, CA) according to the manufacturer's instructions. Following a 15 minute incubation at room temperature, the cells were washed twice in PBS. They were then blocked with human serum (Valley Biomedical, Winchester, VA) and FACS buffer mixed 1:1 for 10 minutes at 4°C. The wells were washed twice with FACS buffer and then resuspended in 50 µl FACS buffer with 1 µl of unloaded CD1b tetramer and 1 µl of each AMSGL-loaded CD1b tetramer labeled with APC or ECD and incubated at room temperature for 40 minutes in the dark. After this incubation period, the cells were washed twice with FACS buffer and then labelled with anti-CD3 ECD (Beckman Coulter, Brea, CA), anti-CD4 APC Ax750 (Beckman Coulter, Brea, CA), and anti-CD8β BB700 (BD Biosciences, San Jose, CA) antibodies for 30 minutes at 4°C. After

two final washes in FACS buffer, the cells were fixed in 1% paraformaldehyde (PFA) (Electron Microscopy Sciences, Hatfield, PA) and acquired on a BD LSRFortessa (BD Biosciences, San Jose, CA) equipped with blue (488 nm), green (532 nm), red (628 nm), violet (405 nm), and ultraviolet (355 nm) lasers.

For tetramer analysis of *in vitro*-derived T cell lines and transduced T cells, T cell lines or transductants were plated at one million cells per well in a 96-well U-bottom plate. Cells were washed twice with PBS and resuspended with Live/Dead Fixable Aqua or with Live/Dead Fixable Green Dead Cell Stain Kit (Life Technologies, Carlsbad, CA) per the manufacturer's instructions. For this step and all subsequent steps, the cells were kept in the dark. Following a 15 minute incubation, cells were washed twice with PBS and blocked with human serum (Valley Biomedical, Winchester, VA) prepared in FACS buffer (1x PBS (Gibco, Waltham, MA) supplemented with 0.2% BSA (Sigma, St. Louis, MO)) mixed 1:1 for 10 minutes at 4°C. Cells were then resuspended in 50 µl of FACS buffer containing 1 µl of AMSGL-loaded CD1b and 1 µl of mock-loaded control CD1b tetramers, then incubated at room temperature for 60 minutes. The tetramer titers were determined prior to use in the present study (data not shown). Following a 15 minute incubation at room temperature, the cells were washed twice in PBS and then stained with anti-CD3 ECD (Beckman Coulter, Brea, CA), CD4 APC Ax750 (Beckman Coulter, Brea, CA) and anti-CD8α PerCP Cy5.5 (BD Biosciences, San Jose, CA). When T cells transduced with exogenous TCR were used anti-mTCRBC APC (BD Biosciences, San Jose, CA) was also included in the antibody cocktail. The optimal titers of all antibodies were determined prior to use (data not shown). After two final washes in FACS buffer, the cells were fixed in 1% paraformaldehyde (PFA) (Electron Microscopy Sciences, Hatfield, PA) and acquired on a BD LSRFortessa (BD Biosciences, San Jose, CA).

3.7.6 *T cell Receptor Cassette Construction*

Codon-optimized A01 and A05 T cell TCR sequences were assembled into a TCR cassette (Linnemann et al. 2013). In this construct, the TCR α and TCR β chain constant regions are replaced with modified murine TCR constant regions to facilitate measurement of TCR expression and to encourage pairing between exogenous TCR chains. The TCR cassettes were synthesized through Thermo Fisher GeneArt Synthesis service and were then cloned into pRRL.PPT.MP.GFPpre (Jing et al. 2016; Zhou et al. 2012) using BamHI and SalI restriction enzymes (New England BioLabs, Ipswich, MA). All plasmids were purified using Maxi Prep kits (Qiagen, Hilden, Germany).

3.7.7 *Generation of Lentivirus*

Lenti-X HEK293T cells (Clontech, Mountain View, CA) were seeded at 2 million cells per 100 mm tissue culture dish and incubated for 48 hours at 37˚C/5% CO2 in DMEM (Gibco, Waltham, MA) or until cells reached 75% confluency. The medium was replaced 4 hours before transfection. Cells were transfected with 10 µg pRRL-TCR plasmid, 5 µg pCI-VSVG envelope plasmid, and 5 µg of a psPAX2 packaging vector (gifted from Dr. Stanley Riddell at Fred Hutchinson Cancer Research Center). Plasmids were mixed with Fugene 6 transfection reagent (Promega, Madison, WI) at a dilution of 1:12 in a total volume of 600 µl. Transfection mixture was added dropwise into the cell culture and incubated overnight in the conditions described above. The medium was then replaced and incubated for an additional 48 hours. After this time, 20 µl of supernatant was titered using Lenti-X GoStix (Clontech, Mountain View, CA) per the manufacturer. Supernatant was then harvested every 12 hours for a total of three collections. At each collection, cell debris was removed by centrifugation at 1500 rpm for 5 minutes, and cleaned

supernatant was reserved in a 50-ml conical and kept at 4˚C until three collections had been acquired. Supernatant was then incubated overnight with Lenti-X concentrator (Clontech, Mountain View, CA) at a ratio of 1:3. The following day, the supernatant was centrifuged at 1500×g for 45 minutes at 4˚C. Supernatant was then discarded, and the pelleted virions were resuspended in 300 µl R10 media and stored at − 80˚C until further use.

3.7.8 *Transduction of Jurkat Cells*

CD8-expressing Jurkat cells were seeded at 1 million cells per well in a 48-well plate in enhanced RPMI. The same day, the Jurkat cells were transduced with TCR lentivirus at an estimated multiplicity of infection (MOI) of 5 with 1 µl of polybrene at a final concentration of 4 µg/ml (Sigma, St. Louis, MO). Cells and virus were incubated for 4 hours at 37˚C/5% CO2 and washed with PBS (Gibco, Waltham, MA) to remove excess virus. Jurkat cells were maintained in culture for 1 week using enhanced RPMI and screened for TCR expression (Jing et al. 2016) using an anti-mouse TCR β chain APC antibody (BD Biosciences, San Jose, CA) and tetramer staining as described above.

3.7.9 *Transduction of Primary T cells*

Cryopreserved PBMC from a random blood bank donor (Bloodworks Inc, Seattle, WA) was thawed as described above and enumerated using trypan blue exclusion. T cells were isolated from PBMC using magnet activated cell sorting (MACS) using the Pan T cell Isolation Kit (negative selection) according to the manufacturer's instructions (Miltenyi Biotec, Germany). Following separation, T cells are enumerated using Trypan Blue exclusion and co-incubated with CD3/CD28 Human T cell Activating Dynabeads (ThermoFisher) at a 3:1 bead:T cell ratio in a total volume of 1 ml TCM supplemented with 50 units/ml recombinant IL-2 in a 48-well plate.

On day 2, lentiviral stock and 4 μg/ml polybrene was added to culture. Viral titer is determined prior to use (data not shown). Following viral addition to the well, the 48-well plate is then centrifuged at 679 x g for 90 minutes at 32˚C. The cells are then incubated at 37˚C/5% CO_2 for 48 hours.

On day 4, the cells are harvested and transferred to a 4 ml FACS tube and rinsed with 3 ml of TCM. The cells are then centrifuged at 1,300 rpm for 5 minutes to remove the polybrene from the cells. Following centrifugation, the cells are resuspended in TCM supplemented with rIL-2 as described above and returned to the original well. The cells are then incubated for 72 hours at 37˚C/5% CO_2.

On day 7, the cells are harvested and moved to a 4ml FACS tube and incubated on a magnetic stand for 10 minutes at room temperature to remove the Dynabeads. The media, which contains the activated T cells, was then removed and added to a 15 ml conical. Fresh media is then added to the 4 ml FACS tube to rinse the beads, and the 4 ml FACS tube is then returned to the magnetic stand and incubated for 5 minutes at room temperature. The media is then removed from the 4 ml FACS tube and added to the 15 ml conical. Cells are then centrifuged at 1,300 rpm for 5 minutes, and resuspended in fresh TCM supplemented with rIL-2 and returned to the 48-well plate. Cells are then incubated for 4 days at 37˚C/5% CO_2 and maintained as necessary.

On day 12, the cells are then assayed to quantify T cell transduction by tetramer staining as described above.

3.7.10 *T cell Sorting*

The transduced T cells are then sorted to purity using a modified version of the tetramer staining method described above. However, after the antibody stain, the transduced T cells are resuspended in 200 μl of FACS buffer and tetramer-positive T cells were sorted at the UW

Department of Immunology Flow Cytometry Core using a FACS Aria II (BD Biosciences, San Jose, CA) cell sorter equipped with blue (488 nm), red (641 nm), and violet (407 nm), lasers. Cells were sorted into 3 ml of TCM in 4 ml FACS tubes.

3.7.11 *Rapid Expansion Method*

Further expansion of the T cells transduced with exogenous TCR was performed using a modified version of a previously established rapid expansion protocol (Riddell et al., 1992). Briefly, 100,000 T cells were mixed with 5 million irradiated EBV-transformed B cells and 25 million irradiated PBMC as feeder cells in R10 in T25 tissue culture flasks (Costar, St. Louis, MO) with 25 ml TCM. Anti-CD3 (clone OKT3) was added at a final concentration of 30 ng/ml, and the mixture was incubated overnight at 37ºC/5% CO_2. The following day, recombinant IL-2 (rIL-2) (Prometheus Pharmaceuticals through UWMC Clinical Pharmacy) was added at a final concentration of 50 U/ml. On day 4, the cells were washed twice in TCM to remove the anti-CD3 antibody and resuspended in fresh media supplemented with rIL-2 at 50 U/ml. Half the media was replaced every three days or split into new T25 tissue culture flasks as determined by cell confluency. After 13 days in culture, the transduced T cells were screened by tetramer staining and then frozen on day 14.

3.7.12 *Limiting Dilution Cloning*

Sorted T cells were washed and resuspended in TCM/HS and plated at 1 or 2 cells per well in each well of a 96-well plate to create single cell clones. Irradiated PBMC (150,000 cells per well) were added as feeder cells along with PHA (Remel, San Diego, CA) at a final concentration of 1.6 µg/ml. After two days in culture at 37˚C/5% CO_2, 10 µl natural IL-2 (Hemagen, Columbia, MD) was added to each well. Half the media was replaced every two days with TCM/HS and

natural IL-2. Cultures were maintained for 14 days and screened for antigen specificity by tetramer staining and IFN-γ ELISPOT.

3.7.13 *IFN-γ ELISPOT*

We used an IFN-γ ELISPOT to determine the antigen specificity of our T cell lines. EMD Multiscreen-IP filter plates (Millipore, Billerica, MA) were coated with 1D1K antibody (Mabtech, Sweden) diluted 1:400 in PBS and incubated overnight at 4˚C. The following day, one thousand T cells were plated 1:50 with K562 cells stably transfected with CD1b or with a mock vector. Lipids antigens were stored in 2:1 chloroform:methanol and appropriate amount was dried using gaseous nitrogen. The lipids were sonicated into media to obtain a 4 μg/ml suspension and plated with the cells at a final concentration of 1 μg/ml. These cultures were incubated at 37˚C for approximately 16 hours. The following day, the cells were washed twice with sterile water to lyse the cells, and the plates were incubated with the detection antibody 7-B6-1-biotin (Mabtech, Sweden) diluted 1:1000 in PBS + 0.5% FCS and incubated for two hours at room temperature. The cells were then washed five times with PBS and incubated in ExtrAvidin-Alkaline Phosphatase (Sigma, St. Louis, MO) diluted 1:1000 in PBS and incubated for one hour at room temperature. The wells were then washed five times and incubated with BCIP/NBT substrate (Sigma, St. Louis, MO) for five minutes to develop the membrane. The wells and IFN-γ spots were counted using an ImmunoSpot S6 Core Analyzer (Cellular Technology Limited, Cleveland, OH).

3.7.14 *Statistical and Computational Methods*

Initial compensation, gating, and quality assessment of flow cytometry data was performed using FlowJo version 9 (FlowJo, TreeStar Inc, Ashland OR). Unless otherwise-stated, the gating strategy for flow cytometry assays began with gating of singlets and viable cells. Lymphocytes

were then identified by size gating, and T cells were identified using anti-CD3. The T cells were further examined for antigen-specificity using AMSGL-CD1b tetramers. Flow cytometry data processing and MFI extraction was performed using the OpenCyto framework in the R programming environment (Finak et al., 2014; R Core Team, 2016). Statistical tests were conducted in R (v3.8.5) or Graph Pad Prism version 6 (GraphPad, GSL Biotech, San Diego, CA).

Chapter 4. TCR CO-RECEPTORS DEFINE DISTINCT FUNCTIONAL SUBSETS OF MYCOBACTERIAL GLYCOLIPID-SPECIFIC T CELLS

4.1 INTRODUCTION

TCR engagement with antigen-loaded antigen presenting molecules triggers intracellular signaling pathways that induce T cell proliferation and cytokine secretion (Weiss and Littman, 1994). The functional outcome of this interaction is affected by the molecular factors within the TCR/antigen presenting molecule interaction at the immunological synapse (Huang et al., 2012). Of these parameters, TCR affinity for the loaded antigen-presenting molecule is one of the most extensively studied (Stone et al., 2009). One model proposes that T cells with the highest affinity TCR have a competitive advantage during the immune response, as they receive more sustained TCR signaling than T cells with a lower affinity TCR (Busch and Pamer, 1999; Zehn et al., 2009). Thus, as the immune response progresses, the T cell repertoire responding to the antigen gets less diverse as high affinity clones become more prevalent (Busch and Pamer, 1999). Further, when peptide-specific T cells are activated with altered peptide antigens, these differences in the affinity of TCR–pMHC engagement can activate different signaling pathways, leading to different effector functions and rates of T cell proliferation (Sloan-Lancaster and Allen, 1996)

However, sustained TCR signaling and proliferation can also lead to T cell senescence and exhaustion, where T cells become terminally differentiated effector cells with limited functional and protective capacity (Schietinger and Greenberg, 2014). In fact, this is one explanation for a model where subdominant T cell clones contribute significantly to protective immune responses to pathogens, as these subdominant responses may be less prone to terminal differentiation and

promote more durable immunity (Moguche et al., 2017). Thus, the level of TCR signaling and engagement during an immune response is a key factor that shapes T cell differentiation and function.

TCR co-receptors also define functional subsets of T cells. Canonically, peptide-specific T cells that express the CD4 co-receptor can be divided into four major functional subsets: Th1, Th2, Th17, and Treg. These functional lineages are driven by the master transcription factors T-bet, GATA3, ROR-γt, and FOXP3, respectively (Fontenot et al., 2003; Hori et al., 2003; Ivanov et al., 2006; Szabo et al., 2000; Zhen and Flavell, 1997). Conversely, peptide-specific T cells that express the CD8 co-receptor are traditionally cytotoxic T cells. However, MHC-restricted T cells exhibit functional plasticity and can alter their functional program over the course of the T cell's life-span (Sallusto et al., 2018). Peptide-specific T cell fate is determined during thymic selection (Taniuchi, 2018). Bipotential DP thymocytes that express a MHC-I or MHC-II specific TCR differentiate into CD8 single positive (SP) or CD4 SP thymocytes, respectively (Taniuchi, 2018). These subsets are committed to either a cytotoxic or helper T cell lineage by epigenetic changes driven by the transcription factors Runx3 or ThPOK, respectively (Taniuchi, 2018).

iNKT and MAIT cells are also divided into distinct functional classes based on the co-receptors they express, yet these T cell subpopulations recognize the same antigens presented by the same antigen-presenting molecule. In humans, iNKT cells that express the CD4 co-receptor are Th0/Th2-like, and DN iNKT cells are Th1 (Gumperz et al., 2002; Lee et al., 2002a). $CD8^+$ MAIT cells express higher levels of IL-12 receptor (IL-12R) and IL-18R, along with higher levels of granulysin, granzyme B, and perforin, suggesting that they are more sensitive to TCR-independent signaling and are more potently cytotoxic (Dias et al., 2018). DN MAIT cells express less IFN-γ and more IL-17 than $CD8^+$ MAIT cells, and have a higher ROR-γt to T-bet ratio,

indicative of a Th17 phenotype (Dias et al., 2018). While the mechanism for this functional distinction is unknown, one discussed model is that the CD8 co-receptor stabilizes and enhances the interaction between the MAIT cell TCR and the MR1-antigen complex (Dias et al., 2018). Consistent with this mechanism, blocking CD8 with a monoclonal antibody leads to decreased MAIT cell responses to *Escherichia coli* (Kurioka et al., 2017) Thus, an emerging model for these functional distinctions between innate-like T cells is that TCR co-receptor expression potentiates T cell activation and affects T cell functional profile. However, whether distinct functional classes exist within mycobacterial glycolipid-specific T cells and how they are defined is unknown.

Some data suggest that TCR affinity for glycolipid-loaded CD1b molecules may be involved. *in vitro*-derived T cell clones with different affinities for GMM-loaded CD1b tetramer have been shown to have different functional capabilities. T cells clones that express the high affinity GEM TCR and the CD4 co-receptor expressed high levels of Th1 cytokines, whereas the T cells clones with lower affinity TCRs expressed Th1 cytokines along with IL-17 (Van Rhijn et al., 2014). Of note, the T cell clones with lower affinity TCRs expressed either the CD8αβ heterodimer or were DN (Van Rhijn et al., 2014). As these data were generated with a panel of *in vitro*-derived T cell clones, it is unclear whether this distinction exists *in vivo*. Further, whether this phenomenon is generalizable to T cells that recognize other mycobacterial lipid antigens is unknown.

In Chapter 3, we showed that mycobacterial glycolipid-specific T cells that express the CD4 co-receptor bind glycolipid-loaded CD1b tetramers with higher intensity than T cells that express the CD8 co-receptor. Here, we address the hypothesis that CD4 and CD8 mycobacterial glycolipid-specific T cells express distinct functional profiles. We show using *in vitro* and *ex vivo*

studies that functional subpopulations of mycobacterial glycolipid-specific T cells can be defined by the expression of the CD4 or CD8 TCR co-receptor.

4.2 Functional Differences Between CD4 and CD8 Ac_2SGL-specific T cell Lines

We used two previously described T cell lines, named A01 and A05 (James et al., 2018). The A01 T cell line expresses a CD8αβ heterodimer, whereas A05 expresses the CD4 co-receptor (Figure 3.2A). As these two T cell lines express different co-receptors, we predicted that they would exhibit differences in their sensitivity to antigen and functional profile.

First, we profiled IFN-γ production by both T cell lines to determine differences in antigen sensitivity and cytokine release in *in vitro*-derived T cell lines. We co-incubated 1,000 tetramer-positive cells with K562-CD1b antigen presenting cells with titrating amounts of the Ac_2SGL analog, AMSGL, and measured IFN-γ production by ELISPOT. The A05 T cell line produced 113 IFN-γ spots per 1,000 tetramer-positive cells after stimulation and exhibited EC_{50} of 0.0007 μg/ml (Figure 4.1A). Conversely, the A01 T cell line produced 89 IFN-γ spots per 1,000 tetramer-positive cells, and exhibited EC_{50} of 0.06 μg/ml (Figure 4.1A). This demonstrates that the CD4 T cell line is more sensitive to activation, particularly at a limiting antigen concentration.

Next, we examined the functional profiles of both T cell lines using a previously optimized intracellular cytokine staining panel (De Rosa et al., 2012). Both T cell lines were stimulated with K562-CD1b or K562-EV antigen presenting cells loaded with AMSGL for six hours, and Th1, Th2, and Th17 cytokine production was measured. 91% of A05 and 81% of A01 T cells express Th1 cytokines after stimulation (e.g., (IFN-γ, TNF, and IL-2) (Figure 4.1B). In addition, 80% of

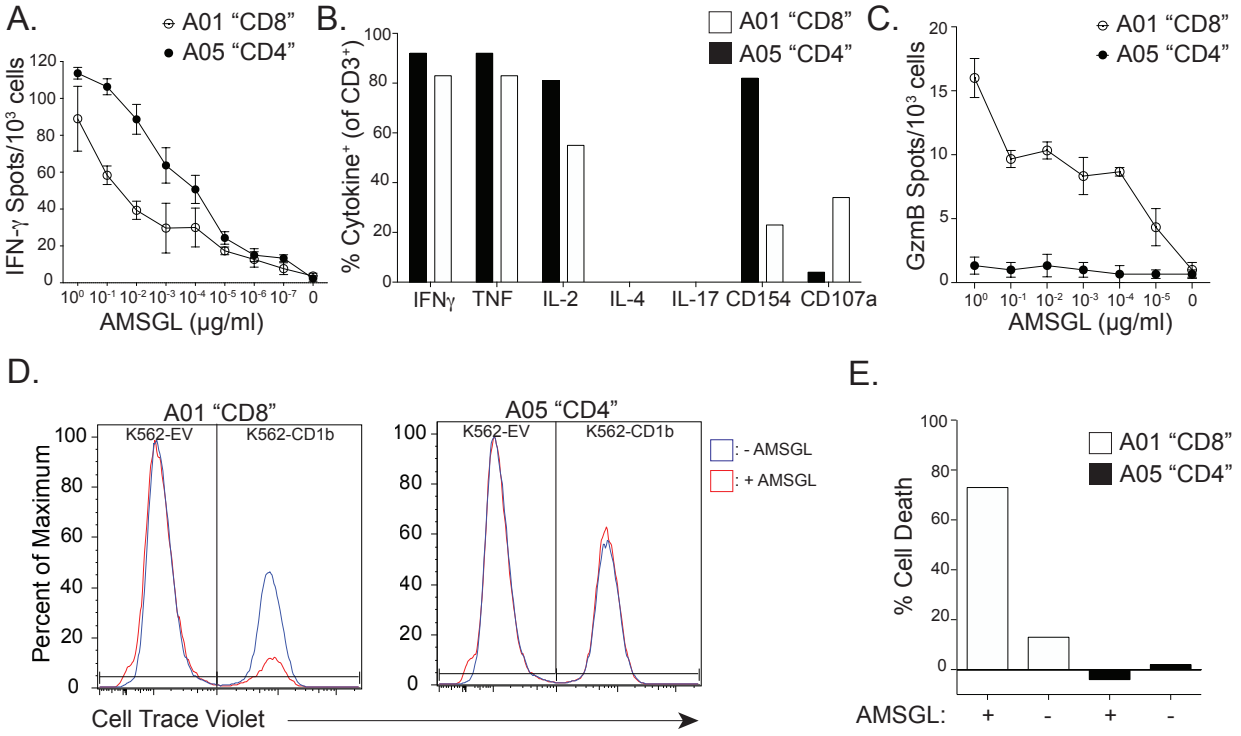

Figure 4.1. **Functional profiles of the A01 and A05 T cell lines.**

We profiled the functional profiles of the A01 and A05 T cell lines. (A) IFN-γ production by 1,000 tetramer-positive T cells from the A01 (white) and A05 (black) T cell lines after co-incubation with K562-CD1b antigen presenting cells and AMSGL antigen. Cells were cultured overnight and IFN-γ production was assessed using IFN-γ ELISPOT. Antigen concentration ranged from 1 µg/ml to 10^{-7} µg/ml in log-fold dilutions. Error bars represent standard deviation of triplicate wells. (B) Cytokine production by the A01 (white) and A05 (black) T cell lines was measured using intracellular cytokine staining after co-incubation with K562-CD1b antigen presenting cells and AMSGL antigen for 6 hours. Data are expressed as a percent of T cells that express the cytokine of total $CD3^+$ T cells. Percentages are corrected for background expression of the cytokine by subtracting the percentage of T cells that express the cytokine after co-incubation with K562-EV antigen presenting cells and AMSGL for 6 hours. (C) Granzyme B (GzmB) production from 1,000 T cells from the A01 (white) and A05 (black) T cell lines after co-incubation with K562-CD1b antigen presenting cells and AMSGL antigen. Cells were cultured overnight and GzmB production was assessed using GzmB ELISPOT. Antigen concentration ranged from 1 µg/ml to 10^{-5} µg/ml in log-fold dilutions. Error bars represent standard deviation of triplicate wells. (D) Cytotoxicity was assayed by co-incubating A01 (left) and A05 (right) T cell lines with K562-EV and K562-CD1b antigen presenting cells labeled "low" and "high" with Cell Trace Violet, respectively. Co-cultures were incubated in the presence (red) or absence (blue) of AMSGL antigen. (E) Cytotoxicity was quantified by calculating the percent of cell number reduction of K562-CD1b cells compared to the K562-EV cells (% Cell Death). Percentages were calculated for the A01 (white) and A05 (black) T cell lines in the presence or absence of AMSGL. All data in this Figure are representative of at least 2 independent experiments.

the cells in the CD4 T cell line expressed CD40 ligand (CD40L) on the surface, which is known to interact with CD40 expressed on B populations. By contrast, only 19% of the T cells in the A01 line express this marker. However, 37% of the A01 T cell line expressed CD107a, a degranulation marker suggesting cytotoxic activity, whereas only 4% of T cells in the A05 line express this marker after stimulation (Figure 4.1B). Thus, these data show that while the CD4 and CD8 T cell lines both express Th1 cytokines, they are functionally distinct. The CD4 T cell expresses CD40L after antigen stimulation, suggesting this T cell population may be involved in B cell help, and the CD8 T cell line expresses CD107a, and may be cytotoxic.

To determine whether these T cell lines exhibit differences in cytotoxic potential, we first measured granzyme B production after overnight stimulation with AMSGL-loaded K562-CD1b cells. Granzyme B production was measured using an ELISPOT assay. After stimulation the A01 T cell line secreted 10-fold more granzyme B per 1,000 cells than the A05 T cell line, as measured by granzyme B ELISPOT (Figure 4.1C). Further, we detected granzyme B production from the A01 T cell line at a 10^{-5} μg/ml concentration of AMSGL (Figure 4.1C).

Next, to determine differences in cytotoxic activity, we co-incubated K562-CD1b and K562-EV antigen presenting cells with the A01 or A05 T cell lines in the presence or absence of AMSGL. We defined specific lysis as the ability of a T cell line to specifically reduce the K562-CD1b cell population in the presence of lipid, while leaving the K562-EV population and the K562-CD1b without pulsed antigen intact after co-incubation. The A01 T cell line specifically killed 78% of K562-CD1b cells in the presence of lipid when compared to K562-EV cells (Figure 4.1D). Further, the A05 T cell line exhibited no cytotoxic capacity (Figure 4.1D, right). Thus, we were able to detect functional differences between the CD4 and CD8 T cell lines. However, these

data are limited by the repeated *in vitro* expansion of these lines, which may affect T cell functional profile.

4.3 Establishing an *ex vivo* Single Cell Phenotyping Workflow

Here, we adapted an established method to profile paired TCR sequences, transcription factor, and cytokine expression from single cells (Han et al., 2014). In brief, single T cells are sorted into wells of a 96-well plate and subjected to three rounds of transcript amplification. First, the single cells are lysed and reverse transcription and pre-amplification of gene targets is performed (gene targets described in Appendix B). Second, nested PCR of gene targets is performed. Lastly, each well is barcoded according to its location within the 96-well plate and Illumina paired-end adapters are added. The amplicons are then pooled and sequenced on an Illumina MiSeq.

The data processing, quality control (QC), and annotation pipeline was based on the VDJfasta pipeline developed by Glanville et al. (Glanville et al., 2009). This pipeline involves trimming, joining, demultiplexing, and then aligning the reads to a set library of genes. This method is computationally superior to another published method for analyzing these data that processes the TCR and phenotype genes separately using an antigen receptor alignment software, MiXCR, and STAR RNA sequencing (RNA-Seq) aligner, respectively (Bolotin et al., 2015; Xu et al., 2019). The latter is computationally intensive, taking over 49 hours to fully process one dataset. In addition, the phenotype alignment method requires such a large amount of computational power that this step in the pipeline must also be submitted to a computer cluster for

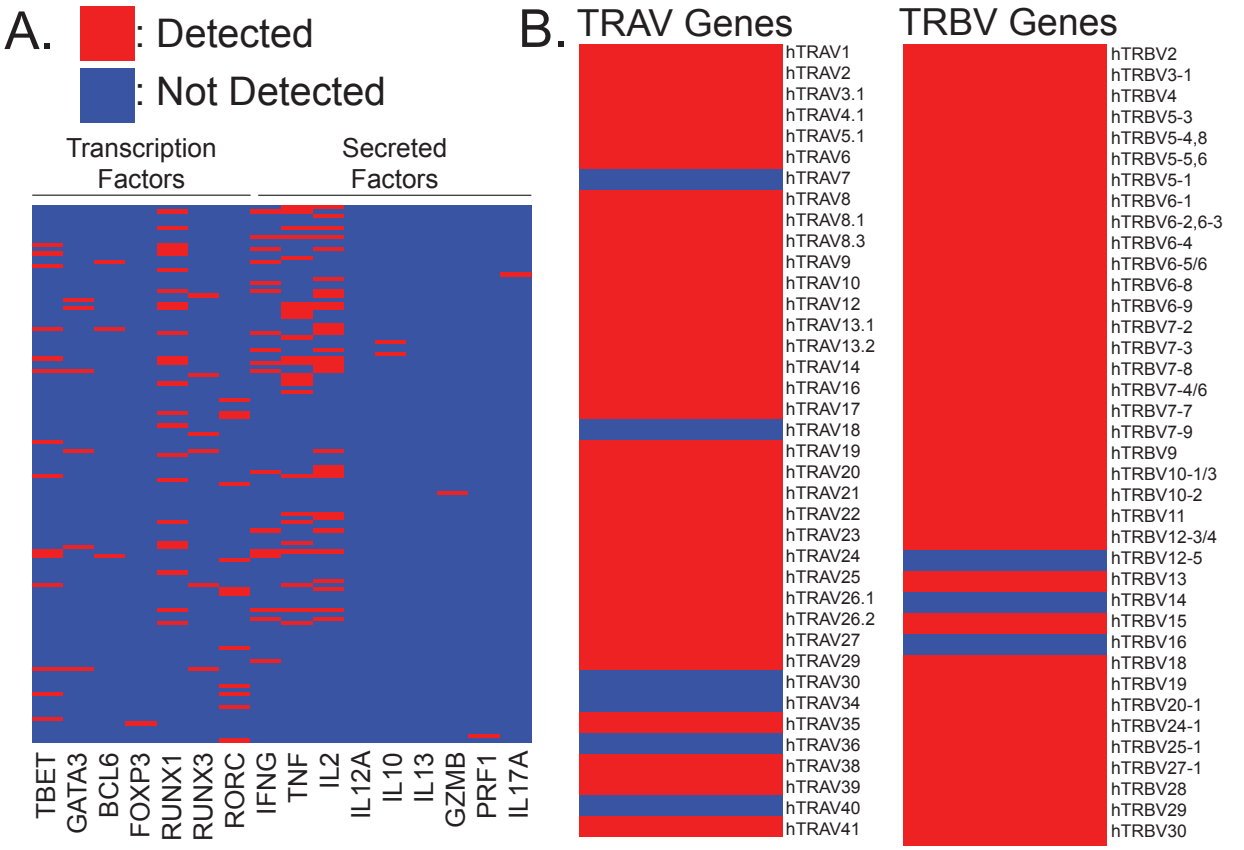

Figure 4.2. **Validation of single cell phenotyping workflow.**

An established single cell phenotyping workflow is adapted here to profile the TCR α and β chains and functional profiles of single T cells. We validated this by sorting single PMA/ionomycin-stimulated $CD3^+$ T cells from cryopreserved PBMC isolated from a random blood bank donor and evaluating amplification of each target gene using this workflow. The amplified transcripts were sequenced using an Illumina MiSeq and detection of each gene target is represented here. Reads were aligned using VDJFasta, and Immunogenetics nomenclature is used. (A) Heatmap displaying the phenotypes of each sorted cell. Each row depicts the genes expressed by one cell (n = 128). Transcription factor and secreted factor and cytokine transcripts that were detected are represented in red, and transcripts that were not detected in that cell are represented in blue. Gene symbols are used. (B) TCR α chain variable (TRAV) genes that were used by reads that aligned to TCR genes are represented in red, and TRAV genes that were not detected are depicted in blue. Each row is one TRAV gene (n = 2,353,192 reads sampled). (C) TCR β chain (TRBV) genes that were used by reads that aligned to TCR genes are represented in red, and TRBV genes that were not detected are depicted in blue. Each row is one TRBV gene (n = 1,922,985 reads sampled).

processing. By processing both the TCR and phenotype genes together, and by aligning the reads to a small library of genes instead of the human reference transcriptome, we were able to reduce the processing time to approximately 36 hours. Further, this task can be handled by most standard desktop computers and is simple to execute, making this method more accessible to users. The software information and bash execution pipeline is described in Appendix B.

To validate this assay, we performed two sets of experiments. First, PBMC were stimulated with PMA/ionomycin for 6 hours and 188 single $CD3^+$ T cells were sorted into two 96-well plates (data not shown). Gene targets were amplified and recovery of each target gene was analyzed. After sorting stimulated T cells, we were able to recover data from 128 (68%) cells after QC (data not shown). We detected seven out of seven transcription factors in these cells in our data set, which are T-bet, GATA3, BCL6, FOXP3, RUNX1, RUNX3, and ROR-γt (RORC) (Figure 4.2B). We were able to detect seven out of nine secreted factors, as we were able to detect expression of IFN-γ, TNF, IL-2, perforin 1 (PRF1), granzyme B (GZMB) , IL-10, *and* IL-17A, but were unable to detect expression of IL-12A and IL-13 (Figure 4.2B). It is possible that a six-hour incubation was insufficient to stimulate expression of these genes. In addition, most of the T cells that were sorted expressed Th1 cytokines (IFN-γ, TNF, IL-2), and only approximately 2% of circulating CD4 T cells are Th2 cells (Tanaka et al., 1998). Therefore, we may not have assayed enough cells to detect this functional subset. Further, IL-12A is not a commonly expressed cytokine by T cells, as it is primarily expressed by dendritic cells and macrophages to induce Th1 differentiation among CD4 T cells (Trinchieri, 1994). This cytokine was also not detected in the original manuscript that described this method (Han et al., 2014). Thus, we concluded that our assay had sufficient sensitivity for the analytes of interest to proceed.

Next, we determined TCR α and β chain gene recovery from our sorted T cells. Out of the 38 TRAV gene primers we included in our assay, we were able to detect amplicon for 32 of the 38 variable genes (86%) (Figure 4.2C). Out of the 38 TRBV gene primers we included in our assay, we were able to detect amplicon from 35 of the 38 variable genes (92%) (Figure 4.2C). Of note, due to the strict QC criteria that assigns TCR sequences to wells, to validate these primers we probed all amplicons that aligned to a TRAV or TRBV gene, even if that TCR transcript was not present at a high enough frequency enough to be included in the final data set. The variable gene segments we did not detect in this experiment are relatively rare in donor PBMC. Each of these undetected genes comprises less than 1% of variable genes used by T cells in healthy donor PBMC, some of which were completely undetected after sampling five donors (Hou et al., 2016; Ruggiero et al., 2015).

In our next validation experiment, we sorted T cells with known TCR α and β chains to verify that we could recover an expected result from this platform. First, we sorted A01 and A05 T cells into 24 wells of a 96-well plate, each (data not shown). After amplification, we recovered the correct TCR α and β chain from 100% of the wells that passed QC (data not shown). Thus, these data demonstrate that this platform can detect a wide variety of transcription factors, cytokines, and TCR genes in a robust manner.

4.4 Identified T cell Receptors Using *ex vivo* Phenotyping Workflow are Consistent with Published Data

To profile *ex vivo* CD4 and CD8 glycolipid-specific T cells, we sorted single cells from two South African adults with newly diagnosed active TB disease using Ac_2SGL-loaded and

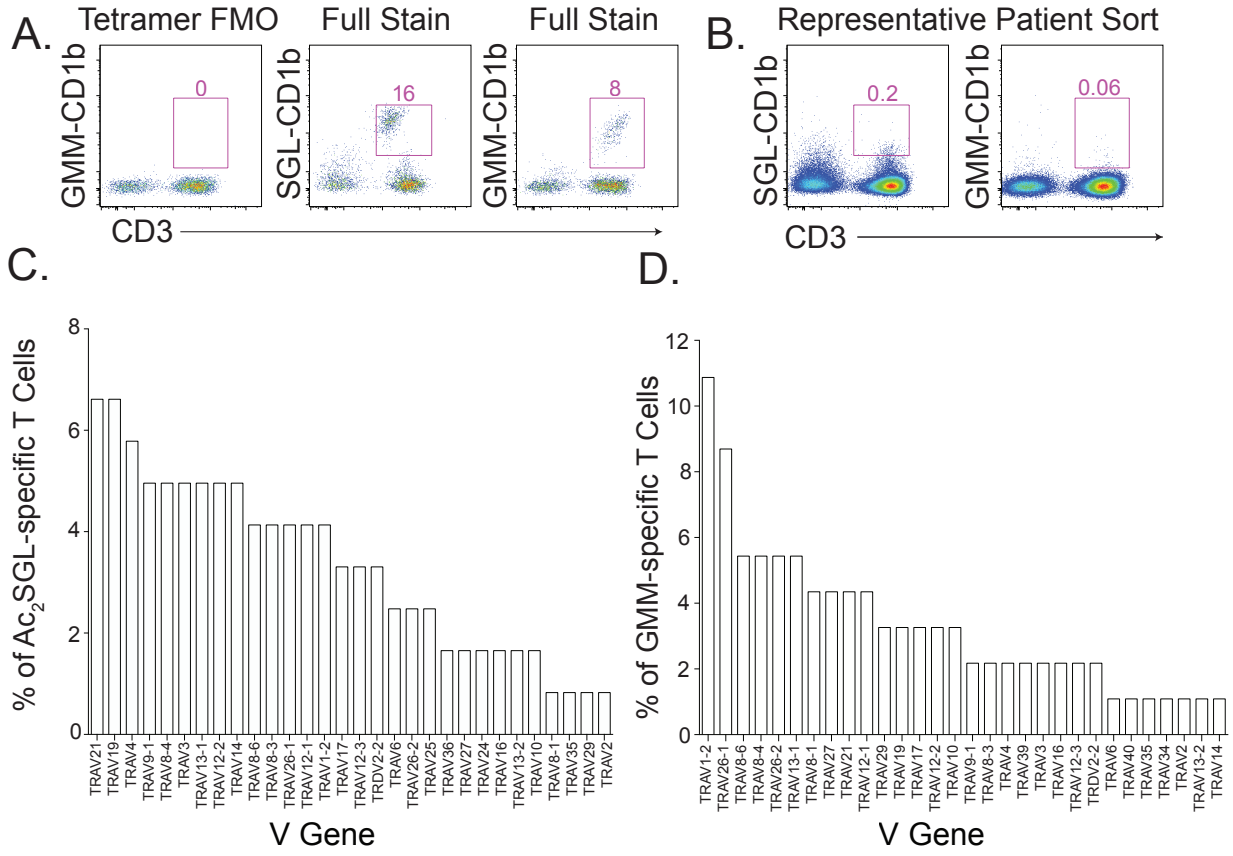

Figure 4.3. ***ex vivo*** **sort of Ac_2SGL- and GMM-specific T cells from individuals with active TB.**

AMSGL-CD1b and GMM-CD1b tetramers were incorporated into a multi-parameter flow cytometry assay to isolate Ac_2SGL-specific and GMM-specific T cells using fluorescence activated cell sorting (FACS). (A) The tetramer positive gate was defined by a 'Fluorescence Minus One' (FMO) negative control (left) and a positive control using Ac_2SGL- and GMM-specific T cell lines diluted in donor PBMC (middle, right). (B) Representative staining from a South African adult blood donor. Ac_2SGL-CD1b and GMM-CD1b tetramer positive T cells in the blood were identified from cryopreserved PBMC obtained from South African adults with new diagnosis of active TB disease (n = 2). (C) Bar plot depicts the percentage of total Ac_2SGL-specific T cell receptor α chains identified that use this V gene (n = 121). V genes were mapped using VDJFasta and IMGT nomenclature is used. (D) Bar plot depicts the percentage of total GMM-specific T cell receptor α chains identified that use this V gene (n = 91).

GMM-loaded CD1b tetramer (Day et al., 2011). Gates defining CD1b tetramer-positive cells were set based on control samples not stained with the tetramers, labeled tetramer fluorescence minus one (FMO) (Figure 4.3A, left). As additional staining controls, we also included an Ac_2SGL-specific and a GMM-specific T cell line at approximately 16% and 8% of total T cells, respectively, (Figure 4.3A, middle, right). The sort gates and tetramer-positive sorted events from one patient sample is shown here (Figure 4.3B). In addition, we sorted 88 tetramer-negative events to serve as a comparator population (data not shown). Of note, the final dataset only includes TCR α chain sequences as we were unable to robustly amplify the TCR β chain from these samples.

After amplification, sequencing, QC, and processing, we analyzed the V gene usage of recovered TCRs from these sorted events and compared them to known V genes from confirmed Ac_2SGL- and GMM-specific TCRs. We were able to identify TRAV8-6 and TRAV13-1, TRAV17, and TRAV14 which are the V genes used by confirmed Ac_2SGL-specific TCRs (James et al., 2018) (Figure 4.3C). In addition, we found that 10.8% of TCRs recovered from wells where a GMM-CD1b tetramer-positive event was sorted used TRAV1-2, which is consistent with the published TCRs of GMM-specific T cells (Figure 4.3D). We also identified other V genes that have been previously shown to be used by GMM-specific TCRs. These include TRAV17, TRAV8, and TRAV13 (Figure 4.3C) (Van Rhijn, et al., 2014; De Witt et al., 2018). Due to the identification of known TCR V genes, we will define these sorted tetramer-positive events as putatively antigen-specific.

In addition to detecting previously described TCR α chain V genes, we also detected previously unidentified genes. Among sorted AMSGL-CD1b tetramer-positive events, we found that approximately 7% used TRAV21 and 7% used TRAV19, making these two variable genes the most commonly recovered V genes (Figure 4.3C). While we did detect these variable genes

within the tetramer-negative sorted events, the frequency was 3.5-fold lower than it was among AMSGL-CD1b tetramer positive events (1 of 43 cells compared to 8 of 121), suggesting these genes may be enriched among Ac_2SGL-specific T cells (data not shown).

4.5 *EX VIVO* CD4 AND CD8 GLYCOLIPID-SPECIFIC T CELLS EXHIBIT DISTINCT FUNCTIONAL PROFILES

Next, we examined the phenotypes of CD4 and CD8 GMM- and Ac_2SGL-specific T cells. We only included cells in this analysis where CD4 or CD8 transcript was detected using this assay (105 of 272 total cells). We then used the Seurat pipeline, which was originally developed to analyze RNA-Seq data, to identify distinct phenotypic clusters within our data set (Satija et al., 2015). This pipeline uses a distance-based clustering approach that uses previously-defined principal components (PC) to construct a K-nearest neighbors graph based on the Euclidean distance between cells in PC space. The implementation of this pipeline in the R programming environment is outlined in Appendix B.

Seurat identified three distinct clusters within our dataset (Figure 4.4A). The cells are visualized here using Uniform Manifold Approximation and Projection (UMAP) (Figure 4.4A) (McInnes et al., 2018). We first visualized the T cells that express the CD4 or CD8 co-receptors (Figure 4.4B). We found that T cells that express the CD4 and CD8 co-receptor are spatially separated when visualized using UMAP, suggesting that the phenotypes these T cells express are distinct (Figure 4.4B).

We then used Seurat to determine which features were driving the differences between the clusters. Cluster 0 is comprised of cells that lack of expression of all markers that drive the other

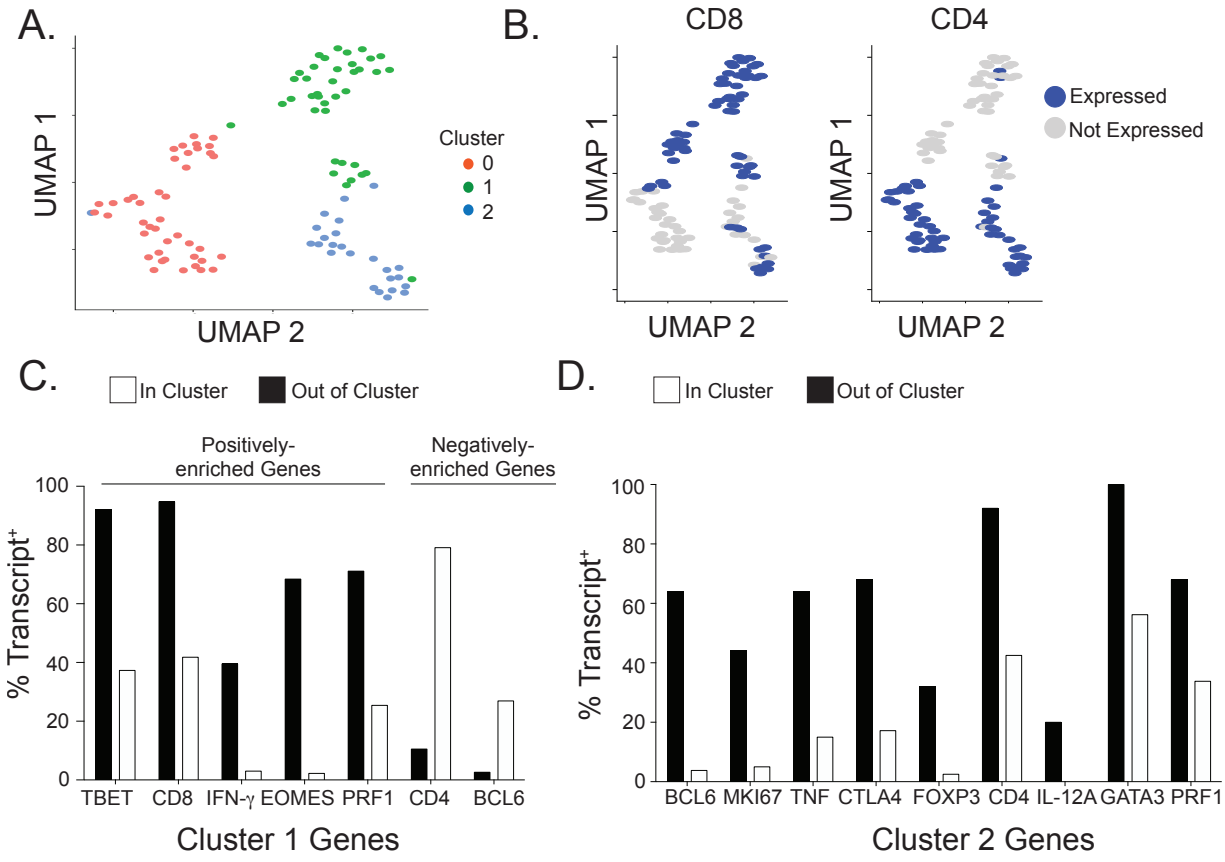

Figure 4.4. ***ex vivo*** **phenotypes of Ac_2SGL- and GMM-specific T cells from individuals with active TB.**

We compared the functional profiles of CD4 and CD8 mycobacterial glycolipid-specific T cells isolated from two individuals with newly diagnosed active TB disease using the Seurat pipeline. (A) Functional profiles of sorted cells were visualized in two dimensional space using the dimensionality reduction method UMAP. Each dot represents one cell. The three distinct clusters are represented in red, blue, and green (n = 105). (B) UMAP visualization of sorted cells colored by CD8 (left) and CD4 (right) expression. Cells that express the respective co-receptor are colored blue and cells that do not express the co-receptor are colored grey. (C) Bars represent the percent of cells within (black) and outside (white) of cluster 1 that express the listed genes. Each listed gene is statistically positively or negatively enriched within cluster 1 (p-values listed in table 4.1, Wilcoxon Rank Sum Test with Bonferroni correction, n = 105). (D) Bars represent the percent of cells within (black) and outside (white) of cluster 2 that express the listed genes. Each listed gene is statistically positively or negatively enriched within cluster 2 (p-values listed in Table 4.1, Wilcoxon Rank Sum Test with Bonferroni correction, n = 105). Adjusted p-values used determine enrichment of genes in each cluster are summarized in Table 4.1.

clusters (Table 4.1). Cluster 1 is characterized by the lack of T cells that express CD4 and BCL6, accompanied by significant enrichment CD8 T cells that express Th1 and cytotoxic markers such as, TBET, IFN-γ, EOMES, and PRF1 (Figure 4.4C, Table 4.1). Cluster 2 is characterized by a strong enrichment of CD4 T cells that express a variety of functional markers. These are Th1 markers such as TNF, Th2 markers such as GATA3, regulatory T cell markers such as CTLA4 and FOXP3, and the Tfh transcription factor BCL6 (Figure 4.4D, Table 4.1). We also detected PRF1 and IL-12A expression by CD4 T cells in cluster 2 (Figure 4.4D, Table 4.1). We did not detect any genes that were negatively enriched in cluster 2 (Table 4.1). Importantly, Ki-67 which is expressed by actively proliferating cells was enriched in the same cluster as CD4 (Figure 4.4D, Table 4.1) (Scholzen and Gerdes, 2000). 18% of CD4 T cells expressed this marker, and these markers exhibit a modest positive correlation ($r = 0.16$). Conversely, 9% of CD8 T cells expressed this marker, and these two markers are not correlated ($r = -0.06$). This suggests that some sorted CD4 T cells may have been actively proliferating at the time of sample collection, which may relate to our findings in Chapter 3 that $CD4^+$ mycobacterial glycolipid-specific T cells are more sensitive to antigen-dependent activation than those that express CD8 and may be more likely to be activated during infection.

Thus, these data show that glycolipid-specific T cells that express CD4 and CD8 co-receptors are functionally distinct. Mycobacterial glycolipid-specific T cells that express the CD8 co-receptor are broadly Th1/cytotoxic T cells. Conversely, glycolipid-specific T cells that express the CD4 co-receptor are very diverse. They express some Th1 markers (TNF), but also can express features of Treg (FOXP3, CTLA4), Th2 (GATA3), and T follicular helper (Tfh) (BCL6) T cell subsets.

Feature	Cluster	Average log Fold Change	Adjusted p-value
PRF1	0	-0.7884891	3.772006e-11
TBET	0	-0.6424331	2.397203e-10
EOMES	0	-0.6975326	9.581073e-09
CD8	0	-0.3333376	2.334034e-03
GATA3	0	-0.2966021	3.748265e-03
IFNG	0	-0.3809424	6.180856e-03
BCL6	0	-0.3022949	9.576098e-02
CD4	1	-0.6920857	3.734865e-10
TBET	1	0.4534103	1.413587e-06
CD8	1	0.4249525	2.564962e-06
IFNG	1	0.4677431	2.975124e-05
EOMES	1	0.4518588	9.200098e-05
PRF1	1	0.4360566	1.394497e-04
BCL6	1	-0.3353254	4.969027e-02
BCL6	2	0.6958855	2.111262e-10
MKI67	2	0.5888951	1.120074e-06
TNF	2	0.4786990	7.224478e-05
CTLA4	2	0.4893367	2.113157e-04
FOXP3	2	0.3721109	2.773426e-03
CD4	2	0.3100052	5.018761e-03
IL12A	2	0.2513780	2.337716e-02
GATA3	2	0.2953271	4.714024e-02

Table 4.3. Adjusted p-values for genes differentially expressed between clusters.

Differentially expressed genes between clusters are listed. The average log-fold-change indicates the log-fold-change in average expression between the cells within the cluster and outside the cluster. Positive values indicate that the gene is more highly expressed within the cluster, and negative values indicate that the gene is more highly expressed outside the cluster. P-values were calculated between the two groups of cells using the Wilcoxon Rank Sum Test and adjusted based on Bonferroni correction using all the genes in the data set.

4.6 SUMMARY

In summary, we have shown that Ac_2SGL-specific T cells that express the CD4 and CD8 co-receptor express distinct functional profiles using *in vitro* and *ex vivo* studies. Our data show that *ex vivo* and *in vitro*-derived Ac_2SGL-specific T cells that express CD8 exhibit a consistent bias towards cytotoxic phenotypes. Further, CD4 mycobacterial glycolipid-specific T cells are more sensitive to antigen-dependent activation *in vitro* and we detected increased markers of T cell proliferation *ex vivo*. Further, they also express many signs that mycobacterial glycolipid-specific T cells may be involved in B cell maturation and antibody class switching. *in vitro* Ac_2SGL-specific T cells express CD40L, and we detected transcripts from the transcription factors BCL6 and GATA3 in sorted mycobacterial glycolipid-specific T cells.

The data described in this chapter have important implications for mycobacterial lipid-specific immunity and should inform future studies to determine how these functional differences we have outlined may be impacting the T cell response to mycobacterial glycolipids. Furthering our data from Chapter 3 that CD4 mycobacterial glycolipid-specific T cells have a higher functional avidity for glycolipid-loaded CD1b molecules than CD8 T cells, we have also shown that they have distinct functional profiles. Whether these differences affect the protective capacity of these T cell subsets is unknown. Based on our results, CD4 and CD8 mycobacterial glycolipid-specific T cell populations exhibit differences in activation, frequency, and functional profiles, which could impact bacterial burden and the extent of lung pathology during M.tb infection.

Further, it has been demonstrated previously that during M.tb infection, T cells that recognize immunodominant antigens exhibit characteristics of T cell exhaustion and terminal differentiation, such as killer cell lectin like receptor G1 (KLRG1) and programmed cell death 1 (PD-1) (Moguche et al., 2017). As some mycobacterial glycolipid antigens have been described as

immunodominant, T cells that recognize these antigens should be evaluated for T cell exhaustion and senescence markers, and the impact these have on protective capacity should be studied (Seshadri et al., 2015). Our data support a model where $CD4^+$ mycobacterial glycolipid-specific T cells undergo higher levels of TCR signaling, leading to an increased propensity towards T cell terminal differentiation and reduced protective capacity.

Conversely, these antigen affinity differences may also lead to an increased protective capacity. Over the course of an infection, the number of cytokines a T cell population produces changes as a function of antigen load and duration of stimulation (Seder et al., 2008). As such, increased levels of stimulation in the short term lead to T cells that produce multiple different cytokines, which are known as polyfunctional T cells (Seder et al., 2008). Polyfunctional $CD4^+$ T cells have been associated with protective immunity to TB (Lewinsohn et al., 2017). In one study, the level of polyfunctionality T cells exhibited differs between CD4 mycobacterial lipid-specific T cells that recognize chemically distinct antigens (Seshadri et al., 2015). One explanation for this finding could be that the TCR affinity or antigen abundance affected the level of polyfunctionality these T cell subsets exhibited. While this study did not evaluate the phenotypes of mycobacterial glycolipid-specific T cells that express the CD8 co-receptor, there may be a relationship between TCR co-receptor expression and the level of polyfunctionality exhibited by $CD4^+$ and $CD8^+$ glycolipid-specific T cells, as they exhibit differences in TCR signaling and functional differentiation.

In conclusion, functional subsets of mycobacterial glycolipid-specific T cells can be defined in part by TCR co-receptor expression. These differences in functional profiles identified in *in vitro* and *ex vivo* studies highlight the need for increased investigation into the impact these differences may have on the immune to M.tb infection. These studies also open new lines of

investigation by suggesting the presence of mycobacterial glycolipid-specific regulatory T cells and T cells that aid in the generation of mycobacterial glycolipid-specific antibodies, both of which have not been previously described.

4.7 Materials and Methods

4.7.1 *Culture Media*

Media (R10) for washing peripheral blood mononuclear cells (PBMC) consisted of RPMI 1640 (Gibco, Waltham, MA) supplemented with 10% fetal calf serum (Hyclone, Logan, UT). Our base T cell media (TCM) consisted of RPMI 1640 supplemented with 10% fetal calf serum, 100 U/ml Penicillin, 100 mg/ml Streptomycin, 55 mM 2-mercaptoethanol, 0.3X Essential Amino Acids, 60 mM Non-essential Amino Acids, 11 mM HEPES, and 800 mM L-Glutamine (Gibco, Waltham, MA) and was sterile-filtered. Our TCM containing human serum (TCM/HS) consisted of 10% human serum (derived from healthy donors), 100 U/ml Penicillin, 100 mg/ml Streptomycin, and 400 mM L-Glutamine (Gibco, Waltham, MA).

4.7.2 *Intracellular Cytokine Staining*

On day 0, cryopreserved T cell lines were thawed, counted, and enumerated using Trypan blue exclusion T cell lines were rested in TCM overnight as described above and enumerated again on day 1. On day 0, AMSGL was evaporated to dryness from chloroform-based solvents under a sterile nitrogen stream and then sonicated into media. This lipid suspension was added to 50,000 K562-EV or K562-CD1b cells at 5 mg/ml final concentrations. K562 cells were incubated for 18 hours at 37˚C, 5% CO2 to facilitate lipid loading.

On day 1, rested T cell lines were split and added to the K562 cells without washing at a final density of 1 million/well. Thus, each T cell line was co-incubated with loaded K562-CD1b and K562-EV antigen presenting cells. The cell mixture was allowed to incubate for 6 hours in the presence of anti-CD28/Ly29d Abs (BD Biosciences, San Jose, CA), brefeldin A at a final concentration of 10 mg/ml (Sigma-Aldrich), and GolgiStop containing Monensin (BD Biosciences, San Jose, CA), after which EDTA, at a final concentration of 2 mmol, was added to disaggregate cells.

On day 2, the samples were washed twice in PBS and then stained with Aqua Live/Dead (Life Technologies, Carlsbad, CA) prepared according to manufacturer's instructions and incubated for 20 minutes at room temperature. Live/Dead staining and all steps following were performed in the dark. The cells were washed twice in PBS and then incubated at room temperature for 10 minutes in 1x FACS Lyse (BD Biosciences, San Jose, CA). Following one wash with FACS buffer, the cells were incubated an additional 10 minutes in 1x FACS Perm II (BD Biosciences, San Jose, CA) at room temperature. The cells were washed twice in FACS buffer and labeled with antibodies for CD3, CD4, CD8, IFN-γ, IL-2, IL-4, CD154 (BD Biosciences, San Jose, CA), and TNF (eBioSciences, Waltham, MA) for 30 minutes at 4°C. Following two final washes in FACS buffer, the cells were fixed in 1% PFA and acquired on a BD LSRFortessa (BD Biosciences, San Jose, CA).

4.7.3 *IFN-γ and Granzyme B ELISPOT*

We used an IFN-γ ELISPOT to determine the antigen specificity of our T cell lines. EMD Multiscreen-IP filter plates (Millipore, Billerica, MA) were coated with 1D1K antibody (Mabtech, Sweden) diluted 1:400 in PBS and incubated overnight at 4˚C. The following day, one thousand T

cells were plated 1:50 with K562 cells stably transfected with CD1b or with a mock vector. Lipids antigens were stored in 2:1 chloroform:methanol and appropriate amount was dried using gaseous nitrogen. The lipids were sonicated into media to obtain a 4 μg/ml suspension and plated with the cells at a final concentration of 1 μg/ml. These cultures were incubated at 37˚C for approximately 16 hours. The following day, the cells were washed twice with sterile water to lyse the cells, and the plates were incubated with the detection antibody 7-B6-1-biotin (Mabtech, Sweden) diluted 1:1000 in PBS + 0.5% FCS and incubated for two hours at room temperature. The cells were then washed five times with PBS and incubated in ExtrAvidin-Alkaline Phosphatase (Sigma, St. Louis, MO) diluted 1:1000 in PBS and incubated for one hour at room temperature. The wells were then washed five times and incubated with BCIP/NBT substrate (Sigma, St. Louis, MO) for five minutes to develop the membrane. The wells and IFN-γ spots were counted using an ImmunoSpot S6 Core Analyzer (Cellular Technology Limited, Cleveland, OH). The granzyme B ELISPOT followed identical methods with the following exceptions: EMD filter plates were coated with GB10 antibody, GB11-biotin was used as the detection antibody, and the culture incubation was extended to 48 hours.

4.7.4 *Cytotoxicity Assay*

To detect cytotoxic activity, the T cell lines were thawed and rested overnight in TCM as described above. The following day, K562-CD1b and K562-EV were stained with Cell Trace Violet (Invitrogen, Carlsbad, CA) at 10 μM and 0.2 μM, respectively, for 20 minutes at 37˚C. Staining was quenched by adding 10 ml cold PBS to the staining solution. Stained K562-CD1b and K562-EV cells were then mixed at a 1:1 ratio. This cell mixture was then co-incubated with the T cell lines at an effector to target ratio of 5:1 in a 96-well plate in a total volume of 200 μl of TCM. AMSGL was added to the culture media at 1 μg/ml, and the cell suspension was centrifuged

briefly to pellet the cells. Cells were incubated for 24 hours at 37˚C/5% CO_2. The following day, the cells were washed twice with PBS, and stained with Aqua Live/Dead (Life Technologies, Carlsbad, CA) prepared according to manufacturer's instructions and incubated for 20 minutes at room temperature. The cells were then washed twice with PBS and then stained with anti-CD3 antibody (BD Biosciences, San Jose, CA) for 30 minutes at 4˚C in FACS buffer. The cells were then washed twice with FACS buffer and fixed in 1% PFA. Samples were acquired on an LSR Fortessa (BD Biosciences, San Jose, CA).

4.7.5 *Clinical Cohorts*

We utilized cryopreserved PBMC samples isolated from South African adults with a new diagnosis of active tuberculosis (Day et al., 2011). Participants were over 18 years of age and HIV uninfected. All patients had positive sputum smear microscopy and/or were positive culture for M.tb. Blood was obtained and PBMC archived prior to or within 7 days of starting standard course anti-TB treatment, which was provided according to South African national health guidelines.

4.7.6 *Single-cell Transcriptional Profiling*

This protocol was established exactly as the methods in Han, et al., 2014 describe. In brief, PBMC from South African adults with active tuberculosis were thawed in warm thaw media (R10 with 2 μL/ml Benzonase (Millipore, Billerica, MA) sterile-filtered) and centrifuged at 1500 rpm for 5 minutes. The supernatant was decanted, and the cells were resuspended in R10 and counted by Trypan Blue (Millipore, Billerica, MA) exclusion. The cells were again centrifuged at 1500 rpm for 5 minutes and plated at a density of 1 million cells per well in a 96-well U-bottom plate. Cells were then tetramer stained as described above, and SGL-specific T cells were sorted based

on staining with their respective AMSGL-CD1b tetramer, and not with the mock-loaded CD1b tetramer.

Cells were sorted into single wells of a 96-well PCR plate (Eppendorf, Hamburg, Germany) containing 5 µl of sort buffer consisting of (1X Qiagen One-step RT PCR Buffer (Qiagen, Hilden, Germany), 0.1 mM dithiothreitol (Invitrogen, Carlsbad, CA), RNaseOUT (Invitrogen, Carlsbad, CA), and molecular-grade nuclease-free water (Fisher, Hampton, NH)). Cells were covered with two layers of AlumaSeal sealing foils (Excel Scientific, Victorville, CA), centrifuged briefly at 1800 rpm for 1 minute, and frozen at -80˚C overnight. The following day, the reverse transcription reaction was performed using 1X Qiagen One-step RT-PCR Buffer (Qiagen, Hilden, Germany), 10 mM dNTP (Qiagen, Hilden, Germany), One-step RT enzyme mix (Qiagen, Hilden, Germany), and primer pools containing TCRAV and TCRBV primers at 0.06 µM final concentration, TCRA and TCRB constant region primers at 0.3 µM final, and phenotype gene primers at 0.1 µM. Primer sequences are as described in Han et al., 2014. Samples then undergo amplification in a Mastercycler Nexus Gradient Thermal Cycler (Eppendorf, Hamburg, Germany) using the following protocol: 50˚C for 36 minutes, 95˚C for 15 minutes, 25 cycles of: 94˚C for 30 seconds, 60˚C for 1 minute, and 72˚C for 1 minute, followed by a final incubation of 72˚C for 5 minutes. Then the second phase of amplification uses 0.4 units of HotStarTaq DNA polymerase (Qiagen, Hilden, Germany), with 1X PCR buffer, 200 µM of dNTPs, 0.06 µM TCRAV and TCRBV primers, and 0.3 µM TCRA and TCRB constant region primer, with 1.2 µl of cDNA template, brought up to 15 µl in molecular grade water. In a second plate, the same reaction is carried out using 0.1 µM of phenotyping primers and 2 µl of cDNA template. Both reactions follow this thermal cycling protocol: 95˚C for 15 minutes, then 25 cycles or 30 cycles for the TCR or phenotyping reactions, respectively, of: 95˚C for 30 seconds, 64˚C for 1 minute, and 72˚C for 1

minute, followed by a final extension of 72˚C for 10 minutes. Lastly, the amplicons were barcoded based on their plate, row, and column location using the barcodes specified in Han et al., 2014. The TCRA, TCRB, and phenotyping genes were all amplified separately at this step. The reaction mixture contains molecular-grade water, 1X PCR buffer, 1X Q buffer, 200 µM dNTPs, and 0.4 units of HotStarTaq DNA. The row and column barcodes were each added at 0.05 µM, and the Illumina MiSeq paired end adapters were used at 0.5 µM. 1.2 µl of TCRA and TCRB and 1.5 µl phenotype template was added to make a total volume of 15 µl. All plates were cycled according to the following program: 95˚C for 15 minutes, 36 cycles of the following: 94˚C for 30 seconds, 66˚C for 1 minute, 72˚C for 1 minute, followed by a final extension of 72˚C for 10 min. After the amplification steps, all wells are pooled from each plate and cleaned using Ampure XP PCR Cleanup Beads (Beckman Coulter, Brea, CA) according to the manufacturer's instructions. Each plate was pooled and the plate libraries were quantified on a Qubit Fluorometer 3.0 using a dsDNA High-sensitivity Kit per manufacturer's instructions (Life Technologies, Carlsbad, CA). The plates were then pooled in equal volumes and the pooled library was then diluted to 6 µM and sequenced using a 500-cycle V3 reagent on an Illumina MiSeq (Illumina, San Diego, CA) at the Fred Hutchinson Cancer Research Center Genomics Core.

4.7.7 *Statistical and Computational Methods*

Raw reads were trimmed and demultiplexed using VDJFasta software (Glanville et al., 2009). Paired end reads were assembled by finding a consensus of at least 100 bases. Amplicons smaller than 100 bases were filtered out. The resulting paired-end reads are then assigned to wells according to barcodes that designate the plate, row, and column. The average read count per well for this study was approximately 47,000.

To map the TCR reads, a cutoff of >95% sequence identity was established to collapse reads and establish a consensus sequence within each well. All sequences exceeding 95% sequence identity are assumed to derive from the same TCR sequence. The 95% cutoff conservatively ensures all sequences derived from the same transcript would be properly assigned. For phenotyping transcripts, the number of reads containing a 95% match to the customized database of transcription factor and cytokine genes are scored. The resulting data is then compiled into a .csv file containing the TCR assignment and number of reads for each phenotype gene for each well.

Data were then input into the R programming environment and further processed and formatted. The resulting matrix was then analyzed using Seurat to cluster the data and perform feature selection (Satija et al., 2015). Pipeline and parameter selection is outlined in Appendix B. Other data visualization and statistical tests were performed in the R programming environment or Graph Pad Prism (v6) (San Diego, CA).

Chapter 5. DISCUSSION

Adapted from James C.A., Seshadri C. (2020). T Cell Responses to Mycobacterial Glycolipids: On the Spectrum of "Innateness". *Frontiers in Immunology.* 11, 170. doi: 10.3389/fimmu.2020.00170.

5.1 SUMMARY

In summary, we have shown that there are several molecular and cellular factors that affect T cell recognition of Ac_2SGL. On the molecular level, Ac_2SGL-specific T cells exhibit such fine specificity for particular structural moieties, that variation in the number of methylations and the addition of one unsaturated bond in the acyl chain of Ac_2SGL is sufficient to abrogate antigenicity. On the cellular level, we have demonstrated that in *ex vivo, in vitro*-derived, and transduced Ac_2SGL-specific T cells exhibit a consistent hierarchy in which CD4 T cells bind AMSGL-CD1b tetramer with a higher MFI, followed by CD8 T cells, and DN T cells. This hierarchy translates to differences in T cell activation and cytokine release. Further, we have demonstrated that the expression of these TCR co-receptors defines functional subsets of Ac_2SGL-specific T cells that more closely align with the functional subsets of peptide-specific T cells than innate-like T cells. The data we have highlighted in this dissertation have significant implications for the development of novel vaccination and diagnostic strategies for TB.

5.2 IMPLICATIONS FOR NOVEL MYCOBACTERIAL VACCINE STRATEGIES

Mycolipid-specific T cells hold significant promise for new vaccine approaches. Immunizing with mycolipids has conferred modest protection to TB in rodent models (Dascher et al., 2003; Larrouy-Maumus et al., 2017). However, which T cell subpopulations mediate this

protective immune response is unknown. Our data and others suggest that each antigen and T cell subpopulation, as defined by TCR affinity or co-receptor expression, should be studied independently to understand how these T cell populations are involved in the immune response to TB.

The next step to increasing vaccine efficacy should be to ensure inclusion of a variety of antigenic types. One strategy of increasing antigenic breadth is by utilizing live-attenuated or killed whole cell vaccines (Scriba et al., 2016). If T cell responses to mycobacterial glycolipid antigens are associated with positive outcomes in these studies, then using lipid-subunit vaccines to target a specific population can also be considered as a novel vaccine strategy. Natural candidates for lipid-subunit vaccine are SGLs, which have only been detected in virulent strains of M.tb (Layre et al., 2011b). Further, SGL-specific T cells are expanded in individuals who have been exposed to M.tb (Gilleron et al., 2004).

Though we have focused our comments on mycolipids as T cell antigens, it is important to note that these lipids may also have adjuvant properties. Indeed, many of these antigens are structurally similar to adjuvants in clinical use, such as GLA-SE and trehalose dibehenate (TDB) (Coler et al., 2011; Werninghaus et al., 2009). Some T cell antigens, such as phosphotidyl-*myo*-inositol mannosides, may fortuitously act as both antigen and adjuvant by activating Toll-like receptor pathways (de la Salle et al., 2005; Jones et al., 2001).

5.3 Implications for Mycobacterial Diagnostics

The diagnosis of mycobacterial disease could be improved by leveraging the biology of mycobacterial glycolipid-specific T cells. Latent TB is typically diagnosed by an interferon gamma release assay, which measures T cell responses to secreted protein antigens but is a poor predictor

for progression to active disease (Abubakar et al., 2018). Notably, diagnostics targeting cell surface mycobacterial glycolipids are already being used for both TB and leprosy. High-affinity IgG antibodies targeting LAM have been incorporated into a urine-based assay for TB and have shown clinical utility in the setting of HIV co-infection (Broger et al., 2019). IgM antibodies targeting phenolic glycolipids (PGLs) are being used for the diagnosis of leprosy (Gurung et al., 2019). Even though the current standard for leprosy diagnosis incorporates IgM antibodies to PGL, this could improve as PGLs also likely contain T cell epitopes, which could be leveraged to develop higher affinity IgG antibodies to PGLs. This is also probably true of LAM, currently the target of antibody-based diagnostics for TB, which actually contains a T cell epitope in the form of PIM (de la Salle et al., 2005). Finally, diagnostics could be improved by targeting specific lipids, such as SGLs, which have been shown to be preferentially expressed by M.tb and are absent from BCG and environmental strains (Goren et al., 1974; Layre et al., 2011b). In this dissertation, we show evidence that Ac_2SGL-specific T cells that express the CD4 co-receptor express markers that suggest these T cells may be involved in generating such antibodies. This finding should be confirmed, and if found true would provide a novel diagnostic target that improves upon current strategies. In addition, CD4 GMM- and MA-specific T cells express CD40 ligand (CD40L), which suggests that these T cells may be involved in B cell maturation and immunoglobulin class-switching (Seshadri et al., 2015). iNKT cells have previously been shown to provide both cognate and non-cognate help to B cell class switching and affinity maturation (Doherty et al., 2018; Leadbetter et al., 2008; Tonti et al., 2009). Similarly, supernatants from activated MAIT cells promote B cell differentiation into plasmablasts, and production of IgA, IgM, and IgG antibodies (Bennet et al., 2017). It is possible that mycolipid-specific T cells provide both cognate and non-cognate help to B cells.

An emerging approach to the diagnosis of infectious diseases is using high-throughput sequencing of TCRs that are expanded in peripheral blood. Using machine learning, a recent study showed that a TCR 'fingerprint' of cytomegalovirus (CMV) infection could be identified (Emerson et al., 2017). This is a notable result because most CMV-specific TCRs would be private due to the highly polymorphic nature of MHC. On the other hand, CD1-restricted TCRs are expected to be public due to the non-polymorphic nature of CD1. Indeed, our group found that both shared and private TCR repertoires of GMM-specific T cells were associated with active TB disease in a South African cohort (DeWitt et al., 2018). Thus, TCRs specific for mycolipids could be developed into a blood-based diagnostic tool.

5.4 CONCLUSION

Together, our data support the emerging model that chemically distinct antigens and T cell subpopulations ought to be studied independently to understand the full breadth of T cell immunity to mycobacterial glycolipids. Our data are consistent with existing literature that demonstrate that subtle changes to the acyl groups within the lipid antigen can in some instances fully abrogate antigenicity within certain T cell populations and that reduction of TCR affinity alters the functional response of mycobacterial glycolipid-specific T cells (Chancellor et al., 2017; Van Rhijn et al., 2017) Thus, as we show that CD4 and CD8 co-receptors can affect T cell functional avidity, and that CD4 and CD8 glycolipid-specific T cells have distinct functional profiles, CD4 and CD8 subpopulations of glycolipid-specific T cells ought to be examined independently in human cohort and animal studies. In this way, we can start to fully appreciate the nuance of glycolipid-specific T cell responses to infection and vaccination, and understand which antigens, subpopulations, and functional responses might participate in protective immune responses to M.tb.

REFERENCES

Abubakar, I., Drobniewski, F., Southern, J., Sitch, A. J., Jackson, C., Lipman, M., et al. (2018). Prognostic value of interferon-γ release assays and tuberculin skin test in predicting the development of active tuberculosis (UK PREDICT TB): a prospective cohort study. *Lancet Infect. Dis.* 18, 1077–1087. doi:10.1016/S1473-3099(18)30355-4.

Adekambi, T., Ibegbu, C. C., Cagle, S., Kalokhe, A. S., Wang, Y. F., Hu, Y., et al. (2015). Biomarkers on patient T cells diagnose active tuberculosis and monitor treatment response. *J. Clin. Invest.* 125, 1827–1838. doi:10.1172/JCI77990.

Arbues, A., Aguilo, J. I., Gonzalo-Asensio, J., Marinova, D., Uranga, S., Puentes, E., et al. (2013). Construction, characterization and preclinical evaluation of MTBVAC, the first live-attenuated M. tuberculosis-based vaccine to enter clinical trials. *Vaccine* 31, 4867–4873. doi:10.1016/j.vaccine.2013.07.051.

Arrenberg, P., Halder, R., Dai, Y., Maricic, I., and Kumar, V. (2010). Oligoclonality and innate-like features in the TCR repertoire of type II NKT cells reactive to a β-linked self-glycolipid. *Proc. Natl. Acad. Sci. U. S. A.* 107, 10984–10989. doi:10.1073/pnas.1000576107.

Artyomov, M. N., Lis, M., Devadas, S., Davis, M. M., and Chakraborty, A. K. (2010). CD4 and CD8 binding to MHC molecules primarily acts to enhance Lck delivery. *Proc. Natl. Acad. Sci. U. S. A.* 107, 16916–16921. doi:10.1073/pnas.1010568107.

Beckman, E. M., Melián, A., Behar, S. M., Sieling, P. A., Chatterjee, D., Furlong, S. T., et al. (1996). CD1c restricts responses of mycobacteria-specific T cells. Evidence for antigen presentation by a second member of the human CD1 family. *J. Immunol.* 157, 2795–803. Available at: http://www.ncbi.nlm.nih.gov/pubmed/8816382.

Beckman, E. M., Porcelli, S. a, Morita, C. T., Behar, S. M., Furlong, S. T., and Brenner, M. B. (1994). Recognition of a lipid antigen by CD1-restricted alpha beta+ T cells. *Nature* 372, 691–694. doi:10.1038/372691a0.

Birkinshaw, R. W., Pellicci, D. G., Cheng, T. Y., Keller, A. N., Sandoval-Romero, M., Gras, S., et al. (2015). alphabeta T cell antigen receptor recognition of CD1a presenting self lipid ligands. *Nat Immunol* 16, 258–266. doi:10.1038/ni.3098.

Bolotin, D. A., Poslavsky, S., Mitrophanov, I., Shugay, M., Mamedov, I. Z., Putintseva, E. V., et al. (2015). MiXCR: Software for comprehensive adaptive immunity profiling. *Nat. Methods* 12, 380–381. doi:10.1038/nmeth.3364.

Brigl, M., Tatituri, R. V. V, Watts, G. F. M., Bhowruth, V., Leadbetter, E. A., Barton, N., et al. (2011). Innate and cytokine-driven signals, rather than microbial antigens, dominate in natural killer T cell activation during microbial infection. *J. Exp. Med.* 208, 1163–1177. doi:10.1084/jem.20102555.

Broger, T., Sossen, B., du Toit, E., Kerkhoff, A. D., Schutz, C., Ivanova Reipold, E., et al. (2019). Novel lipoarabinomannan point-of-care tuberculosis test for people with HIV: a diagnostic accuracy study. *Lancet Infect. Dis.* 19, 852–861. doi:10.1016/s1473-3099(19)30001-5.

Busch, D. H., and Pamer, E. G. (1999). T cell affinity maturation by selective expansion during infection. *J. Exp. Med.* 189, 701–709. doi:10.1084/jem.189.4.701.

Busch, M., Herzmann, C., Kallert, S., Zimmermann, A., Hofer, C., Mayer, D., et al. (2016). Lipoarabinomannan-responsive polycytotoxic T cells are associated with protection in human tuberculosis. *Am. J. Respir. Crit. Care Med.* 194, 345–355.

doi:10.1164/rccm.201509-1746OC.
Calabi, F., Jarvis, J. M., Martin, L., and Milstein, C. (1989). Two classes of CD1 genes. *Eur. J. Immunol.* 19, 285–292. doi:10.1002/eji.1830190211.
Chancellor, A., Tocheva, A. S., Cave-Ayland, C., Tezera, L., White, A., Al Dulayymi, J. R., et al. (2017). CD1b-restricted GEM T cell responses are modulated by Mycobacterium tuberculosis mycolic acid meromycolate chains. *Proc. Natl. Acad. Sci. U. S. A.* 114, E10956–E10964. doi:10.1073/pnas.1708252114.
Chesne-Seck, M. L., Barilone, N., Boudou, F., Asensio, J. G., Kolattukudy, P. E., Martín, C., et al. (2008). A point mutation in the two-component regulator PhoP-PhoR accounts for the absence of polyketide-derived acyltrehaloses but not that of phthiocerol dimycocerosates in Mycobacterium tuberculosis H37Ra. *J. Bacteriol.* 190, 1329–1334. doi:10.1128/JB.01465-07.
Coler, R. N., Bertholet, S., Moutaftsi, M., Guderian, J. A., Windish, H. P., Baldwin, S. L., et al. (2011). Development and characterization of synthetic glucopyranosyl lipid adjuvant system as a vaccine adjuvant. *PLoS One* 6. doi:10.1371/journal.pone.0016333.
Coquet, J. M., Chakravarti, S., Kyparissoudis, K., McNab, F. W., Pitt, L. A., McKenzie, B. S., et al. (2008). Diverse cytokine production by NKT cell subsets and identification of an IL-17-producing CD4-NK1.1- NKT cell population. *Proc. Natl. Acad. Sci. U. S. A.* 105, 11287–11292. doi:10.1073/pnas.0801631105.
Corbett, A. J., Eckle, S. B. G., Birkinshaw, R. W., Liu, L., Patel, O., Mahony, J., et al. (2014). T-cell activation by transitory neo-antigens derived from distinct microbial pathways. *Nature* 509, 361–365. doi:10.1038/nature13160.
Dascher, C. C., Hiromatsu, K., Xiong, X., Morehouse, C., Watts, G., Liu, G., et al. (2003). Immunization with a mycobacterial lipid vaccine improves pulmonary pathology in the guinea pig model of tuberculosis. *Int. Immunol.* 15, 915–925. doi:10.1093/intimm/dxg091.
Day, C. L., Abrahams, D. A., Lerumo, L., Janse van Rensburg, E., Stone, L., O'rie, T., et al. (2011). Functional Capacity of Mycobacterium tuberculosis -Specific T Cell Responses in Humans Is Associated with Mycobacterial Load . *J. Immunol.* 187, 2222–2232. doi:10.4049/jimmunol.1101122.
de la Salle, H., Mariotti, S., Angenieux, C., Gilleron, M., Garcia-Alles, L.-F., Malm, D., et al. (2005). Assistance of microbial glycolipid antigen processing by CD1e. *Science* 310, 1321–4. doi:10.1126/science.1115301.
De Rosa, S. C., Carter, D. K., and McElrath, M. J. (2012). OMIP-014: Validated multi-functional characterization of antigen-specific human T-cells by intracellular cytokine staining. *Cytometry. A* 81, 1019–1021. doi:10.1002/cyto.a.22218.
Dellabona, P., Padovan, E., Casorati, G., Brockhaus, M., and Lanzavecchia, A. (1994). An invariant V alpha 24-J alpha Q/V beta 11 T cell receptor is expressed in all individuals by clonally expanded CD4-8- T cells. *J. Exp. Med.* 180, 1171–6. doi:10.1084/jem.180.3.1171.
DeWitt, W. S., Yu, K. K. Q., Wilburn, D. B., Sherwood, A., Vignali, M., Day, C. L., et al. (2018). A Diverse Lipid Antigen–Specific TCR Repertoire Is Clonally Expanded during Active Tuberculosis. *J. Immunol.* doi:10.4049/jimmunol.1800186.
Dhodapkar, M. V., and Kumar, V. (2017). Type II NKT Cells and Their Emerging Role in Health and Disease. *J. Immunol.* 198, 1015–1021. doi:10.4049/jimmunol.1601399.
Dias, J., Boulouis, C., Gorin, J. B., Van Den Biggelaar, R. H. G. A., Lal, K. G., Gibbs, A., et al. (2018). The CD4−CD8− MAIT cell subpopulation is a functionally distinct subset developmentally related to the main CD8+ MAIT cell pool. *Proc. Natl. Acad. Sci. U. S. A.*

115, E11513–E11522. doi:10.1073/pnas.1812273115.
Doherty, D. G., Melo, A. M., Moreno-Olivera, A., and Solomos, A. C. (2018). Activation and regulation of B cell responses by invariant natural killer T cells. *Front. Immunol.* 9. doi:10.3389/fimmu.2018.01360.
Eckle, S. B. G., Birkinshaw, R. W., Kostenko, L., Corbett, A. J., McWilliam, H. E. G., Reantragoon, R., et al. (2014). A molecular basis underpinning the T cell receptor heterogeneity of mucosal-associated invariant T cells. *J. Exp. Med.* 211. doi:10.1084/jem.20140484.
Emerson, R. O., DeWitt, W. S., Vignali, M., Gravley, J., Hu, J. K., Osborne, E. J., et al. (2017). Immunosequencing identifies signatures of cytomegalovirus exposure history and HLA-mediated effects on the T cell repertoire. *Nat. Genet.* 49, 659–665. doi:10.4049/jimmunol.1800186.
Farhat, M., Greenaway, C., Pai, M., and Menzies, D. (2006). False-positive tuberculin skin tests: What is the absolute effect of BCG and non-tuberculous mycobacteria? *Int. J. Tuberc. Lung Dis.* 10, 1192–1204. doi:10.1136/OEM.2006.028068.
Felio, K., Nguyen, H., Dascher, C. C., Choi, H.-J., Li, S., Zimmer, M. I., et al. (2009). CD1-restricted adaptive immune responses to Mycobacteria in human group 1 CD1 transgenic mice. *J. Exp. Med.* 206, 2497–2509. doi:10.1084/jem.20090898.
Fine, P. E. M. (1995). Variation in protection by BCG: implications of and for heterologous immunity. *Lancet* 346, 1339–1345. doi:10.1016/S0140-6736(95)92348-9.
Fontenot, J. D., Gavin, M. A., and Rudensky, A. Y. (2003). Foxp3 programs the development and function of CD4+CD25+ regulatory T cells. *Nat. Immunol.* 4, 330–336. doi:10.1038/ni904.
Fox, L. M., Cox, D. G., Lockridge, J. L., Wang, X., Chen, X., Scharf, L., et al. (2009). Recognition of lyso-phospholipids by human natural killer T lymphocytes. *PLoS Biol.* 7. doi:10.1371/journal.pbio.1000228.
Gadola, S. D., Zaccai, N. R., Harlos, K., Shepherd, D., Castro-Palomino, J. C., Ritter, G., et al. (2002). Structure of human CD1b with bound ligands at 2.3 A, a maze for alkyl chains. *Nat. Immunol.* 3, 721–726. doi:10.1038/ni821.
Garcia-Alles, L. F., Collmann, A., Versluis, C., Lindner, B., Guiard, J., Maveyraud, L., et al. (2011). Structural reorganization of the antigen-binding groove of human CD1b for presentation of mycobacterial sulfoglycolipids. *Proc Natl Acad Sci U S A* 108, 17755–17760. doi:10.1073/pnas.1110118108.
Garner, L. C., Klenerman, P., and Provine, N. M. (2018). Insights into mucosal-associated invariant T cell biology from studies of invariant natural killer T cells. *Front. Immunol.* 9. doi:10.3389/fimmu.2018.01478.
Gau, B., Lemétais, A., Lepore, M., Garcia-Alles, L. F., Bourdreux, Y., Mori, L., et al. (2013). Simplified deoxypropionate acyl chains for mycobacterium tuberculosis sulfoglycolipid analogues: Chain length is essential for high antigenicity. *ChemBioChem* 14, 2413–2417. doi:10.1002/cbic.201300482.
Geerdink, D., Horst, B. ter, Lepore, M., Mori, L., Puzo, G., Hirsch, A. K. H., et al. (2013). Total synthesis, stereochemical elucidation and biological evaluation of Ac $_2$ SGL; a 1,3-methyl branched sulfoglycolipid from Mycobacterium tuberculosis. *Chem. Sci.* 4, 709–716. doi:10.1039/C2SC21620E.
Geerdink, D., and Minnaard, A. J. (2014). Total synthesis of sulfolipid-1. *Chem Commun* 50, 2286–2288. doi:10.1039/c3cc48087a.

Gherardin, N. A., Souter, M. N. T., Koay, H. F., Mangas, K. M., Seemann, T., Stinear, T. P., et al. (2018). Human blood MAIT cell subsets defined using MR1 tetramers. *Immunol. Cell Biol.* 96, 507–525. doi:10.1111/imcb.12021.

Gilleron, M., Stenger, S., Mazorra, Z., Wittke, F., Mariotti, S., Böhmer, G., et al. (2004). Diacylated Sulfoglycolipids Are Novel Mycobacterial Antigens Stimulating CD1-restricted T Cells during Infection with Mycobacterium tuberculosis. *J. Exp. Med. J. Exp. Med* 36491100, 649–659. doi:10.1084/jem.20031097.

Glanville, J., Zhai, W., Berka, J., Telman, D., Huerta, G., Mehta, G. R., et al. (2009). Precise determination of the diversity of a combinatorial antibody library gives insight into the human immunoglobulin repertoire. *Proc. Natl. Acad. Sci. U. S. A.* 106, 20216–20221. doi:10.1073/pnas.0909775106.

Gold, M. C., Cerri, S., Smyk-Pearson, S., Cansler, M. E., Vogt, T. M., Delepine, J., et al. (2010). Human mucosal associated invariant T cells detect bacterially infected cells. *PLoS Biol.* 8, 1–14. doi:10.1371/journal.pbio.1000407.

Gold, M. C., McLaren, J. E., Reistetter, J. A., Smyk-Pearson, S., Ladell, K., Swarbrick, G. M., et al. (2014). MR1-restricted MAIT cells display ligand discrimination and pathogen selectivity through distinct T cell receptor usage. *J. Exp. Med.* 211, 1601–1610. doi:10.1084/jem.20140507.

Gonzalo, J.-A., Delaney, T., Corcoran, J., Goodearl, A., Gutierrez-Ramos, J. C., and Coyle, A. J. (2001). Cutting Edge: The Related Molecules CD28 and Inducible Costimulator Deliver Both Unique and Complementary Signals Required for Optimal T Cell Activation. *J. Immunol.* 166, 1–5. doi:10.4049/jimmunol.166.1.1.

Goren, M. B. (1970). Sulfolipid I of Mycobacterium tuberculosis, strain H37Rv II. Structural studies. *Biochim. Biophys. Acta (BBA)/Lipids Lipid Metab.* 210, 127–138. doi:10.1016/0005-2760(70)90068-8.

Goren, M. B., Brokl, O., Das, B. C., and Lederer, E. (1971). Sulfolipid I of Mycobacterium tuberculosis, strain H37RV. Nature of the acyl substituents. *Biochemistry* 10, 72–81.

Goren, M. B., Brokl, O., and Schaefer, W. B. (1974). Lipids of putative relevance to virulence in Mycobacterium tuberculosis: Correlation of virulence with elaboration of sulfatides and strongly acidic lipids. *Infect. Immun.* 9, 142–149.

Gras, S., Van Rhijn, I., Shahine, A., Cheng, T.-Y., Bhati, M., Tan, L. L., et al. (2016). T cell receptor recognition of CD1b presenting a mycobacterial glycolipid. *Nat. Commun.* 7, 13257. doi:10.1038/ncomms13257.

Gudmundsdottir, H., Wells, A. D., and Turka, L. A. (1999). Dynamics and requirements of T cell clonal expansion in vivo at the single-cell level: effector function is linked to proliferative capacity. *J. Immunol.* 162, 5212–23. Available at: http://www.ncbi.nlm.nih.gov/pubmed/10227995.

Guiard, J., Collmann, A., Garcia-Alles, L. F., Mourey, L., Brando, T., Mori, L., et al. (2009). Fatty acyl structures of mycobacterium tuberculosis sulfoglycolipid govern T cell response. *J. Immunol.* 182, 7030–7037. doi:10.4049/jimmunol.0804044.

Guiard, J., Collmann, A., Gilleron, M., Mori, L., De Libero, G., Prandi, J., et al. (2008). Synthesis of diacylated trehalose sulfates: Candidates for a tuberculosis vaccine. *Angew. Chemie - Int. Ed.* 47, 9734–9738. doi:10.1002/anie.200803835.

Gumperz, J. E., Miyake, S., Yamamura, T., and Brenner, M. B. (2002). Functionally distinct subsets of CD1d-restricted natural killer T cells revealed by CD1d tetramer staining. *J. Exp. Med.* 195, 625–636. doi:10.1084/jem.20011786.

Gurung, P., Gomes, C. M., Vernal, S., and Leeflang, M. M. G. (2019). Diagnostic accuracy of tests for leprosy: a systematic review and meta-analysis. *Clin. Microbiol. Infect.* doi:10.1016/j.cmi.2019.05.020.

Gutierrez-Arcelus, M., Teslovich, N., Mola, A. R., Polidoro, R. B., Nathan, A., Kim, H., et al. (2019). Lymphocyte innateness defined by transcriptional states reflects a balance between proliferation and effector functions. *Nat. Commun.* 10. doi:10.1038/s41467-019-08604-4.

Han, A., Glanville, J., Hansmann, L., and Davis, M. M. (2014). Linking T-cell receptor sequence to functional phenotype at the single-cell level. *Nat. Biotechnol.* 32, 684–692. doi:10.1038/nbt.2938.

Han, M., Hannick, L. I., DiBrino, M., and Robinson, M. a (1999). Polymorphism of human CD1 genes. *Tissue Antigens* 54, 122–127. doi:10.1034/j.1399-0039.1999.540202.x.

Hori, S., Nomura, T., and Sakaguchi, S. (2003). Control of Regulatory T Cell Development by the Transcription Factor Foxp3 *Science (80-.)*. 299, 1057 LP-1061. doi:10.1126/science.1079490.

Hou, X., Lu, C., Chen, S., Xie, Q., Cui, G., Chen, J., et al. (2016). High throughput sequencing of T cell antigen receptors reveals a conserved tcr repertoire. *Med. (United States)* 95. doi:10.1097/MD.0000000000002839.

Huang, J., Meyer, C., and Zhu, C. (2012). T cell antigen recognition at the cell membrane. *Mol. Immunol.* 52, 155–164. doi:10.1016/j.molimm.2012.05.004.

Hutchinson, S. L., Wooldridge, L., Tafuro, S., Laugel, B., Glick, M., Boulter, J. M., et al. (2003). The CD8 T Cell Coreceptor Exhibits Disproportionate Biological Activity at Extremely Low Binding Affinities. *J. Biol. Chem.* 278, 24285–24293. doi:10.1074/jbc.M300633200.

Ivanov, I. I., McKenzie, B. S., Zhou, L., Tadokoro, C. E., Lepelley, A., Lafaille, J. J., et al. (2006). The Orphan Nuclear Receptor RORγt Directs the Differentiation Program of Proinflammatory IL-17+ T Helper Cells. *Cell* 126, 1121–1133. doi:10.1016/j.cell.2006.07.035.

Jahng, A., Maricic, I., Aguilera, C., Cardell, S., Halder, R. C., and Kumar, V. (2004). Prevention of Autoimmunity by Targeting a Distinct, Noninvariant CD1d-reactive T Cell Population Reactive to Sulfatide. *J. Exp. Med.* 199, 947–957. doi:10.1084/jem.20031389.

James, C. A., Yu, K. K. Q., Gilleron, M., Prandi, J., Yedulla, V. R., Moleda, Z. Z., et al. (2018). CD1b Tetramers Identify T Cells that Recognize Natural and Synthetic Diacylated Sulfoglycolipids from Mycobacterium tuberculosis. *Cell Chem. Biol.* doi:10.1016/j.chembiol.2018.01.006.

Janeway, C. A. (1992). The T Cell Receptor as a Multicomponent Signalling Machine: CD4/CD8 Coreceptors and CD45 in T Cell Activation. *Annu. Rev. Immunol.* 10, 645–674. doi:10.1146/annurev.iy.10.040192.003241.

Jones, B. W., Means, T. K., Heldwein, K. A., Keen, M. A., Hill, P. J., Belisle, J. T., et al. (2001). Different Toll-like receptor agonists induce distinct macrophage responses. *J. Leukoc. Biol.* 69, 1036–44. doi:10.1189/jlb.1106655.

Kabouridis, P. S. (2006). Lipid rafts in T cell receptor signalling (review). *Mol. Membr. Biol.* 23, 49–57. doi:10.1080/09687860500453673.

Kasmar, A. G., van Rhijn, I., Cheng, T.-Y., Turner, M., Seshadri, C., Schiefner, A., et al. (2011). CD1b tetramers bind T cell receptors to identify a mycobacterial glycolipid-reactive T cell repertoire in humans. *J. Exp. Med.* 208, 1741–1747. doi:10.1084/jem.20110665.

Kasprowicz, V. O., Cheng, T. Y., Ndung'u, T., Sunpath, H., Moody, D. B., and Kasmar, A. G. (2016). HIV disrupts human T cells that target mycobacterial glycolipids. *J. Infect. Dis.*

213, 628–633. doi:10.1093/infdis/jiv455.
Kee, S. J., Kwon, Y. S., Park, Y. W., Cho, Y. N., Lee, S. J., Kim, T. J., et al. (2012). Dysfunction of natural killer T cells in patients with active Mycobacterium tuberculosis infection. *Infect. Immun.* 80, 2100–2108. doi:10.1128/IAI.06018-11.
Keller, A. N., Eckle, S. B. G., Xu, W., Liu, L., Hughes, V. A., Mak, J. Y. W., et al. (2017). Drugs and drug-like molecules can modulate the function of mucosal-associated invariant T cells. *Nat. Immunol.* 18, 402–411. doi:10.1038/ni.3679.
Kersh, G. J., Kersh, E. N., Fremont, D. H., and Allen, P. M. (1998). High- and Low-Potency Ligands with Similar Affinities for the TCR. *Immunity* 9, 817–826. doi:10.1016/s1074-7613(00)80647-0.
Kinjo, Y., Wu, D., Kim, G. S., Xing, G. W., Poles, M. A., Ho, D. D., et al. (2005). Recognition of bacterial glycosphingolipids by natural killer T cells. *Nature* 434, 520–525. doi:10.1038/nature03407.
Kitamura, H., Iwakabe, K., Yahata, T., Nishimura, S., Ohta, A., Ohmi, Y., et al. (1997). CD1d-restricted and TCR-mediated activation of Vα14 NKT cells by glycosylceramides. *Science (80-.).* 278, 1626–1629. doi:10.1084/jem.189.7.1121.
Kjer-Nielsen, L., Patel, O., Corbett, A. J., Le Nours, J., Meehan, B., Liu, L., et al. (2012). MR1 presents microbial vitamin B metabolites to MAIT cells. *Nature* 491, 717–723. doi:10.1038/nature11605.
Kurioka, A., Jahun, A. S., Hannaway, R. F., Walker, L. J., Fergusson, J. R., Sverremark-Ekström, E., et al. (2017). Shared and distinct phenotypes and functions of human cD161++ Vα7.2+ T cell subsets. *Front. Immunol.* 8. doi:10.3389/fimmu.2017.01031.
Larrouy-Maumus, G., Layre, E., Clark, S., Prandi, J., Rayner, E., Lepore, M., et al. (2017). Protective efficacy of a lipid antigen vaccine in a guinea pig model of tuberculosis. *Vaccine* 35, 1395–1402. doi:10.1016/j.vaccine.2017.01.079.
Layre, E., Collmann, A., Bastian, M., Mariotti, S., Czaplicki, J., Prandi, J., et al. (2009). Mycolic Acids Constitute a Scaffold for Mycobacterial Lipid Antigens Stimulating CD1-Restricted T Cells. *Chem. Biol.* 16, 82–92. doi:10.1016/j.chembiol.2008.11.008.
Layre, E., Paepe, D. C.-D., Larrouy-Maumus, G., Vaubourgeix, J., Mundayoor, S., Lindner, B., et al. (2011a). Deciphering sulfoglycolipids of Mycobacterium tuberculosis. *J. Lipid Res.* 52, 1098–110. doi:10.1194/jlr.M013482.
Layre, E., Sweet, L., Hong, S., Madigan, C. A., Desjardins, D., Young, D. C., et al. (2011b). A comparative lipidomics platform for chemotaxonomic analysis of mycobacterium tuberculosis. *Chem. Biol.* 18, 1537–1549. doi:10.1016/j.chembiol.2011.10.013.
Layton, E. D., Yu, K. K. Q., Smith, M. T., Scriba, T. J., De Rosa, S. C., and Seshadri, C. (2018). Validation of a CD1b tetramer assay for studies of human mycobacterial infection or vaccination. *J. Immunol. Methods* 458, 44–52. doi:10.1016/j.jim.2018.04.004.
Leadbetter, E. A., Brigl, M., Illarionov, P., Cohen, N., Luteran, M. C., Pillai, S., et al. (2008). NK T cells provide lipid antigen-specific cognate help for B cells. *Proc. Natl. Acad. Sci. U. S. A.* 105, 8339–8344. doi:10.1073/pnas.0801375105.
Lee, J. S., Krause, R., Schreiber, J., Mollenkopf, H. J., Kowall, J., Stein, R., et al. (2008). Mutation in the Transcriptional Regulator PhoP Contributes to Avirulence of Mycobacterium tuberculosis H37Ra Strain. *Cell Host Microbe* 3, 97–103. doi:10.1016/j.chom.2008.01.002.
Lee, P. T., Benlagha, K., Teyton, L., and Bendelac, A. (2002a). Distinct functional lineages of human Vα24 natural killer T cells. *J. Exp. Med.* 195, 637–641. doi:10.1084/jem.20011908.

Lee, P. T., Putnam, A., Benlagha, K., Teyton, L., Gottlieb, P. A., and Bendelac, A. (2002b). Testing the NKT cell hypothesis of human IDDM pathogenesis. *J. Clin. Invest.* 110, 793–800. doi:10.1172/JCI0215832.

Lee, Y. J., Holzapfel, K. L., Zhu, J., Jameson, S. C., and Hogquist, K. A. (2013). Steady-state production of IL-4 modulates immunity in mouse strains and is determined by lineage diversity of iNKT cells. *Nat. Immunol.* 14, 1146–1154. doi:10.1038/ni.2731.

Lepore, M., Kalinichenko, A., Calogero, S., Kumar, P., Paleja, B., Schmaler, M., et al. (2017). Functionally diverse human T cells recognize non-microbial antigens presented by MR1. *Elife* 6. doi:10.7554/eLife.24476.

Lepore, M., Kalinichenko, A., Kalinicenko, A., Colone, A., Paleja, B., Singhal, A., et al. (2014). Parallel T-cell cloning and deep sequencing of human MAIT cells reveal stable oligoclonal TCRβ repertoire. *Nat. Commun.* 5, 3866. doi:10.1038/ncomms4866.

Lewinsohn, D. A., Lewinsohn, D. M., and Scriba, T. J. (2017). Polyfunctional CD4+ T cells as targets for tuberculosis vaccination. *Front. Immunol.* 8. doi:10.3389/fimmu.2017.01262.

Lin, P. L., Rutledge, T., Green, A. M., Bigbee, M., Fuhrman, C., Klein, E., et al. (2012). CD4 T cell depletion exacerbates acute mycobacterium tuberculosis while reactivation of latent infection is dependent on severity of tissue depletion in cynomolgus macaques. *AIDS Res. Hum. Retroviruses* 28, 1693–1702. doi:10.1089/aid.2012.0028.

London, C. A., Lodge, M. P., and Abbas, A. K. (2000). Functional Responses and Costimulator Dependence of Memory CD4 + T Cells . *J. Immunol.* 164, 265–272. doi:10.4049/jimmunol.164.1.265.

Lopez, K., Iwany, S. K., Suliman, S., Reijneveld, J. F., Ocampo, T. A., Jimenez, J., et al. (2020). CD1b Tetramers Broadly Detect T Cells That Correlate With Mycobacterial Exposure but Not Tuberculosis Disease State. *Front. Immunol.* 11, 199. doi:10.3389/fimmu.2020.00199.

Mahomed, H., Hawkridge, T., Verver, S., Geiter, L., Hatherill, M., Abrahams, D., et al. (2011). Predictive factors for latent tuberculosis infection among adolescents in a high-burden area in South Africa. *Int. J. Tuberc. Lung Dis.* 15, 331–6. Available at: http://www.ncbi.nlm.nih.gov/pubmed/21333099.

Malka-Ruimy, C., Youssef, G. Ben, Lambert, M., Tourret, M., Ghazarian, L., Faye, A., et al. (2019). Mucosal-associated invariant T cell levels are reduced in the peripheral blood and lungs of children with active pulmonary tuberculosis. *Front. Immunol.* 10. doi:10.3389/fimmu.2019.00206.

Mangtani, P., Abubakar, I., Ariti, C., Beynon, R., Pimpin, L., Fine, P. E. M., et al. (2014). Protection by BCG vaccine against tuberculosis: A systematic review of randomized controlled trials. *Clin. Infect. Dis.* 58, 470–480. doi:10.1093/cid/cit790.

Martin, L. H., Calabi, F., and Milstein, C. (1986). Isolation of CD1 genes: A family of major histocompatibility complex-related differentiation antigens. *Proc. Natl. Acad. Sci. U. S. A.* 83, 9154–9158. doi:10.1073/pnas.83.23.9154.

McInnes, L., Healy, J., Saul, N., and Großberger, L. (2018). UMAP: Uniform Manifold Approximation and Projection. *J. Open Source Softw.* 3, 861. doi:10.21105/joss.00861.

Meermeier, E. W., Laugel, B. F., Sewell, A. K., Corbett, A. J., Rossjohn, J., McCluskey, J., et al. (2016). Human TRAV1-2-negative MR1-restricted T cells detect S. pyogenes and alternatives to MAIT riboflavin-based antigens. *Nat. Commun.* 7. doi:10.1038/ncomms12506.

Méndez-Samperio, P. (2018). Development of tuberculosis vaccines in clinical trials: Current status. *Scand. J. Immunol.* 88. doi:10.1111/sji.12710.

Moguche, A. O., Musvosvi, M., Penn-Nicholson, A., Plumlee, C. R., Mearns, H., Geldenhuys, H., et al. (2017). Antigen Availability Shapes T Cell Differentiation and Function during Tuberculosis. *Cell Host Microbe* 21, 695–706.e5. doi:10.1016/j.chom.2017.05.012.

Mogues, B. T., Goodrich, M. E., Ryan, L., Lacourse, R., and North, R. J. (2001). The Relative Importance of T Cell Subsets in Immunity and Immunopathology of Airborne Mycobacterium tuberculosis Infection in Mice. *J. Exp. Med.* 193, 271–280. doi:10.1084/jem.193.3.271.

Montoya, C. J., Pollard, D., Martinson, J., Kumari, K., Wasserfall, C., Mulder, C. B., et al. (2007). Characterization of human invariant natural killer T subsets in health and disease using a novel invariant natural killer T cell-clonotypic monoclonal antibody, 6B11. *Immunology* 122, 1–14. doi:10.1111/j.1365-2567.2007.02647.x.

Moody, D. B. (1997). Structural Requirements for Glycolipid Antigen Recognition by CD1b-Restricted T Cells. *Science (80-.).* 278, 283–286. doi:10.1126/science.278.5336.283.

Moody, D. B., Reinhold, B. B., Guy, M. R., Beckman, E. M., Frederique, D. E., Furlong, S. T., et al. (1997). Structural requirements for glycolipid antigen recognition by CD1b- restricted T cells. *Science (80-.).* 278, 283–6. doi:10.1126/science.278.5336.283.

Moody, D. B., Ulrichs, T., Mühlecker, W., Young, D. C., Gurcha, S. S., Grant, E., et al. (2000). CD1c-mediated T-cell recognition of isoprenoid glycolipids in Mycobacterium tuberculosis infection. *Nature* 404, 884–888. doi:10.1038/35009119.

Moody, D. B., Young, D. C., Cheng, T. Y., Rosat, J. P., Roura-Mir, C., O'Connor, P. B., et al. (2004). T Cell Activation by Lipopeptide Antigens. *Science (80-.).* 303, 527–531. doi:10.1126/science.1089353.

Murphy, K. (2017). *Immunobiology 9th Edition*. doi:10.1007/s13398-014-0173-7.2.

Nguyen, T. K. A., Koets, A. P., Santema, W. J., van Eden, W., Rutten, V. P. M. G., and Van Rhijn, I. (2009). The mycobacterial glycolipid glucose monomycolate induces a memory T cell response comparable to a model protein antigen and no B cell response upon experimental vaccination of cattle. *Vaccine* 27, 4818–4825. doi:10.1016/j.vaccine.2009.05.078.

O'Reilly, V., Zeng, S. G., Bricard, G., Atzberger, A., Hogan, A. E., Jackson, J., et al. (2011). Distinct and overlapping effector functions of expanded human CD4 +, cd8α + and CD4 - CD8α - invariant natural killer T cells. *PLoS One* 6. doi:10.1371/journal.pone.0028648.

Pai, M., Denkinger, C. M., Kik, S. V., Rangaka, M. X., Zwerling, A., Oxlade, O., et al. (2014). Gamma interferon release assays for detection of Mycobacterium tuberculosis infection. *Clin. Microbiol. Rev.* 27, 3–20. doi:10.1128/CMR.00034-13.

Paquin-Proulx, D., Costa, P. R., Silveira, C. G. T., Marmorato, M. P., Cerqueira, N. B., Sutton, M. S., et al. (2018). Latent Mycobacterium tuberculosis infection is associated with a higher frequency of mucosal-associated invariant T and invariant natural killer T cells. *Front. Immunol.* 9. doi:10.3389/fimmu.2018.01394.

Parra-Cuadrado, J. F., Navarro, P., Mirones, I., Setién, F., Oteo, M., and Martínez-Naves, E. (2000). A study on the polymorphism of human MHC class I-related MR1 gene and identification of an MR1-like pseudogene. *Tissue Antigens* 56, 170–172. doi:10.1034/j.1399-0039.2000.560211.x.

Patel, O., Cameron, G., Pellicci, D. G., Liu, Z., Byun, H.-S., Beddoe, T., et al. (2011). NKT TCR Recognition of CD1d-α- C -Galactosylceramide . *J. Immunol.* 187, 4705–4713. doi:10.4049/jimmunol.1100794.

Porcelli, S., Morita, C., and Brenner, M. (1992). CD1b restricts the response of human CD4-8- T

lymphocytes to a microbial antigen. *Nature* 360, 593–597. doi:10.1038/360593a0.
Porcelli, S., Yockey, C. E., Brenner, M. B., and Balk, S. P. (1993). Analysis of T cell antigen receptor (TCR) expression by human peripheral blood CD4−8− αβ T cells demonstrates preferential use of several Vβ genes and an invariant TCR α chain. *J. Exp. Med.* 178, 1–16. doi:10.1084/jem.178.1.1.
Rahimpour, A., Koay, H. F., Enders, A., Clanchy, R., Eckle, S. B. G., Meehan, B., et al. (2015). Identification of phenotypically and functionally heterogeneous mouse mucosal-associated invariant T cells using MR1 tetramers. *J. Exp. Med.* 212, 1095–1108. doi:10.1084/jem.20142110.
Rasappan, R., and Aggarwal, V. K. (2014). Synthesis of hydroxyphthioceranic acid using a traceless lithiation–borylation–protodeboronation strategy. *Nat. Chem.* 6, 810–814. doi:10.1038/nchem.2010.
Report, G. T. (2018). *Global tuberculosis Report WHO 2018*.
Rogers, P. R., Dubey, C., and Swain, S. L. (2000). Qualitative Changes Accompany Memory T Cell Generation: Faster, More Effective Responses at Lower Doses of Antigen. *J. Immunol.* 164, 2338–2346. doi:10.4049/jimmunol.164.5.2338.
Roh, K. H., Lillemeier, B. F., Wang, F., and Davis, M. M. (2015). The coreceptor CD4 is expressed in distinct nanoclusters and does not colocalize with T-cell receptor and active protein tyrosine kinase p56lck. *Proc. Natl. Acad. Sci. U. S. A.* 112, E1604–E1613. doi:10.1073/pnas.1503532112.
Rosat, J. P., Grant, E. P., Beckman, E. M., Dascher, C. C., Sieling, P. a, Frederique, D., et al. (1999). CD1-restricted microbial lipid antigen-specific recognition found in the CD8+ alpha beta T cell pool. *J. Immunol.* 162, 366–371.
Rothchild, A. C., Jayaraman, P., Nunes-Alves, C., and Behar, S. M. (2014). iNKT Cell Production of GM-CSF Controls Mycobacterium tuberculosis. *PLoS Pathog.* 10. doi:10.1371/journal.ppat.1003805.
Rowland, R., and McShane, H. (2011). Tuberculosis vaccines in clinical trials. *Expert Rev. Vaccines* 10, 645–658. doi:10.1586/erv.11.28.
Ruggiero, E., Nicolay, J. P., Fronza, R., Arens, A., Paruzynski, A., Nowrouzi, A., et al. (2015). High-resolution analysis of the human T-cell receptor repertoire. *Nat. Commun.* 6. doi:10.1038/ncomms9081.
Ruhl, C. R., Pasko, B. L., Khan, H. S., Kindt, L. M., Stamm, C. E., Franco, L. H., et al. (2020). Mycobacterium tuberculosis Sulfolipid-1 Activates Nociceptive Neurons and Induces Cough. *Cell*. doi:10.1016/j.cell.2020.02.026.
Sada-Ovalle, I., Chiba, A., Gonzales, A., Brenner, M. B., and Behar, S. M. (2008). Innate invariant NKT cells recognize Mycobacterium tuberculosis-infected macrophages, produce interferon-γ, and kill intracellular bacteria. *PLoS Pathog.* 4. doi:10.1371/journal.ppat.1000239.
Sallusto, F., Cassotta, A., Hoces, D., Foglierini, M., and Lanzavecchia, A. (2018). Do memory CD4 T cells keep their cell-type programming: Plasticity versus fate commitment?: T-cell heterogeneity, plasticity, and selection in humans. *Cold Spring Harb. Perspect. Biol.* 10. doi:10.1101/cshperspect.a029421.
Satija, R., Farrell, J. A., Gennert, D., Schier, A. F., and Regev, A. (2015). Spatial reconstruction of single-cell gene expression data. *Nat. Biotechnol.* 33, 495–502. doi:10.1038/nbt.3192.
Schieffer, D., Naware, S., Bakun, W., and Bamezai, A. K. (2014). Lipid raft-based membrane order is important for antigen-specific clonal expansion of CD4 T lymphocytes. *BMC*

Immunol. 15. doi:10.1186/s12865-014-0058-8.
Schietinger, A., and Greenberg, P. D. (2014). Tolerance and exhaustion: Defining mechanisms of T cell dysfunction. *Trends Immunol.* 35, 51–60. doi:10.1016/j.it.2013.10.001.
Schlienger, K., Craighead, N., Lee, K. P., Levine, B. L., and June, C. H. (2000). Efficient priming of protein antigen-specific human CD4+T cells by monocyte-derived dendritic cells. *Blood* 96, 3490–3498.
Scholzen, T., and Gerdes, J. (2000). The Ki-67 protein: From the known and the unknown. *J. Cell. Physiol.* 182, 311–322. doi:10.1002/(SICI)1097-4652(200003)182:3<311::AID-JCP1>3.0.CO;2-9.
Scriba, T. J., Kaufmann, S. H. E., Henri Lambert, P., Sanicas, M., Martin, C., and Neyrolles, O. (2016). Vaccination Against Tuberculosis With Whole-Cell Mycobacterial Vaccines. *J. Infect. Dis.*, 1–22. doi:10.1093/infdis/jiw228.
Seder, R. A., Darrah, P. A., and Roederer, M. (2008). T-cell quality in memory and protection: Implications for vaccine design. *Nat. Rev. Immunol.* 8, 247–258. doi:10.1038/nri2274.
Seshadri, C., Lin, L., Scriba, T. J., Peterson, G., Freidrich, D., Frahm, N., et al. (2015). T Cell Responses against Mycobacterial Lipids and Proteins Are Poorly Correlated in South African Adolescents. *J. Immunol.* 195, 4595–4603. doi:10.4049/jimmunol.1501285.
Shahine, A., Reinink, P., Reijneveld, J. F., Gras, S., Holzheimer, M., Cheng, T.-Y., et al. (2019). A T-cell receptor escape channel allows broad T-cell response to CD1b and membrane phospholipids. *Nat. Commun.* 10, 56. doi:10.1038/s41467-018-07898-0.
Sidobre, S., Naidenko, O. V., Sim, B.-C., Gascoigne, N. R. J., Garcia, K. C., and Kronenberg, M. (2002). The Vα14 NKT Cell TCR Exhibits High-Affinity Binding to a Glycolipid/CD1d Complex. *J. Immunol.* 169, 1340–1348. doi:10.4049/jimmunol.169.3.1340.
Sieling, P. A., Chatterjee, D., Porcelli, S. A., Prigozy, T. I., Mazzaccaro, R. J., Soriano, T., et al. (1995). CD1-restricted T cell recognition of microbial lipoglycan antigens. *Science (80-.).* 269, 227–230.
Sieling, P. A., Ochoa, M.-T., Jullien, D., Leslie, D. S., Sabet, S., Rosat, J.-P., et al. (2000). Evidence for Human CD4 + T Cells in the CD1-Restricted Repertoire: Derivation of Mycobacteria-Reactive T Cells from Leprosy Lesions. *J. Immunol.* 164, 4790–4796. doi:10.4049/jimmunol.164.9.4790.
Slichter, C. K., McDavid, A., Miller, H. W., Finak, G., Seymour, B. J., McNevin, J. P., et al. (2016). Distinct activation thresholds of human conventional and innate-like memory T cells. *JCI Insight* 1, 1–16. doi:10.1172/jci.insight.86292.
Sloan-Lancaster, J., and Allen, P. M. (1996). ALTERED PEPTIDE LIGAND–INDUCED PARTIAL T CELL ACTIVATION: Molecular Mechanisms and Role in T Cell Biology. *Annu. Rev. Immunol.* 14, 1–27. doi:10.1146/annurev.immunol.14.1.1.
Spertini, F., Audran, R., Chakour, R., Karoui, O., Steiner-Monard, V., Thierry, A. C., et al. (2015). Safety of human immunisation with a live-attenuated Mycobacterium tuberculosis vaccine: A randomised, double-blind, controlled phase I trial. *Lancet Respir. Med.* 3, 953–962. doi:10.1016/S2213-2600(15)00435-X.
Stenger, S., Mazzaccaro, R. J., Uyemura, K., Cho, S., Barnes, P. F., Rosat, J. P., et al. (1997). Differential effects of cytolytic T cell subsets on intracellular infection. *Science* 276, 1684–1687. doi:10.1126/science.276.5319.1684.
Stone, J. D., Chervin, A. S., and Kranz, D. M. (2009). T-cell receptor binding affinities and kinetics: impact on T-cell activity and specificity. *Immunology* 126, 165–176. doi:10.1111/j.1365-2567.2008.03015.x.

Stone, J. D., and Kranz, D. M. (2013). Role of T cell receptor affinity in the efficacy and specificity of adoptive T cell therapies. *Front. Immunol.* 4. doi:10.3389/fimmu.2013.00244.

Szabo, S. J., Kim, S. T., Costa, G. L., Zhang, X., Fathman, C. G., and Glimcher, L. H. (2000). A novel transcription factor, T-bet, directs Th1 lineage commitment. *Cell* 100, 655–669. doi:10.1016/S0092-8674(00)80702-3.

Tanaka, K., Kemmotsu, K., Ogawa, K., Ishii, N., Minami, M., Nagata, K., et al. (1998). Flow cytometric analysis of helper T cell subsets (Th1 and Th2) in healthy adults. *Rinsho Byori.* 46, 1247–1251.

Taniuchi, I. (2018). CD4 Helper and CD8 Cytotoxic T Cell Differentiation. *Annu. Rev. Immunol.* 36, 579–601. doi:10.1146/annurev-immunol-042617-053411.

Thedrez, A., de Lalla, C., Allain, S., Zaccagnino, L., Sidobre, S., Garavaglia, C., et al. (2007). CD4 engagement by CD1d potentiates activation of CD4⁺ invariant NKT cells. *Blood* 110, 251 LP-258. Available at: http://www.bloodjournal.org/content/110/1/251.abstract.

Tonti, E., Galli, G., Malzone, C., Abrignani, S., Casorati, G., and Dellabona, P. (2009). NKT-cell help to B lymphocytes can occur independently of cognate interaction. *Blood* 113, 370–376. doi:10.1182/blood-2008-06-166249.

Trinchieri, G. (1994). Interleukin-12: A cytokine produced by antigen-presenting cells with immunoregulatory functions in the generation of T-helper cells type 1 and cytotoxic lymphocytes. *Blood* 84, 4008–4027. doi:10.1182/blood.v84.12.4008.bloodjournal84124008.

Trunz, B. B., Fine, P., and Dye, C. (2006). Effect of BCG vaccination on childhood tuberculous meningitis and miliary tuberculosis worldwide: a meta-analysis and assessment of cost-effectiveness. *Lancet* 367, 1173–1180. doi:10.1016/S0140-6736(06)68507-3.

Ulrichs, T., Moody, D. B., Grant, E., Kaufmann, S. H. E., and Porcelli, S. A. (2003). T-cell responses to CD1-presented lipid antigens in humans with Mycobacterium tuberculosis infection. *Infect. Immun.* 71, 3076–3087. doi:10.1128/IAI.71.6.3076-3087.2003.

Ussher, J. E., Bilton, M., Attwod, E., Shadwell, J., Richardson, R., de Lara, C., et al. (2014). CD161++CD8+ T cells, including the MAIT cell subset, are specifically activated by IL-12+IL-18 in a TCR-independent manner. *Eur. J. Immunol.* 44, 195–203. doi:10.1002/eji.201343509.

Van Rhijn, I., Gherardin, N. a, Kasmar, A., de Jager, W., Pellicci, D. G., Kostenko, L., et al. (2014). TCR bias and affinity define two compartments of the CD1b-glycolipid-specific T Cell repertoire. *J. Immunol.* 192, 4054–60. doi:10.4049/jimmunol.1400158.

Van Rhijn, I., Iwany, S. K., Fodran, P., Cheng, T. Y., Gapin, L., Minnaard, A. J., et al. (2017). CD1b-mycolic acid tetramers demonstrate T-cell fine specificity for mycobacterial lipid tails. *Eur. J. Immunol.* 47, 1525–1534. doi:10.1002/eji.201747062.

Van Rhijn, I., Kasmar, A., de Jong, A., Gras, S., Bhati, M., Doorenspleet, M. E., et al. (2013). A conserved human T cell population targets mycobacterial antigens presented by CD1b. *Nat. Immunol.* 14, 706–13. doi:10.1038/ni.2630.

Viganò, S., Utzschneider, D. T., Perreau, M., Pantaleo, G., Zehn, D., and Harari, A. (2012). Functional avidity: A measure to predict the efficacy of effector T cells? *Clin. Dev. Immunol.* 2012. doi:10.1155/2012/153863.

Wang, G. C., Dash, P., Mccullers, J. A., Doherty, P. C., and Thomas, P. G. T Cell Receptor ab Diversity Inversely Correlates with Pathogen-Specific Antibody Levels in Human Cytomegalovirus Infection.

Weiss, A., and Littman, D. R. (1994). Signal transduction by lymphocyte antigen receptors. *Cell*

76, 263–274. doi:10.1016/0092-8674(94)90334-4.
Werninghaus, K., Babiak, A., Groß, O., Hölscher, C., Dietrich, H., Agger, E. M., et al. (2009). Adjuvanticity of a synthetic cord factor analogue for subunit Mycobacterium tuberculosis vaccination requires FclRγ-Syk- Card9-dependent innate immune activation. *J. Exp. Med.* 206, 89–97. doi:10.1084/jem.20081445.
Xu, Y., Morales, A. J., Cargill, M. J., Towlerton, A. M. H., Coffey, D. G., Warren, E. H., et al. (2019). Preclinical development of T-cell receptor-engineered T-cell therapy targeting the 5T4 tumor antigen on renal cell carcinoma. *Cancer Immunol. Immunother.* 68, 1979–1993. doi:10.1007/s00262-019-02419-4.
Zehn, D., Lee, S. Y., and Bevan, M. J. (2009). Complete but curtailed T-cell response to very low-affinity antigen. *Nature* 458, 211–214. doi:10.1038/nature07657.
Zhao, J., Siddiqui, S., Shang, S., Bian, Y., Bagchi, S., He, Y., et al. (2015). Mycolic acid-specific T cells protect against Mycobacterium tuberculosis infection in a humanized transgenic mouse model. *Elife* 4. doi:10.7554/eLife.08525.
Zhen, W., and Flavell, R. A. (1997). The Transcription Factor GATA-3 Is Necessary and Sufficient for Th2 Cytokine Gene. *Cell* 89, 587–596. doi:10.1016/S0030-6657(08)70226-9.
Zhou, D., Mattner, J., Cantu, C., Schrantz, N., Yin, N., Gao, Y., et al. (2004). Lysosomal glycosphingolipid recognition by NKT cells. *Science (80-.).* 306, 1786–1789. doi:10.1126/science.1103440.
Zhu, J., Yamane, H., and Paul, W. E. (2010). Differentiation of Effector CD4 T Cell Populations. *Annu. Rev. Immunol.* 28, 445–489. doi:10.1146/annurev-immunol-030409-101212.

APPENDIX A: EX VIVO IDENTITIFICATION OF Ac_2SGL-SPECIFIC T CELLS

Appendix A.I: Table of demographic information for patient samples included in *ex vivo* analysis of Ac_2SGL-specific T cells.

Cohort	PTID	IGRA	TST Result	Age	Sex	Race
HVTN SAC	SAC1011	N/A	N/A	N/A	N/A	N/A
HVTN SAC	SAC212671	N/A	N/A	N/A	N/A	N/A
HVTN SAC	SAC218703	N/A	N/A	N/A	N/A	N/A
HVTN SAC	SAC246764	N/A	N/A	N/A	N/A	N/A
HVTN SAC	SAC283958	N/A	N/A	N/A	N/A	N/A
ACS	11-0097	Positive	12	18	M	White
ACS	11-0116	Negative	0	14	F	Coloured
ACS	11-0117	Negative	0	14	M	White
ACS	11-0178	Negative	0	13	F	Coloured
ACS	09-0210	Positive	17	14	M	Coloured
ACS	03-0548	Positive	15.1	12	M	Black
ACS	01-0676	Negative	0	15	M	Coloured
ACS	01-0678	Negative	0	15	M	Coloured
ACS	03-0707	Positive	13	15	M	Black
ACS	01-0774	Positive	15	12	F	Black

Demographic information for patient samples included in the *ex vivo* analysis of Ac_2SGL-specific T cells. Demographic information was not available for the HIV Vaccine Trials Network Seattle Assay Control (HVTN SAC) cohort, but is comprised of cryopreserved PBMC isolated from healthy donors from Seattle, WA. The Adolescent Cohort Study (ACS) cohort is comprised cryopreserved PBMC isolated from M.tb-infected or M.tb-uninfected adolescents from South Africa. Interferon-g release assay (IGRA) results are reported as Positive or Negative and are indicative of M.tb infection status. These individuals have concordant tuberculin skin test (TST) results. The size of the induration is reported here in mm. Age reflects the age at last birthday at the time the sample was collected. Sex is self-reported. Race classification of individuals as 'White,' 'Coloured,' and 'Black' is based on a system that is used in South Africa as a proxy for socio-economic status in the original study (Mahomed et al., 2011)

Appendix A.II: Flow cytometry panel used for *ex vivo* identification of Ac_2SGL-specific T cells.

Specificity	Purpose	Fluorophore	Clone	Supplier
CD3	Lineage	BUV395	UCHT1	BD Biosciences
CD4	Lineage	APC H7	13B8.2	BD Biosciences
CD8β	Lineage	BB700	2ST8.5H7	BD Biosciences
CD45RA	Memory	BUV737	HI100	BD Biosciences
CCR7	Memory	BV711	150503	BD Biosciences
Pan-γδ	γδ T cells	PE-Vio770	11f2	Miltenyi Biotech
Vδ2	Vγ9δ2 T cells	AF700	B6	BioLegend
TRAV1-2	TCR Identification	BV605	3C10	BioLegend
CD14	Exclusion	BV785	M5E2	BioLegend
CD19	Exclusion	BV785	SJ25C1	BioLegend
CD1b-AMSGL	M.tb lipid antigen-specific T cells	ECD	N/A	Custom
CD1b-AMSGL	M.tb lipid antigen-specific T cells	PE	N/A	Custom
Fixable Green Dead Cell Stain	Viability	FITC	N/A	Life Technologies
Mock-loaded Tetramer	Dump	V510	N/A	Custom

12-color multi-parameter flow cytometry panel for identification of Ac_2SGL-specific T cells. The results reported in Figure 3.1 of this dissertation explored the TCR co-receptor expression Ac_2SGL-specific T cells using a 12-color flow cytometry panel. AMSGL-loaded CD1b tetramer (CD1b-AMSGL) was included for identification of sulfoglycolipid -specific T cells. For the CD1b-SGL tetramers, monomers were obtained from the NIH Tetramer Core Facility, and lipids were loaded onto the monomers and tetramerized in-house. Controls for our studies included Mock-loaded tetramers, and these were obtained from the NIH Tetramer Core Facility as monomers and tetramerized in-house. Additional markers in the panel allowed us to identify γδ T cells, distinguish between T cell lineages, and determine the memory phenotypes of each T cell population.

Appendix A.III. Gating strategy for *ex vivo* analysis of Ac_2SGL-specific T cells.

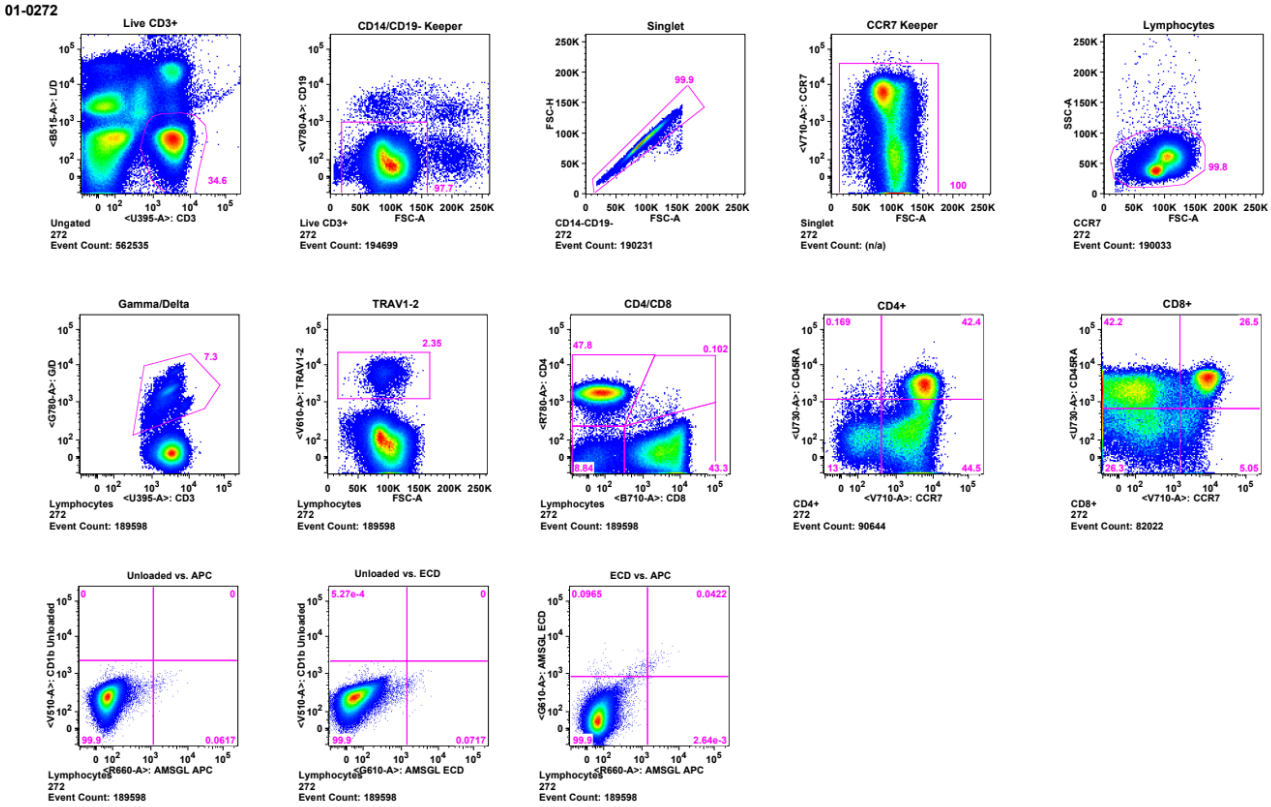

Representative Gating Strategy for identification of Ac_2SGL-specific T cells for patient identification (PTID) number 01-0272. The gating strategy proceeded from Live and $CD3^+$ events to $CD14^-$ and $CD19^-$ events to single cell events to a keeper gate using CCR7 to remove staining artifact to lymphocytes by size gating. After this point, gates were drawn for γδ T cells, TRAV1-2, CD4 and CD8, and CD45RA and CCR7 gates were drawn independently for CD4 and CD8 T cells. Then, gates were drawn for AMSGL-CD1b tetramer-positive events as defined by dual staining with two AMSGL-CD1b tetramers, but negative for Mock-loaded CD1b. From here, the gating set was imported into OpenCyto and cell count and MFI information was extracted for Boolean subsets of interest.

APPENDIX B: COMPUTATIONAL PIPELINE FOR ANALYSIS OF SINGLE-CELL PHENOTYPE DATA

Appendix B.I: Bash script for data processing, QC, and annotation. The script is implemented in the command line. These commands call VDJFasta scripts that are implemented in perl. These VDJFasta scripts can be downloaded here: https://github.com/immunoengineer/vdjfasta.git

```
#Specify paths to samples, library location, and vdjfasta .pl scripts.
#Specify name of projects and names of .fastq files

export SAMPLEPATH=/Users/seshadrilab/Desktop/NGS_TCRSeq
export SOURCE=/Users/seshadrilab/Desktop/NGS_TCRSeq/alpha-pheno/Demultiplex
export READ1=alpha-pheno_S1_L001_R1_001.fastq
export READ2=alpha-pheno_S1_L001_R2_001.fastq
export SAMPLE=alpha-pheno
export vdjfastapath=/Users/seshadrilab/vdjfasta/vdjfasta/bin

#Convert Read 1 and Read2 files from .fastq to .fasta

$vdjfastapath/fastq2fasta.pl --file $SOURCE/$READ1 > $SOURCE/$READ1.fasta
$vdjfastapath/fastq2fasta.pl --file $SOURCE/$READ2 > $SOURCE/$READ2.fasta

#Join paired end reads.input = .fasta files, output = joined reads in .fasta
#file and reads that failed QC in a .fasta file.

$vdjfastapath/fasta-hiseq-join-slow.pl --forward $SOURCE/$READ1.fasta --
reverse $SOURCE/$READ2.fasta --outputfile $SOURCE/$SAMPLE-joined.fasta --
ignoredfile $SOURCE/$SAMPLE-failqc.fasta

#Demultiplex using “Han Plate” MID (these are the barcodes used in Han et
#al., 2014, which are the same barcodes we use.

$vdjfastapath/fasta-demux.pl --dnafile $SOURCE/$SAMPLE-joined.fasta --
hanplate=1

#VDJ TCR Assignment and Phenotype read mapping (this step takes the longest
#(~24 hours). This will loop through each well indepedently.

for file in *-[0-9][A-Z][0-9].fa *-[0-9][0-9][A-Z][0-9].fa *-[0-9][A-Z][0-
9][0-9].fa *-[0-9][0-9][A-Z][0-9][0-9].fa
    do
$vdjfastapath/fasta-vdj-pipeline.pl --file=$SOURCE/$file
done

#Compile mapped reads into .csv summary table. The first line initiates the
#.csv file and the loop compiles the data.

$vdjfastapath/fasta-cell-summary.pl --header=1 > $SOURCE/$SAMPLE-mapped.csv
for file in *dnaH3.fa
do
  $vdjfastapath/fasta-cell-summary.pl --file=$SOURCE/$file
done >> $SOURCE/$SAMPLE-mapped.csv
```

Appendix B.II: R markdown file for running Seurat pipeline on data annotated using bash script above.

```
#Setup
library(tidyverse)
library(ggplot2)
library(scales) # for scales::squish() when coloring
library(cowplot)
library(umap)
library(Seurat)

#Read .csv file into R and clean and format data frame

d <- read.csv(("~/Desktop/alpha-pheno-mapped_FINAL.csv"), header=T, na.string
s=c("NA", "null", "<NA>", ""))
dput(colnames(d))

## c("platewell", "Antigen", "PTID", "wellcount.alpha", "wellcount.pheno",
## "Va", "Ja", "CDR3a", "Va..clone.dominance", "Va.counts", "alt.Va",
## "alt.Ja", "alt.CDR3a", "alt.Va..clone.dominance", "alt.Va.counts",
## "BCL6", "CD4", "CD8", "CTLA4", "EOMES", "FOXP3", "GATA3", "GZMB",
## "IFNG", "IL10", "IL12A", "IL13", "IL17A", "IL2", "MKI67", "PDCD1",
## "PRF1", "RORC", "RUNX1", "RUNX3", "TBET", "TGFB1", "TNF")

d$wellID <- seq_len(nrow(d))
#Remove wells that don't pass threshold read count
d <- subset(d, d$wellcount.alpha >5000)

#Clean and format data table

d[d==""] <- NA
temp <- d[,(16:38)]
temp$BCL6 <- sub(".*? (.+)", "\\1", temp$BCL6)
temp$GATA3 <- sub(".*? (.+)", "\\1", temp$GATA3)
temp$GZMB <- sub(".*? (.+)", "\\1", temp$GZMB)
temp$IFNG <- sub(".*? (.+)", "\\1", temp$IFNG)
temp$IL10 <- sub(".*? (.+)", "\\1", temp$IL10)
temp$IL12A <- sub(".*? (.+)", "\\1", temp$IL12A)
temp$IL13 <- sub(".*? (.+)", "\\1", temp$IL13)
temp$IL2 <- sub(".*? (.+)", "\\1", temp$IL2)
temp$PRF1 <- sub(".*? (.+)", "\\1", temp$PRF1)
temp$RORC <- sub(".*? (.+)", "\\1", temp$RORC)
temp$RUNX1 <- sub(".*? (.+)", "\\1", temp$RUNX1)
temp$RUNX3 <- sub(".*? (.+)", "\\1", temp$RUNX3)
temp$TBET <- sub(".*? (.+)", "\\1", temp$TBET)
temp$TGFB1 <- sub(".*? (.+)", "\\1", temp$TGFB1)
temp$TNF <- sub(".*? (.+)", "\\1", temp$TNF)
temp$CD4 <- sub(".*? (.+)", "\\1", temp$CD4)
temp$CD8 <- sub(".*? (.+)", "\\1", temp$CD8)
```

```
temp$EOMES <- sub(".*? (.+)", "\\1", temp$EOMES)
temp$CTLA4 <- sub(".*? (.+)", "\\1", temp$CTLA4)
temp$MKI67 <- sub(".*? (.+)", "\\1", temp$MKI67)
temp$PDCD1 <- sub(".*? (.+)", "\\1", temp$PDCD1)
temp$FOXP3 <- sub(".*? (.+)", "\\1", temp$FOXP3)

temp$FOXP3 <- as.numeric(temp$FOXP3)
temp$BCL6 <- as.numeric(temp$BCL6)
temp$GATA3 <- as.numeric(temp$GATA3)
temp$GZMB <- as.numeric(temp$GZMB)
temp$IFNG <- as.numeric(temp$IFNG)
temp$IL10 <- as.numeric(temp$IL10)
temp$IL12A <- as.numeric(temp$IL12A)
temp$IL13 <- as.numeric(temp$IL13)
temp$IL2 <- as.numeric(temp$IL2)
temp$PRF1 <- as.numeric(temp$PRF1)
temp$RORC <- as.numeric(temp$RORC)
temp$RUNX1 <- as.numeric(temp$RUNX1)
temp$RUNX3 <- as.numeric(temp$RUNX3)
temp$TBET <- as.numeric(temp$TBET)
temp$TGFB1 <- as.numeric(temp$TGFB1)
temp$TNF <- as.numeric(temp$TNF)
temp$CD8 <- as.numeric(temp$CD8)
temp$CD4 <- as.numeric(temp$CD4)
temp$EOMES <- as.numeric(temp$EOMES)
temp$CTLA4 <- as.numeric(temp$CTLA4)
temp$MKI67 <- as.numeric(temp$MKI67)
temp$PDCD1 <- as.numeric(temp$PDCD1)

#"Booleanize" the dataset. set all genes with reads to 1, all else, set to 0.
Note that genes with fewer than 5 reads did not pass QC and are not included
in this data set.
temp[temp >= 1] <- 1
temp[is.na(temp)] <- 0

#recombine with metadata
subs <- d[,-(16:38)]
d <- cbind(subs, temp)

#Subset data frame to include only cells of interest. Here, I selected only T
cells where CD4 or CD8 was detected.

alphapheno <- d
CD4 <- subset(alphapheno, CD4 == 1)
CD8 <- subset(alphapheno, CD8 == 1)
alphapheno <- rbind(CD4, CD8)

#Add rows containing TCR V gene assignment data to include as features in Seu
rat analysis
```

```
#Included due to high prevalence
alphapheno$TRAV12 <- ifelse(grepl("TRAV12",alphapheno$Va),1,0)
alphapheno$TRAV1.2 <- ifelse(grepl("TRAV1-2",alphapheno$Va),1,0)
alphapheno$TRAV8 <- ifelse(grepl("TRAV8",alphapheno$Va),1,0)
alphapheno$TRAV19 <- ifelse(grepl("TRAV19",alphapheno$Va),1,0)

#Included due to biological interest (LDN5-like and A01/A05-like)
alphapheno$TRAV17 <- ifelse(grepl("TRAV17", alphapheno$Va),1,0)
alphapheno$TRAV13 <- ifelse(grepl("TRAV13", alphapheno$Va),1,0)

cytokine_cols <- c("PTID", "Antigen", "BCL6" ,"CD4" ,"CD8", "CTLA4" , "EOMES"
,"FOXP3", "GATA3", "GZMB", "IFNG","IL10","IL12A","IL13","IL17A","IL2","MKI67"
,"PDCD1","PRF1","RORC", "RUNX1","RUNX3","TBET","TGFB1", "TNF", "TRAV1.2", "TR
AV13", "TRAV17", "TRAV8", "TRAV12")
```

```
#Data is then converted into a matrix that contains only the Boolean gene exp
ression data

d4tsne_withmeta <- alphapheno %>%
  dplyr::select(c("Antigen", "PTID", "wellID", cytokine_cols))

d4tsne_numericonly <- d4tsne_withmeta %>%
  dplyr::select(-Antigen, -PTID, -wellID) %>%
  data.matrix()
```

```
#Seurat Pipeline

# counts data has features as rows, not columns


d4tsne_numericonly <- as.matrix(d4tsne_numericonly)
d4_seurat <- t(d4tsne_numericonly)
seuratOb <- CreateSeuratObject(counts = d4_seurat,
                  project = "GMM_SGLseurat", min.cells = 3, min.features = 0)


# Clustering is dependent on running PCA/dimensionality reduction, which is f
urther dependent on scaling and finding variable features

seuratOb <- FindVariableFeatures(seuratOb, selection.method = "vst", nfeature
s = 2000)

#Scale features

seuratOb <- ScaleData(seuratOb, features = NULL)

#  The ScaleData function:
# Shifts the expression of each gene, so that the mean expression across cell
```

```
s is 0
# Scales the expression of each gene, so that the variance across cells is 1
# This step gives equal weight in downstream analyses, so that highly-express
ed genes do not dominate

#Run PCA
seuratOb<- RunPCA(seuratOb, features = VariableFeatures(object = seuratOb))

#Cluster the cells (dims are the number of Principal Components to include in
analysis)

seuratOb <- FindNeighbors(seuratOb, dims = 1:5)

seuratOb <- FindClusters(seuratOb, resolution = 1, random.seed = 20200420) #
lower res -> fewer clusters

#Visualize data using UMAP

seuratOb <- RunUMAP(seuratOb, dims = 1:3, seed.use = 20200420)

# Finding differentially expressed features (cluster biomarkers)
# find all markers of cluster 0
cluster0.markers <- FindMarkers(seuratOb, ident.1 = 0, min.pct = 0.1)
cluster0.markers

# find all markers of cluster 1
cluster1.markers <- FindMarkers(seuratOb, ident.1 = 1, min.pct = 0.1)
cluster1.markers

# find all markers of cluster 2
cluster2.markers <- FindMarkers(seuratOb, ident.1 = 2, min.pct = 0.1)
cluster2.markers
```